Mathematical Modeling of the Pharyngeal Phase of Swallowing

by

Brigette Marie Rosendall

A dissertation submitted in partial fulfillment
of the requirements for the degree of

Doctor of Philosophy

University of Washington

1996

Approved by Bruce A Finlayson
(Co-Chairperson of Supervisory Committee)

(Co-Chairperson of Supervisory Committee)

Program Authorized
to Offer Degree Chemical Engineering

Date November 8, 1996

In presenting this dissertation in partial fulfillment of the requirements for the Doctoral degree at the University of Washington, I agree that the Library shall make its copies freely available for inspection. I further agree that extensive copying of this dissertation is allowable only for scholarly purposes, consistent with "fair use" as prescribed in the U.S. Copyright Law. Requests for copying or reproduction of this dissertation may be referred to University Microfilms, 1490 Eisenhower Place, P.O. Box 975, Ann Arbor, MI 48106, to whom the author has granted "the right to reproduce and sell (a) copies of the manuscript in microform and/or (b) printed copies of the manuscript made from microform."

Signature_____

Date_____

University of Washington

Abstract

Mathematical Modeling of the Pharyngeal Phase of Swallowing

by: Brigette Marie Rosendall

Chairpersons of the Supervisory Committee
Professor Bruce A. Finlayson
Department of Chemical Engineering
Professor Michael W. Chang
Department of Rehabilitation Medicine

A significant portion of the population suffers from difficulty in swallowing, known as dysphagia, including 12 to 13% of hospitalized patients and 40% of nursing home residents. Dysphagia can make it impossible for a person to eat and drink normally which can lead to malnutrition, cachexia, and dehydration. During the pharyngeal phase of swallowing, the food or liquid to be swallowed, known as the bolus, passes the entrance to the larynx. If the bolus penetrates into the larynx, aspiration or choking can occur. Chronic aspiration can lead to serious lung infections such as pneumonia. Approximately 8,000 people in the United States choke to death each year.

In this research, a mathematical model that simulates swallowing was developed to analyze the parameters affecting the transport of the bolus through the pharynx. This work is a first attempt at modeling the pharyngeal phase of swallowing. The pharyngeal phase of swallowing is a complex, 3-dimensional, moving-boundary problem involving both fluid and solid motion. The model developed is a 2-dimensional representation of the fluid dynamics as the bolus passes through the pharynx. The mechanics of the pharyngeal muscle was not modeled, but was accounted for by prescribing the motion of the boundaries of the bolus in contact with the pharyngeal musculature. This boundary

motion was found through image analysis of individual videofluoroscopy studies. The model was solved with a commercial computational fluid dynamics program, FIDAP.

The model was applied to analyze data from a normal subject to investigate the effect of bolus volume, bolus viscosity, head positioning, and gravitational forces on the pharyngeal swallow. It was found that the viscosity had the greatest effect on the transport of the bolus through the pharynx. The most significant effect of modifying bolus volume or head positioning was to change the geometry of the bolus as it passed through the pharynx. Gravitational forces were found insignificant in the transport of the bolus except in the case of low-viscosity fluids.

The effect of these parameters on swallowing disorders was also investigated by modifying the model and applying the same modeling techniques to data from a dysphagic subject. These studies provided insight into how laryngeal penetration can be reduced by modifying bolus properties.

TABLE OF CONTENTS

TABLE OF CONTENTS (continued)

TABLE OF CONTENTS (continued)

LIST OF TABLES

LIST OF FIGURES

LIST OF FIGURES (continued)

LIST OF FIGURES (continued)

LIST OF FIGURES (continued)

ACKNOWLEDGMENTS

Financial support for this project was provided by the Whitaker Foundation and the Department of Chemical Engineering at the University of Washington. I must thank Dr. Finlayson for supporting me through all my endeavors here at the University of Washington. I have learned much more from him than what is reflected in this dissertation. I consider myself very fortunate to have had the opportunity to learn from him. I must also thank Dr. Chang for bringing this project to my attention. He organized the Dysphagia Study Group, without which, I wouldn't have been able to learn about the physics of swallowing so quickly. The members of the group, Drs. Charles Rohrmann, Kathryn Yorkston, Robert Miller, Charles Pope, and Susan Herring, also deserve my gratitude. I would like to give additional acknowledgment to Dr. Rohrmann for assisting greatly in the fluoroscopy studies.

I also need to thank research group members. Ken Westerberg was a great influence early in my education. He set a fine example of how to be successful as a graduate student. Christophe Poulain and I worked together throughout much of my time here. He was very considerate and easy to work with. Tristan Seitz did much of the work organizing the fluoroscopy studies in the summer of 1995 as a medical student research project. I would also like to thank Len Higashi, who has been extremely considerate in allowing me first priority with computing time.

My family deserves special thanks. My mother and father's support throughout my education, both financial and emotional, has made this possible. My sister Erin has also been a great support. She has given me a great deal of good advice these past few years. I'd also like to thank my brother, Eric, for being my first teacher.

I must give special thanks to a few people who have taken very good care of me during my studies. First, I'd like to thank Willard Foss for his tremendous support and understanding over this past year. He kept me focused on what was important. He was always willing to help with anything I needed. I also need to thank Stephen Porter and Kip Hauch. They have been like family to me. They listened to all my complaints, frustrations, and success stories. They were instrumental in the success of my dissertation defense.

I must also thank Basil Bourque for proofreading the document. He had the patience to read carefully through the entire document, having no background in chemical engineering or medicine. He also had many good suggestions on how to improve the appearance of the document. He deserves gratitude not only from me, but from everyone who reads this document.

Lastly, I'd like to thank all the friends I have made in the department—faculty, staff, and students. Because of them, the past six years have been some of the best years of my life. Their advice and support has meant a great deal to me. I hope these friendships will last a lifetime.

CHAPTER 1.--INTRODUCTION

A significant portion of the population, most commonly the elderly, suffer from difficulty in swallowing, known as dysphagia. Twelve to thirteen percent of hospitalized patients and 40% of nursing home residents suffer from dysphagia (Groher and Bukatman 1986 and Donner 1986). Dysphagia can make it impossible for a person to eat and drink normally which can lead to malnutrition, cachexia, and dehydration.

During the pharyngeal phase of swallowing, the food or liquid to be swallowed, known as the bolus, passes the entrance to the larynx. If the bolus penetrates into the larynx, aspiration or choking can occur. Chronic aspiration can lead to serious lung infections such as pneumonia. Approximately 8,000 people in the United States choke to death each year (Donner and Jones 1985).

There are many causes dysphagia including anatomic, neurologic, and muscular. Specific causes are listed in table 1.1 (Castell and Castell 1993). Anatomical causes result in difficulty in swallowing due to blocking problems. The path of the bolus is disrupted by abnormal formations. Neurological causes are a result of miscommunication between the brain and the nerves related to swallowing. The muscles that propel the bolus are weakened by muscular diseases. A mathematical model can allow investigation of the parameters affecting swallowing function without having to expose the patient to the invasiveness of manometry or excessive radiation exposure from fluoroscopy.

There are four phases of swallowing: the preparatory phase, the oral phase, the pharyngeal phase, and the esophageal phase. We are interested in modeling the pharyngeal phase. During the pharyngeal phase, the food or liquid to be swallowed, known as the bolus, passes the entrance to the larynx. If the bolus penetrates into the larynx, aspiration or choking can occur. Choking occurs when solid food enters and

becomes trapped in the airway. Aspiration occurs during normal breathing when liquid enters the airway and soils the bronchial tree.

A mathematical model that simulates swallowing in the pharynx can be used to understand the mechanisms involved in the transport of the bolus from the mouth to the esophagus. With this model, we hope to learn the effect of various parameters on bolus transport through the pharynx. One of the goals of this model is to investigate the parameters influencing laryngeal penetration. These parameters include bolus size, bolus properties (viscosity, density, etc.), head positioning, and body position. Many of these effects have been studied extensively. The most common techniques used to study these effects include videofluoroscopy and manometry. A mathematical model for bolus transport through the esophagus has been developed, but no models for the pharyngeal phase of swallowing have been published in the literature.

This dissertation covers the literature relevant to swallowing, the mathematical background required to develop the model, the development of the model, the data gathering procedure, and the results of the model applied to normal and disordered swallowing. Chapter 2 covers the literature relevant to swallowing. This chapter covers the biomechanics of the normal swallow, common evaluation techniques, literature data reporting on the normal swallow, and variations due to bolus variables and head and body positioning. Chapter 3 covers the mathematical background including the governing equations, solution methods, and solutions to similar problems. A review of the physical properties required for a model of swallowing is also discussed in chapter 3. A preliminary model was developed to gain insight on what should be included in the next stage of the model. What was learned from this preliminary model is discussed in chapter 4. Chapter 5 presents the details of the next generation of the mathematical model. Chapter 6 focuses on how the data is obtained for the implementation of the model. With the model, the effect of bolus volume, bolus viscosity, gravitational forces,

and head positioning on the pharyngeal phase of swallowing is studied. These results are presented in chapter 7. Verification of the model is also covered in chapter 7. The model is modified to study the effect of bolus variables on laryngeal penetration. The model is also applied to data from a dysphagic patient to study the effect of bolus variables on the swallowing function. These models are presented in chapter 8. The final chapter summarizes this dissertation and discusses possibilities for future studies and model improvements.

Table 1.1.--Causes of Dysphagia

ANATOMIC CAUSES
Postcricoid web
Cervical osteophyte
Hypopharyngeal diverticula
Head and neck tumors
NEUROLOGIC CAUSES
Cerebrovascular accidents
Poliomyelitis
Amyotrophic lateral sclerosis
Parkinson's disease
Cerebral palsy
Tumors
MUSCULAR DISEASE CAUSES
Oculopharyngeal muscular dystrophy
Myasthenia gravis

CHAPTER 2.--SWALLOWING

2.1.--Introduction

The chapter presents a literature review pertinent to swallowing. Studies of the pharyngeal phase cover many normal and disordered swallows. Many techniques have been used for these studies. The most common techniques include videofluoroscopy, manometry, and manofluorography. These studies can provide insight into the geometry of the pharynx and the pressures generated during the swallow.

The next section describes the biomechanics of oral and pharyngeal phase of swallowing. In that section, the anatomy and definitions relevant to swallowing are presented. Techniques to evaluate swallowing in the pharynx are presented in section 2.3. Data describing the normal swallow are detailed in section 2.4. Section 2.5 reviews literature reporting variations of the normal swallow and summarizes the results.

2.2.--Biomechanics of the Swallow

An excellent review of the normal swallow is given by Dodds, *et al.* (1990). The process of ingestion can be broken down into 4 phases. The first is called the preparatory phase. The preparatory phase is simply mastication of the food to be swallowed. This phase ends with the food or liquid bolus on top of the tongue with the tip of the tongue positioned against the maxillary incisors or alveolar ridge{1}. The back of the tongue and the soft palate{2} close together to prevent the bolus from escaping prematurely into the pharynx. This closure is commonly referred to as the glossopalatal junction or sphincter (GPJ){3}. Figures 2.2.1 show the anatomical features important to the oral and pharyngeal phases. The swallowing sequence is sketched in figure 2.2.2 from the anterior-posterior (AP) view. Figure 2.2.3 shows the swallowing sequence from the lateral view. Structures followed by numbers in brackets are marked on figures 2.2.1 and 2.2.3.

The transport of the bolus from the mouth to the pharynx is the oral phase of the swallow. At this stage, the glossopalatal junction opens as the tongue rolls to push the bolus back toward the pharynx. The glossopalatal junction opens by the lifting of the soft palate and the downward and forward movement of the tongue base. The lifting of the soft palate also serves to close the nasopharynx{4} by sealing with the posterior wall of the oropharynx{5}. The movement of the base of the tongue widens the opening to the hypopharynx{6} providing a channel for into which the bolus can fall. At this time, the larynx{7} and the hyoid{8} begin to move forward and upward expanding the hypopharynx.

The pharyngeal phase begins with the head of the bolus entering the oropharynx. The oral and pharyngeal phases overlap as the bolus passes through the glossopalatal junction. This piston like action of the tongue forces the bolus into the pharynx. The tongue base contacts the posterior pharyngeal wall closing the glossopalatal junction. Many events occur as the bolus passes through the pharynx. The peristalsis in the pharynx results in complete closure of the pharyngeal lumen behind the bolus. This begins with the closure of the glossopalatal junction. Closure of the pharyngeal lumen is due to the contraction of the pharyngeal constrictors and the tongue base contacting the posterior pharyngeal wall.

Continuing from the oral phase, the movement of the hyoid induces the elevation of the larynx. The elevation of the larynx also causes the cricopharyngeal muscle{9} to elevate. This whole process has many effects. First, the elevation of the larynx closes the airway preventing aspiration and/or choking. Second, the elevation results in shortening of the pharynx reducing the distance the bolus must travel to be transported to the esophagus. Third, the traction on the cricopharyngeal muscle causes the upper esophageal sphincter (UES){10} to rise and open allowing the bolus to pass into the esophagus. The elevation also moves the epiglottis{11} to a horizontal position. The

contraction of the muscles near the entrance of the larynx results in the flipping of the epiglottis and also acts as a sphincter. The flipped epiglottis covers the entrance of the larynx further protecting the airway.

The hyoid remains elevated until the bolus has passed through the UES into the esophagus{12}. The passage of the bolus tail through the UES ends the pharyngeal phase. The esophageal phase begins when the head of the bolus passes into the esophagus. This phase is characterized by a peristaltic wave contracting the cylindrical lumen transporting the bolus to the stomach.

2.3.--Evaluation Techniques

2.3.1.--Videofluoroscopy

Videofluoroscopy is the dynamic recording of fluoroscopic images. It provides visual information about the temporal and spatial parameters of movements during swallowing. For a standard US video system, complete images are displayed at a rate of 30 per second. For a typical system, the patient is positioned between the X-ray source and the fluoroscope. A video camera is attached to the fluoroscope. The images recorded by the camera are transmitted to a video screen and video tape recorder. A detailed review of the principles of videofluoroscopy along with radiation information is given by Beck and Gayler (1990).

The main advantage of videofluoroscopy is the ability to see what is happening during the swallow. If aspiration occurs, the degree, timing, and possibly the cause can be determined. Other abnormalities can also be determined. Videofluoroscopy can provide detailed geometric and timing information when combined with image processing techniques. Current technology warrants the use of computer analysis. A computerized imaging process for videofluoroscopy is detailed by Dengel, *et al.* (1991). Limitations of videofluoroscopy include the inability to quantify the propulsive forces on the bolus and the radiation exposure to the patient and the examiner.

2.3.2.--Manometry

Manometry is a diagnostic test that measures intralumenal pressures. Pressure measurements are made by the insertion of a catheter through the nose for placement in the pharynx and esophagus. Two types of manometers are commonly used (Castell and Dalton 1992). The first is a water infusion system. It this system, the catheter has many small capillary tubes. These tubes have openings at fixed locations along the length of the catheter. An infusion pump pumps water through the capillary tubes at a constant rate. Each capillary tube is connected to an external transducer to record changes in pressure. Infusion systems are most commonly used in the esophagus where there are no rapid changes and response times can be slow. Kahrilas, *et al.* (1994) state that the recording characteristics of perfused manometric systems are unsuitable for accurate pharyngeal pressure measurements.

Another type of manometry commonly used is known as solid-state manometry. This manometer assembly has strain-gauge sensors and solid-state electronics. This system has a much greater frequency range compared to the perfusion systems. The typical frequency range for this type of system is 0-20,000 Hz. This gives response times suitable for measuring the pressure activity within the pharynx. The frequency response required to reproduce pharyngeal pressure waves is 0-56 Hz. The maximum dP/dt generated during the pharyngeal phase of swallowing is 4000 mmHg/s (Kahrilas, *et al.* 1994).

Manometry is used in the pharynx and UES to determine the resting pressure of the UES, the onset of relaxation of the UES, pharyngeal contraction and peristalsis, and the coordination between UES relaxation and pharyngeal contraction. It is limited by the inability to tell if the pressures measured are applied to the bolus or if these pressures are due to the pharyngeal walls contracting upon the catheter. This tool is also invasive. The presence of the catheter will affect the fluid dynamics (Brasseur and Dodds 1991). Also,

studies have shown that the diameter of the catheter affects the pressures measured (Castell and Castell 1993).

The validity of manometric measurements in the pharynx is examined by McConnel, *et al.* in 1991 and 1992. They investigate the effects of asymmetric pressure measurements and the clinical significance of the vertical motion of the pharynx and catheter. They concluded that asymmetry of the pharynx does not invalidate manometric measurements because the pressures are not asymmetric when the bolus is passing. It is also noted that the use of a manometric sleeve to give an average pressure results in a loss of accuracy in timing. In the second study, they find the elevation of the catheter and the UES are not coordinated. The sensor originally placed in the UES is not in the UES at the peak of the elevation. It is concluded that this difficulty is insignificant because for the period of time where the sensor is not within the UES, the UES is open and the bolus is passing thus equalizing the pressure. They say that the pressure measured by the sensor is the same as within the UES. This is verified with the use of a special catheter with sensors place 1 cm apart in the area of the UES.

2.3.3.--Manofluorography

The correct interpretation of manometric data is important in determining the difference between pressures within the bolus and pressures caused by the lumen contracting on the catheter (Brasseur and Dodds 1991). An effective way to determine if the pressures being measured occur while the bolus is passing the sensors is by combined manometry and videofluoroscopy. This process is called manofluorography. The use of manofluorography for the study of swallowing disorders is detailed by McConnel, *et al.* (1986).

2.3.4.--Other Evaluation Techniques

Manometry and videofluoroscopy are not the only methods used to study swallowing. Logemann (1994) reviews non-imaging techniques for the study of

swallowing. Other methods that have been used to study the pharyngeal phase of the swallow are listed in table 2.3.1 with a reference that describes the technique.

2.4.--The Normal Swallow

2.4.1.--Pressure Measurements

Mendelsohn and McConnel (1987) introduce the use of manofluorography for the study of the function of the pharyngoesophageal segment (UES). They demonstrate the advantage of using combined manometry and videofluoroscopy to asses the cause of pharyngeal pressure events. With this method, they are able to correlate movement of the UES with bolus passage and manometric events. They also present variations due to different swallowing disorders.

Many articles were published by McConnel, *et al.* in 1988. These studies present measurements of various transit times in the pharyngeal phase, velocities, and pressures at various locations. Detailed analysis of the timing of the fluoroscopic, bolus and manometric events are given. They also show the clinical application of manofluorography to many case studies of various forms of dysphagia.

A paper published by Cerenko, *et al.* (1989) presents the major findings of the pressure measurements from McConnel's group. They used solid-state manometry with videofluoroscopy to measure pressure applied to the bolus at three locations: the tongue base, the level of the laryngeal entrance, and the point of highest resting pressure in the PE segment (UES). They explain that the use of solid-state manometry is necessary in order to resolve the rapid changes in the pharynx. Also, simultaneous fluoroscopy shows where the pressures are being measured. This is important due to the geometry changes the pharynx undergoes during the swallow. The distance between each sensor is 4 cm, giving a total length of 8 cm between the base of the tongue and the UES at rest. This study is limited to 10 mL swallows using 26 subjects. Pressure tracings as a function of time are presented in figure 2.4.1. The pressure tracings are from a single subject. The

pressure exerted on the bolus tail by the tongue is referred to as the tongue driving pressure (TDP). The average TDP is 17 mmHg for 10 mL swallows and is measured over a duration of 130 ms at the tongue base. The pressure measurement at the entrance to the larynx is called the oropharyngeal propulsion pump (OPP). It is composed of two pressure waves. The first of these waves is termed the total tongue driving force (TTDF). The average pressure over its 226 ms duration is 18 mmHg. The second pressure wave measured at this location is the pharyngeal clearing force (PCF). This force is said to clear the bolus tail from this level. At the end of the TTDF, the majority of the bolus is in the esophagus. A third sensor is placed at the UES. The negative pressure is measured before the head of bolus reaches this location. This negative pressure wave is called the hypopharyngeal suction pump (HSP). The average value over the 358 ms duration is (-)18 mmHg. When the bolus completely fills the UES, the pressure increases to 0 mmHg and above. The positive pressure wave is referred to as the positive flow integral (PFI). The average pressure value for the PFI is not reported. The average force is defined as the pressure-time integral and is reported as 3.4 mmHg-s.

2.4.2.--Geometry Information

Adnerhill, *et al.* (1989) found that the normal volume for a thin liquid bolus to be approximately 21 ± 5 mL. The average bolus volume for men is 25 mL, and 20 mL for women. Bolus volumes typically used in fluoroscopy studies range from 1 to 30 mL; 5, 10, and 20 being most common. The size and shape of the pharyngeal chamber changes rapidly during the swallow. As mentioned above, fluoroscopic images can be digitized to obtain geometry information.

The length of the pharynx (distance bolus travels from GPJ to UES) is not extensively reported in the literature. Kahrilas, *et al.* (1992) report the distance between the tongue base and the top of the UES to be 48 mm (see figure 2.4.2). The length of the UES is approximately 1 cm (Kahrilas, *et al.* 1988). The length of the pharynx also varies

during the swallow. Kahrilas, *et al.* (1992) refer to this as pharyngeal shortening. The pharynx shortens by about 40% of the original length during the swallow. The duration of this shortening is dependent on the volume swallowed. Other length data can be inferred from the locations of manometric sensors. The distance between the three manometric sensors in Cerenko, *et al.* (1989) is 4 cm. The first sensor was located at the base of the tongue, the second at the entrance of the larynx, and the third at the UES.

The cross-sectional area of the pharynx is a function of both location and time during the swallow. The lateral dimension is greater than the anterior-posterior dimension. Areas reported in the literature are often calculated assuming an ellipsoid shape. Kahrilas, *et al.* (1992) report anterior-posterior coordinates of the pharyngeal surfaces for 5-mL swallows as a function of time and axial location. Cross-sectional areas for an ellipse as a function of bolus volume and axial location are also reported by Kahrilas, *et al.* (1993). Cook, *et al.* (1989) give UES diameter and ellipsoid area as a function of bolus volume.

2.4.3.--Timing

Transit times are also extensively detailed in the literature. Cook, *et al.* (1989) and McConnel, *et al.* (1988) report detailed temporal descriptions of the pharyngeal swallow. Logemann, *et al.* (1987) provide definitions for various timing measures. Kahrilas, *et al.* (1993) also give a time line for the pharyngeal swallow and explain how the timing should be based.

Various velocities are also given in the literature. Jones and Donner (1989) report the pharyngeal peristalsis velocity as 12 to 25 cm/s and the esophageal peristaltic velocity as 1 to 4 cm/s. Kahrilas, *et al.* (1988) calculate hypopharyngeal peristaltic velocities as a function of swallow volumes ranging from 14 to 17 cm/s and conclude that there is no significant difference in peristaltic velocity for different volumes. This conclusion was also reached by Ekberg, *et al.* (1988). Kahrilas, *et al.* (1992) measure the velocity of

lumenal closure as a function of axial location and swallow volume and again find no correlation with swallow volume.

2.5.--Variations of the Normal Swallow

Many studies have investigated differences in the pharyngeal phase of swallowing due to certain variations. Table 2.5.1 lists many of these studies and the corresponding variations. An M in the middle column represents a study using manometry, VF represents videofluoroscopy, CF represents cinefluoroscopy, Endo represents endoscopy, UCT represents ultrafast computerized tomography, and EMG represents electromyography.

Emotional stress increases the UES pressure significantly. Swallowing in the elderly is significantly different that younger subjects: resting pressure of the UES is significantly lower, relaxation of the UES is delayed, duration of the UES opening is decreased, and peristaltic amplitude and velocity are decreased. Cold stimulation has little to no effect on normal subjects. The effect of certain drugs are also found to be minimal. The Mendelsohn maneuver increase the duration of laryngeal elevation.

Changes in body position has two major effects, gravitational and spatial. Studies investigating supine versus upright swallows using manometry have shown a slight shift in the pressure waves (Castell, *et al.* 1990). The time between the minimum UES pressure and the maximum pharyngeal pressure (5 cm proximal to the UES sensor) decreases for upright swallows. This can be interpreted as a slight increase in time for bolus passage for supine swallows. Changes in head position change the geometry of the pharynx. Details of the effect of head position can be found in the references listed in table 2.5.1 and in section 7.4.

The effect of different swallow volumes has been studied extensively. As mentioned previously, swallow volume has no effect on peristaltic velocity. The mean flow rate through the pharynx and UES increase with increasing volume. This is

accomplished by an increase in the cross-sectional area of the pharynx and UES for increasing volume. The UES also opens earlier in comparison to the onset of the stripping wave of peristalsis. The onset of the stripping wave of peristalsis is also later compared to the maximal UES opening. The duration of UES opening and glossopalatal junction opening also increases with increasing volume. This is effectively an increase in the bolus wavelength of peristalsis. The peristaltic pressure wave amplitude and duration is not a function of swallow volume. This is the squeeze of the pharyngeal lumen closing behind the bolus. This essentially means the muscle contraction is not any different for different swallow volumes. Intrabolus pressures increase with increasing volume at the level of the valleculae and within the UES. The pressure drop across the UES (pressure 1 cm proximal - pressure 1 cm distal) decreases with increasing swallow volumes. This is because the hypopharynx increases more in diameter relative to the esophagus for increasing swallow volumes. Maximal superior and anterior movements of the hyoid and larynx increase with increasing volume.

In most instances, the investigators fail to report numerical data for the consistency of substances used in their studies. In one study (Dantas, *et al.* 1990), the effect of boluses of differing viscosity was investigated by comparing liquid barium, with a density and viscosity of 1.4 g/cm^3 and 200 cP, to paste barium, with a density of 2.8 g/cm^3 and a viscosity of 60,000 cP. Pharyngeal and oral transit times are longer for paste than liquid. This implies the velocity of peristalsis is less for paste that liquid boluses, but this is not reported in the literature. Also, there is a delay in UES opening for paste boluses. This also could be attributed to a reduction in peristaltic velocity, but a shorter bolus wavelength would have the same effect. The study does find the bolus wavelength is shortened for paste. For the same volume of liquid and paste, the pharynx and UES distend more for paste boluses. Other effects of high viscosity include an increase in intrabolus pressure. This increase is more profound for higher volume boluses. The

amplitude of the peristaltic pressure wave is slightly increased for higher viscosity but is statistically insignificant. The duration of the peristaltic pressure wave is also increased and is statistically significant. This indicates the muscle contraction is dependent on viscosity. It also implies a decrease in peristaltic velocity for increasing viscosity.

Table 2.3.1.--Other Evaluation Techniques

TECHNIQUE	REFERENCE
Turbo-FLASH Magnetic Resonance Imaging	Suto, *et al.* (1995)
Electrical Impedance Tomography	Hughes, *et al.* (1994)
Ultrafast Computerized Tomography	Ergun, *et al.* (1993)
Videoendoscopy	Bastian (1993)
Electromyography	Perlman (1993)
Electroglottograph	Motta, *et al.* (1990)
Scintigraphy	Holt, *et al.* (1990)
Cineradiography	Jones, *et al.* (1985)

Table 2.5.1.--Variations of the Normal Swallow

VARIATION	METHOD	REFERENCE
Age - Position -Temperature - Volume	M,VF,Endo	Shaker, *et al.* (1994)
Age - Volume	Scint	Cook, *et al.* (1994)
Position	M,VF	Dejaeger, *et al.* (1994)
Volume	VF	Wintzen, *et al.* (1994)
Volume	M,VF	Maddock, *et al.* (1993)
Volume - Consistency - Multiple	VF	Lazarus, *et al.* (1993)
Volume	UCT	Ergun, *et al.* (1993)
Age - Volume - Temperature -	M	Shaker, *et al.* (1993)
Age - Volume - Temperature	M,Endo	Ren, *et al.* (1993)
Age - Sex - Volume - Viscosity	M	Perlman, *et al.* (1993)
Head Position	M	Castell, *et al.* (1993)
Head Position	CF	Welch, *et al.* (1993)
Volume	M,VF	Kahrilas, *et al.* (1992, 1988)
Consistency	VF,EMG	Palmer, *et al.* (1992)
Age	VF	Ekberg, *et al.* (1991)
Drug Effects - Temperature	M	Knauer, *et al.* (1990)
Volume - Viscosity	M,VF,EMG	Dantas, *et al.* (1990)
Body Position	M	Castell, *et al.* (1990)
Age	M	Fulp, *et al.* (1990)
Volume	M,VF	Dantas, *et al.* (1989)
Age - Sex - Smoking	M	Wilson, *et al.* (1990)
Position	CF	Borgstrom, *et al.* (1989)
Volume	M,VF	Jacob, *et al.* (1989)
Head Position	VF	Logemann, *et al.* (1989)
Age - Volume	M,VF	Tracy, *et al.* (1989)
Consistency	M	Wilson, *et al.* (1989)
Volume	M,VF	Cook, *et al.* (1989)
Volume	CF	Ekberg, *et al.* (1988)
Volume	VF	Dodds, *et al.* (1988)
Age - Position	CF	Borgstrom, *et al.* (1988)
Stress	M	Cook, *et al.* (1987, 1989)
Head Position	CF	Ekberg, *et al.* (1986)

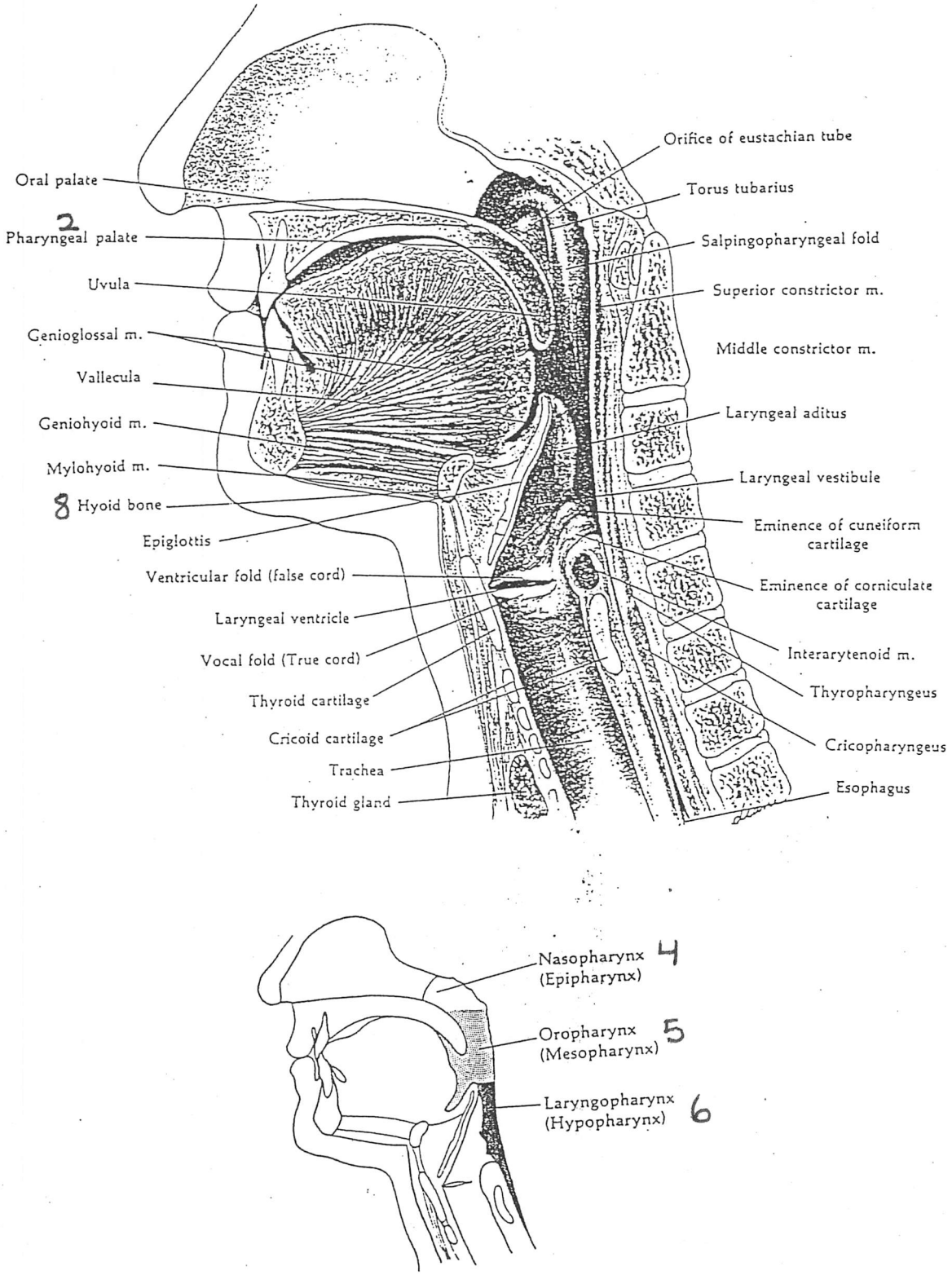

Figure 2.2.1.--Anatomical structures relevant to swallowing. (from Bosma, *et al.* 1986)

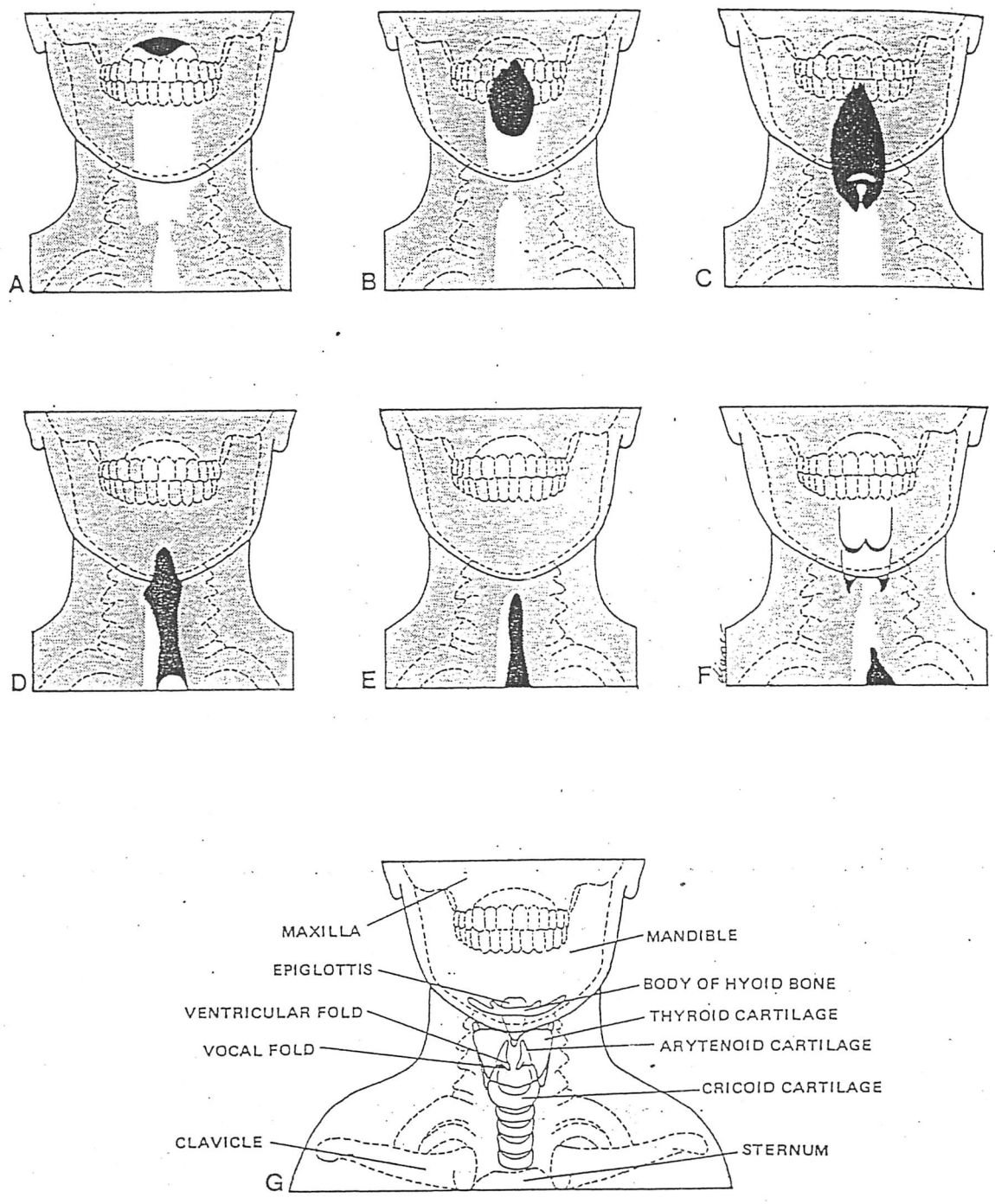

Figure 2.2.2.--Anterior-posterior view of the swallowing sequence. (from Donner, *et al.* 1985)

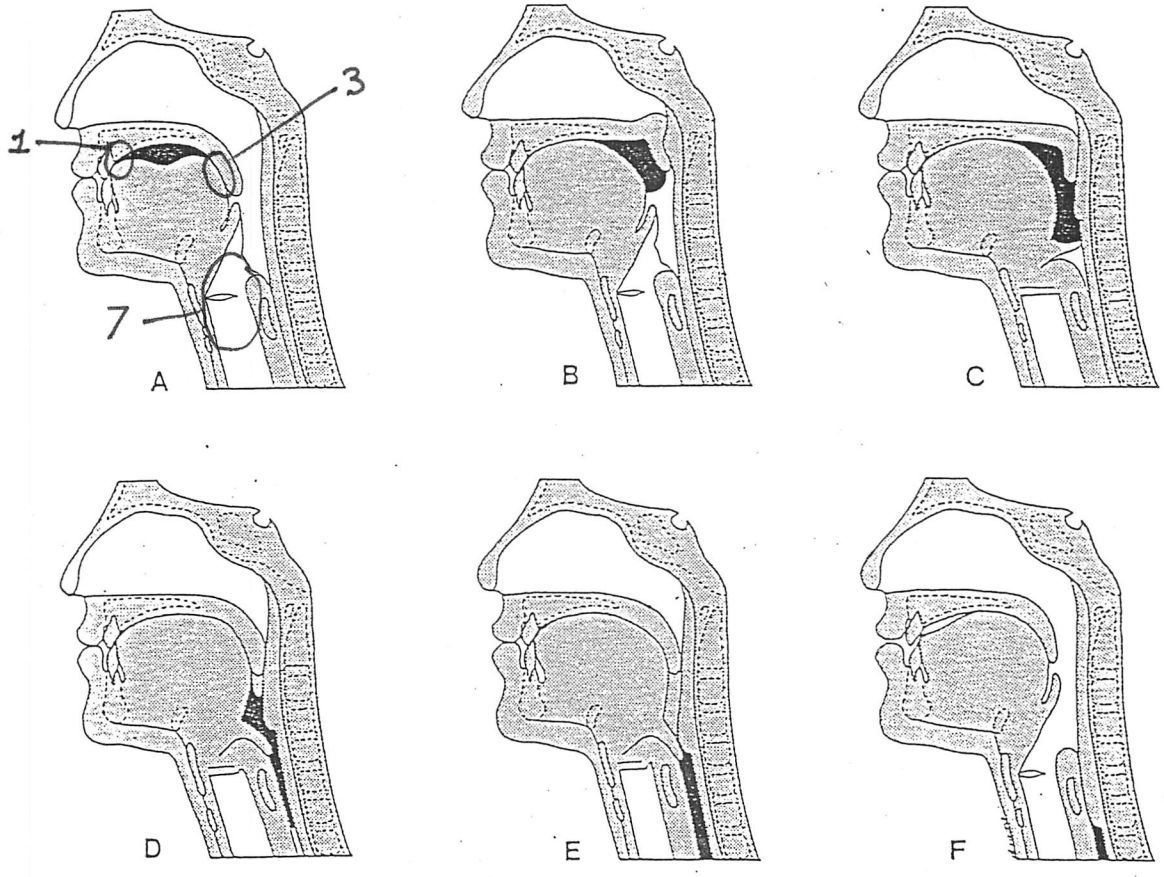

Figure 2.2.3.--Lateral view of the swallowing sequence. (from Donner, *et al.* 1985)

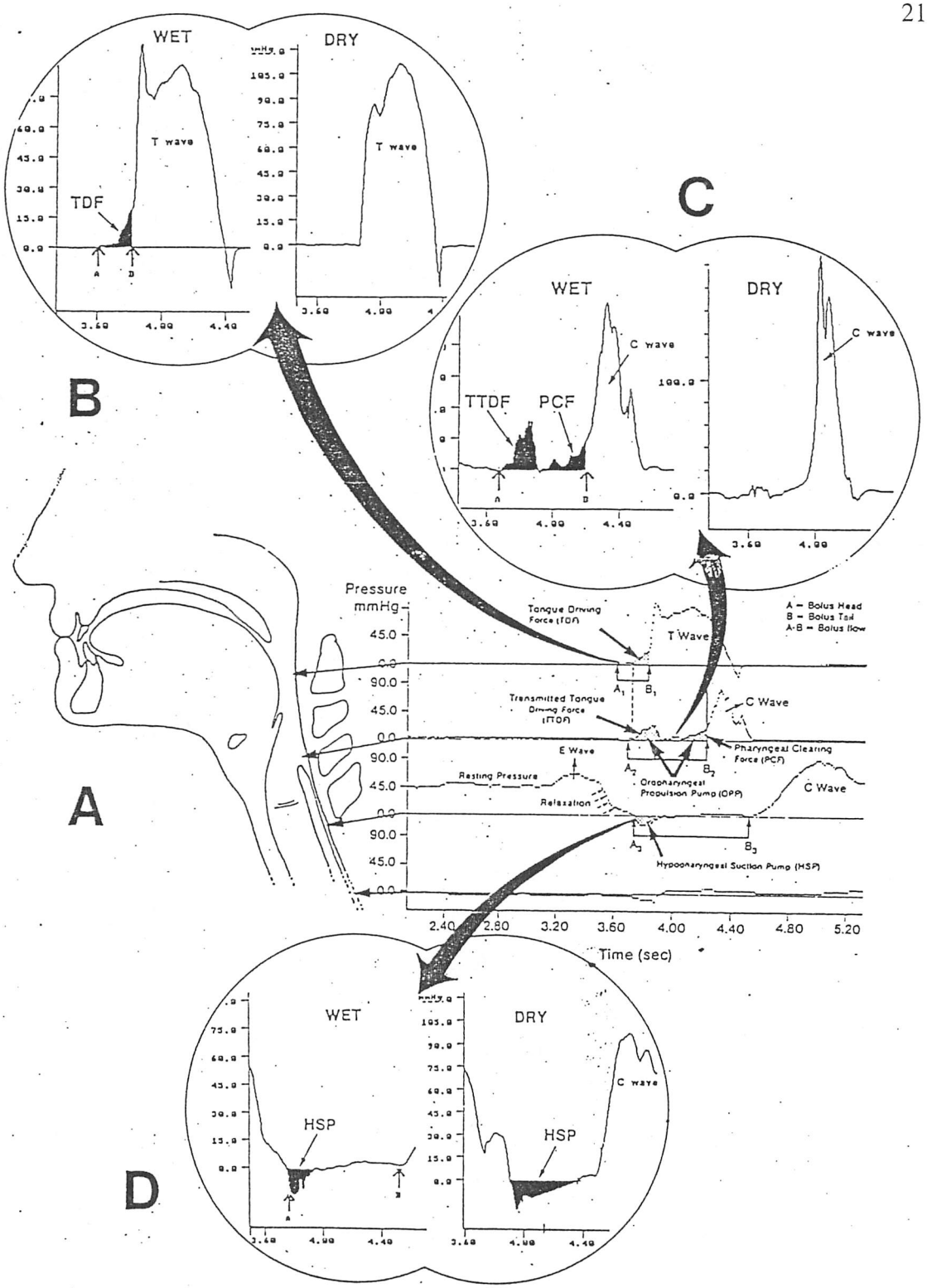

Figure 2.4.1.--Pressure tracings from manometry for a 10 mL barium swallow in a normal subject. (from Cerenko, *et al.* 1989)

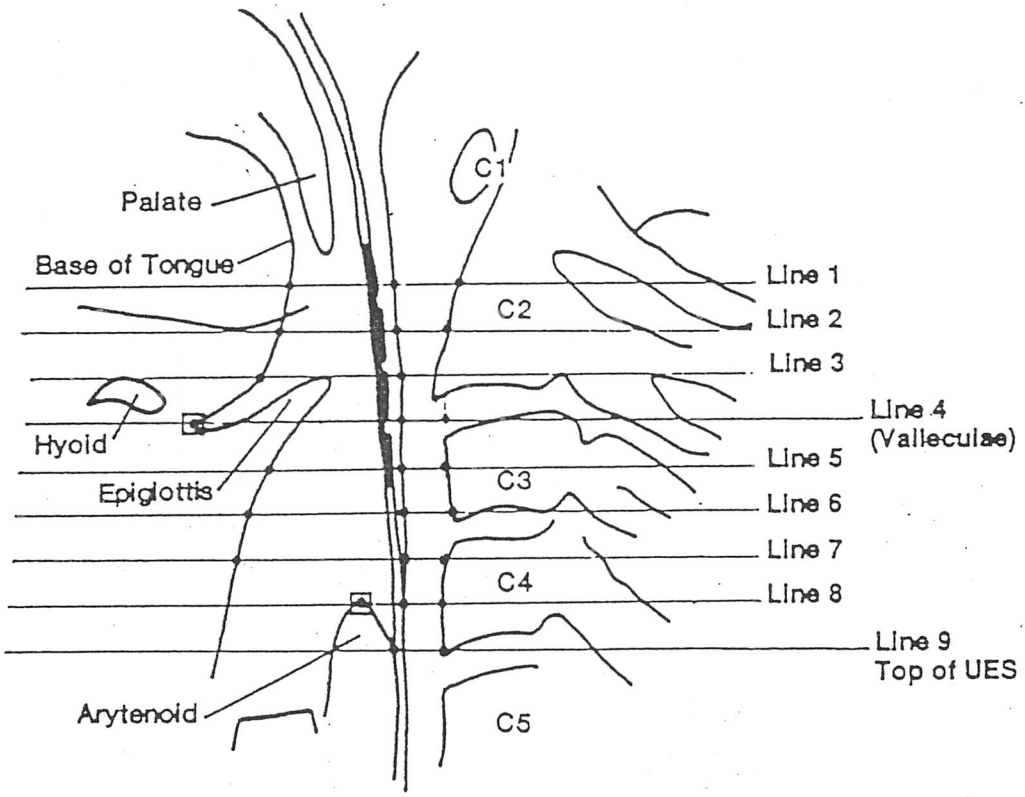

Figure 2.4.2.--Gridlines used by Kahrilas, *et al.* (1992) to normalize anatomic data. The mean distance between grid lines is 6 mm at rest.

CHAPTER 3.--MATHEMATICAL BACKGROUND

3.1.--Introduction

The mathematical background required for modeling the pharyngeal phase of swallowing is presented in this chapter. The equations governing the motion of a fluid are presented in section 3.2. A method for the solution of these equations using computational fluid dynamics with the finite element method is presented in section 3.3. Having the mathematical background, a review of the literature on flow situations similar to swallowing in the pharynx is presented. General peristaltic flow is covered in section 3.4. Section 3.5 presents a mathematical model developed for the esophageal phase of swallowing. No mathematical models for the pharyngeal phase of swallowing currently exist in the literature. Section 3.6 derives an analytical solution for squeezing flow. These models provide insight on how to approach modeling the pharynx. The last section reviews physical properties for the model.

3.2.--Governing Equations

The most general form of the continuum equations for a fluid are presented below. The continuity equation, (3.2.1), is a mathematical statement of the conservation of mass.

$$\frac{\partial \rho}{\partial t} = -(\nabla \cdot \rho \mathbf{v}) \tag{3.2.1}$$

∇ is the divergence operator, ρ is the density of the fluid, $\mathbf{v}$ is the velocity vector, and t is time. The equation of motion is a mathematical statement of the conservation of linear momentum.

$$\frac{\partial}{\partial t}\rho \mathbf{v} = -[\nabla \cdot \rho \mathbf{v}\mathbf{v}] - \nabla p - [\nabla \cdot \tau] + \rho \mathbf{g} \tag{3.2.2}$$

p is the pressure, **g** is vector representing the body force per unit mass (most commonly gravity), and τ is the stress tensor. Equation (3.2.3) represents the conservation of thermal energy.

$$\rho c_{\upsilon}\left(\frac{\partial T}{\partial t}+\mathbf{u}\cdot\nabla T\right)=-(\nabla\cdot\mathbf{q})-T\left(\frac{\partial p}{\partial T}\right)_{V}(\nabla\cdot\mathbf{u})-(\tau:\nabla\mathbf{u})+\mathbf{H} \qquad (3.2.3)$$

c_{υ} is the heat capacity of the fluid, T is temperature, **q** is the heat flux, V is the volume, and **H** is a source term. Derivations of these equations can be found in Bird, *et al.* (1960).

When the fluid can be represented as Newtonian and incompressible, the equations of motion are commonly referred to as the Navier-Stokes equations. For a Newtonian fluid, the stress tensor is linearly proportional to the instantaneous value of the rate of deformation tensor. An equation that describes the functionality of the stress is known as a constitutive relation. The constitutive relation for a Newtonian fluid is defined by equation (3.2.4).

$$\tau=-\mu\mathbf{d} \qquad (3.2.4)$$

In equation (3.2.4), μ is the viscosity of the fluid and **d** is the rate of deformation tensor. Non-Newtonian fluids are simply fluids that do not follow Newtonian behavior. A constitutive relation for a non-Newtonian fluid can take many forms. A viscoelastic fluid is a non-Newtonian fluid that exhibits both viscous (fluid) and elastic (solid) behavior.

3.3.--Solution Methods

The equations for the fluid dynamics model are solved using a software package written by Fluid Dynamics International, Inc. called FIDAP. FIDAP uses the Galerkin formulation of the finite element method to solve the governing equations. Details of all the solution methods discussed in this section can be found in the FIDAP 7.0 Theory Manual (FDI 1993). The finite element method reduces a system of differential equations to a system algebraic equations by breaking up the continuum into discrete pieces called

elements. The unknowns, velocity ($\mathbf{u}(\mathbf{x},t)$), pressure ($p(\mathbf{x},t)$), and temperature ($T(\mathbf{x},t)$), are estimated by polynomials on the element level.

$$\mathbf{u}(\mathbf{x},t) = \sum_{i=1}^{N} \varphi_i \mathbf{U}_i \tag{3.3.1}$$

$$p(\mathbf{x},t) = \sum_{i=1}^{N} \psi_i P_i \tag{3.3.2}$$

$$T(\mathbf{x},t) = \sum_{i=1}^{N} \vartheta_i T_i \tag{3.3.3}$$

The polynomials, φ, ψ, and ϑ are known as interpolation or basis functions; N is the number of nodal points. FIDAP chooses φ and ϑ to be the same, ψ is of equal or lesser order. The form of the basis functions depend on the element type. Element types supported by FIDAP are discussed in detail in the FIDAP Theory Manual (FDI 1993). In the equations above, $\mathbf{U}_i$, P_i, and T_i are the values of the velocity components, pressure, and temperature at the nodal points of the elements. For notational ease, the differential equations for momentum and mass conservation can be represented as follows.

$$\mathbf{f}_1(\mathbf{u}, p, T) = 0 \qquad \text{Momentum} \tag{3.3.4}$$

$$\mathbf{f}_2(\mathbf{u}) = 0 \qquad \text{Mass} \tag{3.3.5}$$

$$\mathbf{f}_3(\mathbf{u}, p, T) = 0 \qquad \text{Energy} \tag{3.3.6}$$

Substituting the approximations given in equations (3.3.1 - 3.3.3) into these differential equations gives the residuals, $\mathbf{R}_i$.

$$\mathbf{f}_1(\varphi, \psi, \vartheta, \mathbf{U}_i, P_i, T_i) = \mathbf{R}_1 \qquad \text{Momentum} \tag{3.3.7}$$

$$\mathbf{f}_2(\varphi, \mathbf{U}_i) = \mathbf{R}_2 \qquad \text{Mass} \tag{3.3.8}$$

$$\mathbf{f}_3(\varphi, \vartheta, \mathbf{U}_i, T_i) = \mathbf{R}_3 \qquad \text{Energy} \tag{3.3.9}$$

These residuals are forced to zero on the problem domain by using the method of weighted residuals (see also Finlayson 1972).

$$\begin{aligned} \int_\Omega W_j R_1 &= 0 \qquad j = 1,N \qquad \text{Momentum} \\ \int_\Omega W_j R_2 &= 0 \qquad j = 1,N \qquad \text{Mass} \\ \int_\Omega W_j R_3 &= 0 \qquad j = 1,N \qquad \text{Energy} \end{aligned} \tag{3.3.10}$$

The Galerkin formulation sets these weighting functions, W_j, equal to the basis functions making the residual orthogonal to the basis function. Since the basis functions for the velocity and pressure discretizations are not necessarily the same, FIDAP chooses the following formulation.

$$\begin{aligned} \int_\Omega \varphi_j R_1 &= 0 \qquad j = 1,N \qquad \text{Momentum} \\ \int_\Omega \psi_j R_2 &= 0 \qquad j = 1,N \qquad \text{Mass} \\ \int_\Omega \vartheta_j R_3 &= 0 \qquad j = 1,N \qquad \text{Energy} \end{aligned} \tag{3.3.11}$$

Using this formulation, the differential equations can be represented by the following set of algebraic equations in matrix notation assuming incompressible flow for clarity.

$$\begin{bmatrix} M & 0 & 0 \\ 0 & N & 0 \\ 0 & 0 & 0 \end{bmatrix} \begin{bmatrix} \dot{U} \\ \dot{T} \\ \dot{P} \end{bmatrix} + \begin{bmatrix} A(U)+K(U,T) & B(T) & -C \\ 0 & D(U)+L(T) & 0 \\ -C^T & 0 & 0 \end{bmatrix} \begin{bmatrix} U \\ T \\ P \end{bmatrix} = \begin{bmatrix} F(T) \\ G(U,T) \\ 0 \end{bmatrix} \tag{3.3.12}$$

Note U represents all components of the velocity. The advection (convection) of momentum and energy are represented by the A and D matrices, respectively. The K and L matrices represent the diffusion of momentum and energy, respectively. The mass and capacitance terms in the field equations are represented by the M and N matrices. The B matrix represents the buoyancy term for strongly coupled flows (FIDAP uses the

Boussinesq approximation). The vectors F and G are forcing functions for the system in terms of volume forces, surface forces, and viscous dissipation.

The discrete problem can be broken into two classes, steady-state and transient analyses. For steady-state analyses, the problem is a set of algebraic equations, almost always non-linear. The solution on non-linear algebraic equations can be broken into two types of solution methods, successive substitution and Newton-type solvers (see also Finlayson 1980). The Newton-type solvers include the Newton-Raphson method, a modified Newton-Raphson method, and a quasi-Newton method. In many situations, the successive substitution method will have a larger radius of convergence than the Newton-type solvers. The Newton-type solvers have the advantage of a much quicker rate of convergence. FIDAP allows the use of a combined strategy. The first few iterations can use the successive substitution method to get within the radius of convergence of the Newton-type solvers. The remaining iterations can then take advantage of the quicker convergence rate of the Newton-type solvers.

Incremental methods can also be used with the Newton-type solvers in steady-state analyses. The equations are solved in increments of some parameter so that convergence is more readily obtained. The natural parameter for fluid mechanics is the Reynolds number. FIDAP solves the equations for a small Reynolds number and uses that solution for the initial guess for a larger Reynolds number. The process is repeated until the solution at the desired Reynolds number is obtained. FIDAP also allows the incremental parameter to be a boundary condition (applied stresses or velocities).

A segregated method is also available for the solution of steady-state analyses. This method is recommended for large 2-D and 3-D, weakly-coupled simulations. With this method, the global matrix is decoupled into sub-matrix systems that require considerably less storage space. Each sub-matrix is associated with one conservation

equation (each component of momentum, mass, energy, and nodal locations for free surface analyses). The equations are then solved in a sequential manner.

Linear equations generated by these methods are solved by direct Gaussian elimination. Iterative procedures can be implemented using the segregated method.

There are two implicit methods and an explicit method for the solution of transient analyses. The explicit method uses a fixed-time step and is based on a forward Euler scheme (Gresho, *et al.* 1984). Explicit methods have the disadvantage of being conditionally stable (see also Finlayson 1992). FIDAP has two optional stabilization techniques depending on the type of instability. When using the Galerkin formulation, there are two main sources of numerical instabilities. One results from the presence of advection terms. This can result in spurious node to node oscillations in the velocity field. The stabilization technique is the addition of a streamline upwind Petrov-Galerkin term (SUPG) to the field equations. Another type of instability can be caused by an inappropriate combination of interpolation functions for the velocity and pressure discretizations. The result is oscillations in the pressure field. The stabilization technique adds a pressure stabilizing Petrov-Galerkin (PSPG) term.

Both implicit integration methods are designed for variable time stepping. The backward Euler method is a first-order accurate scheme. This method uses an explicit forward Euler scheme and a backward Euler scheme to calculate the local truncation error to estimate the next time step. The other implicit method is a second-order accurate trapezoid rule. This method uses an Adams-Bashforth predictor step with a non-dissipative completely stable trapezoid rule corrector step. Both these methods can be used with fixed time steps also. These methods use the same algebraic procedures as for the steady-state problems excluding the combined, incremental, and segregated strategies.

FIDAP can handle a variety of viscosity models including Newtonian, non-Newtonian, and viscoelastic models. Non-Newtonian models built into FIDAP include a

model for a Bingham fluid, a generalized power law relation, and a Carreau model. Also, the user can define their own non-Newtonian model using a FORTRAN subroutine. For a viscoelastic model, FIDAP represents the elastic contribution to the stress tensor using a generalized second-order fluid model. FIDAP includes a subroutine for the specification of constants for the generalized second-order fluid, however, no time dependence is allowed in the second-order model; memory effects cannot be modeled.

3.4.--Peristaltic Pumping

Peristaltic pumping is a form of fluid transport that is used by many systems in the living body to propel or mix the contents of a tube. Examples include the ureter, the gastrointestinal tract (including the pharynx and esophagus), small blood vessels, and glandular ducts. Many studies have investigated the fluid dynamics of peristaltic motion.

The most basic studies investigate the fluid dynamics in a planar channel or axisymmetric geometry with an infinite train of sinusoidal waves traveling down the channel. Typical boundary conditions include symmetry at the centerline and no-slip at the wall. The dimensionless parameters which characterize this flow are the amplitude ratio ($\phi = \varepsilon/h$), wavenumber ($\alpha = h/\lambda$), Reynolds number ($Re = ch\alpha/\nu$), and the dimensionless time-mean flow. The amplitude ratio is the ratio of the maximum amplitude of the wave, ε, to the average height of the wave, h. The wavenumber relates the average height of the wave to the wavelength, λ. The Reynolds number is a dimensionless number that relates the relative significance of inertial forces to viscous forces in the equations of motion. If the Reynolds number is greater than 1, inertial forces are more important. If the Reynolds number is less than 1, viscous forces dominate. The equations of motion are easier to solve when viscous forces dominate and the inertial terms in the equation of motion can be ignored.

Most analytical solutions assume something about the magnitude of the Reynolds number, amplitude ratio, wavenumber, or the time-mean flow. Other approaches have

been to employ asymptotic expansions around Re, α, or ϕ. Shapiro, *et al.* (1969) present the lubrication-theory model. In this model the equations are simplified by assuming inertia effects are negligible (Re = 0), and that the wavenumber is small enough ($\alpha = 0$) so that the pressure can be assumed uniform over the cross-section. The amplitude ratio (ϕ) remains arbitrary. Fung and Yih (1968) present a solution as an expansion up to second order of ϕ with Reynolds number and wavenumber arbitrary requiring the amplitude ratio to be small.

There are also many numerical investigations. Most have explored the basic fluid mechanical issues rather that describe a particular physiological flow. Takabatake and Ayukawa (1982) present a finite difference solution for general plane channel flow. Takabatake, *et al.* (1988) compare this solution with a finite difference solution for general axisymmetric flow.

Other authors have expanded on these basic models by including other effects. Examples include studies of the effect of a non-uniform tube (Gupta and Seshadri 1976), non-Newtonian fluids (Böhme and Friedrich 1983; Siddiqui, *et al.* 1991; and Siddiqui and Schwarz 1993), a peripheral layer of different viscosity (Brasseur, *et al.* 1987), and finite length tube, single-wave peristalsis, and non-integral wavenumber (Li and Brasseur 1993). This last study was to describe bolus transport in the esophageal phase of swallowing.

3.5.--Esophageal Model

Li and Brasseur published a mathematical model for the esophageal phase of the swallow in 1994. Figure 3.5.1 is a diagram of the model parameters. The Navier-Stokes equations are simplified by using the lubrication theory approximation. The lubrication theory approximation ignores the inertial terms in the equations of motion by assuming the Reynolds number can be set to zero. In order for this approximation to be valid, the

Reynolds number must be less that unity (Jaffrin 1973). The Reynolds number for peristaltic transport is defined below (Shapiro, *et al.* 1969).

$$Re = \frac{\rho c h}{\mu}\alpha \qquad (3.5.1)$$

Where ρ and μ are the bolus density and viscosity, respectively, h is the average radius of the bolus, and α is the wavenumber. Standard e·z·hd barium has a density of 1.8 g/mL and a viscosity of approximately 150-200 cP (Li, *et al.* 1992). For the cases presented with the mathematical model, bolus volumes ranged from 5 to 15 mL and occupied 1 to 20 cm of the lumen. These values result in a range of Reynolds numbers from 0.005 to 0.2. Using these values, their assumption is valid. Note, this assumption would not be valid for water for the entire range of parameters (Re = 0.55 to 16.7).

The model assumes the esophagus to be a straight distensible tube of finite length with a circular cross-section at every axial location. The barium mixture is treated as a Newtonian, incompressible fluid. Li, *et al.* (1992) has shown that the e·z·hd barium mixture is Newtonian except at shear rates less than $3s^{-1}$.

The velocity and geometry of the esophageal wall is specified at all times based on fluoroscopic data. Complete occlusion is not modeled because a mathematical singularity exists in the pressure using the lubrication theory approximation (Dusey 1993). "However, by carefully evaluating the source and magnitude of this singularity, we have learned that the singularity is mathematically 'weak' and that the lubrication theory model actually provides a good approximation of the pressures within the contractile zone. The existence of unrealistically high pressures for small occlusion, it turns out, is due to the geometrical details that are not resolved in radiographic images. Our studies indicate that in the physiological system a very thin layer of bolus fluid must exist at the tail of the bolus between the mucosa and the manometric catheter." (Li, *et al.* 1994) They model this "lubrication layer" as a certain thickness throughout the

esophagus determined by matching the results of their model with manometric data. The pressure is forced to be constant in this lubrication layer certain distances upstream (B) and downstream (A) from the bolus (see figure 3.5.1). This is "mathematically equivalent to forcing the bolus fluid velocity to zero and effectively sealing the esophageal lumen in these regions. In effect, we are replacing the manometric catheter in these regions by a column of static fluid at constant pressure, physically equivalent to sealing the tube ends by the UES and LES." The equations for the model are given below.

The Navier-Stokes equations simplify to equation (3.5.2) using the lubrication theory approximation. The simplified continuity equation is given by (3.5.3)

$$\frac{\partial P}{\partial x} = \frac{1}{r}\frac{\partial}{\partial r}\left(r\frac{\partial U}{\partial r}\right) \tag{3.5.2}$$

$$\frac{1}{r}\frac{\partial (rV)}{\partial r} + \frac{\partial U}{\partial x} = 0 \tag{3.5.3}$$

The pressure (P), x-velocity (U), y-velocity (V), the radial (r) and axial (x) directions, and time (t) are non-dimensionalized as follows.

$$x = \frac{\hat{x}}{\lambda}, \quad r = \frac{\hat{r}}{a}, \quad t = \frac{c\hat{t}}{\lambda}, \quad U = \frac{\hat{U}}{c}, \quad V = \frac{\hat{V}}{c}, \quad P = \frac{\hat{P}a^2}{\mu c \lambda} \tag{3.5.4}$$

λ is the wavelength, a is the average radius, c is the peristaltic velocity, and μ is the viscosity. The boundary conditions are listed below.

$$U|_{r=H} = 0, \quad V|_{r=H} = \frac{\partial H}{\partial t}; \quad \left.\frac{\partial U}{\partial r}\right|_{r=0} = 0, \quad V|_{r=0} = 0 \tag{3.5.5}$$

$$P|_{x \le x_a} = P_a, \quad P|_{x \ge x_b} = P_b \tag{3.5.6}$$

Integration of the equations give expressions for the velocity.

$$U = \frac{1}{4}\frac{\partial P}{\partial x}\left(r^2 - H^2\right) \tag{3.5.7}$$

$$V = \frac{r}{4}\left[H\frac{\partial H}{\partial x}\frac{\partial P}{\partial x} - \frac{\partial^2 P}{\partial x^2}\left(\frac{1}{4}r^2 - \frac{1}{2}H^2\right)\right] \tag{3.5.8}$$

Evaluating (3.5.8) at r = H results in an expression relating the wall motion to the pressure gradient.

$$\frac{H^3}{16}\frac{\partial^2 P}{\partial x^2} + \frac{H^2}{4}\frac{\partial H}{\partial x}\frac{\partial P}{\partial x} = \frac{\partial H}{\partial t} \tag{3.5.9}$$

The shape of the bolus is shown in figure 3.5.1 and is defined by the following equations.

$$H(x,t) = \varepsilon + 0.5A\left[1 - \cos 2\pi\left(x - x_0\right)/\lambda_t\right] \qquad \text{for } x_0 \le x \le x_1 \tag{3.5.10}$$

$$H(x,t) = \varepsilon + A \qquad \text{for } x_1 < x < x_2 \tag{3.5.11}$$

$$H(x,t) = \varepsilon + 0.5A\left[\cos 2\pi\left(x - x_3\right)/\lambda_h\right] \qquad \text{for } x_2 \le x \le x_3 \tag{3.5.12}$$

x_1, x_2, and x_3 are defined below.

$$\begin{aligned} x_1 &= x_0 + 0.5\lambda_t \\ x_2 &= x_1 + \lambda_m \\ x_3 &= x_2 + 0.5\lambda_h \end{aligned} \tag{3.5.13}$$

x_0, λ_t, λ_h, and λ_m are functions of time found from videofluoroscopic data. The amplitude, A, is also a function of time chosen to conserve volume.

The resulting equation for the pressure profile is given by equation (3.5.14).

$$P(x,t) = P_a + \int_{x_a}^{x}\frac{G_a}{H^4}dx + \int_{x_a}^{x}\frac{16}{H^4}\left(\int_{x_a}^{x} H\frac{\partial H}{\partial t}dx\right)dx \tag{3.5.14}$$

G_a is given by equation (3.5.15).

$$G_a = \frac{P_b - P_a - 16\int_{x_a}^{x_b}\frac{1}{H^4}\left(\int_{x_a}^{x_b} H\frac{\partial H}{\partial t}dx\right)dx}{\int_{x_a}^{x_b}\frac{1}{H^4}dx} \tag{3.5.15}$$

These equations were solved by integrating numerically using a Simpson's method with second-order accuracy. The derivatives were evaluated analytically. Further mathematical details can be found in Li, *et al.* (1994) and in Li and Brasseur (1993).

This model was tested with manometric and fluoroscopic data provided by Kahrilas, *et al.* (1988) for 4 case studies. The most significant result of the model was the prediction of two separate peristaltic waves within the esophagus. The only way to match both the manometric and videofluoroscopic data for a case where bolus retention was simulated was to assume two separate peristaltic waves, one distal to the aortic arch and one proximal. They support this observation by noting the existence of two types of muscle within the esophagus; striated muscle proximal to the aortic arch and smooth muscle distal to the aortic arch. Figure 3.5.2 compares the measured data with the simulated data.

For the parameters used in the above model, the lubrication theory approximation is a valid modeling technique. Chapter 4 demonstrates why this technique is not applicable to the pharyngeal phase of swallowing. Many of the features of this model, however, can be used to interpret modeling of the pharyngeal phase of swallowing.

3.6.--Squeezing Flow

Due to the complete closure of the pharyngeal lumen behind the bolus, flow through the pharynx can be characterized as squeezing flow. Many solutions of squeezing flow situations exist in the literature, most commonly pertaining to viscometry (see McClelland and Finlayson (1983), McClelland and Finlayson (1988), and Bird, *et al.* (1987). Developed here is an analytical solution for squeezing flow in cartesian geometry to compare with the model in the pharynx.

The problem is simplified by ignoring inertial effects, assuming incompressible, laminar flow, and applying the lubrication approximation. Figure 3.6.1 is a graphical

representation of the model. With these assumptions, the continuity equation and equation of motion simplify to (3.6.1) and (3.6.2), respectively.

$$\frac{\partial v_x}{\partial x} + \frac{\partial v_y}{\partial y} = 0 \tag{3.6.1}$$

$$0 = -\frac{dP}{dy} + \mu\left[\frac{\partial^2 v_x}{\partial x^2}\right] \tag{3.6.2}$$

These equations are solved with the following boundary conditions.

$$v_x\big|_{x=0} = 0 \tag{3.6.3}$$

$$v_x\big|_{x=h} = V_w \tag{3.6.4}$$

$$v_y\big|_{x=h} = 0 \tag{3.6.5}$$

$$v_y\big|_{y=0} = 0 \tag{3.6.6}$$

$$\left.\frac{\partial v_y}{\partial x}\right|_{x=0} = 0 \tag{3.6.7}$$

Integrating continuity applying (3.6.4) gives

$$V_w L + \int_0^h v_y dx = 0. \tag{3.6.8}$$

Integrating the equation of motion invoking (3.6.5) and (3.6.7) gives equation (3.6.9).

$$v_y = \frac{h^2}{2\mu}\left(-\frac{dP}{dy}\right)\left[1 - \left(\frac{x}{h}\right)^2\right] \tag{3.6.9}$$

Combining and integrating (3.6.8) and (3.6.9) specifying $P = P_a$ at $y = L$ gives

$$P - P_a = -\frac{3\mu V_w L^2}{2h^2}\left[1 - \left(\frac{y}{L}\right)^2\right]. \tag{3.6.10}$$

Substituting (3.6.10) into (3.6.9) gives an expression for v_y.

$$v_y = -\frac{3V_w y}{2h}\left[1-\left(\frac{x}{h}\right)^2\right] \tag{3.6.11}$$

To analyze the forces at the wall, the stress tensor is integrated over the area.

$$F = \int_A \sigma_{ij} dA \tag{3.6.12}$$

The stress tensor is given in (3.6.13).

$$\sigma_{ij} = P\delta_{ij} + \tau_{ij} \tag{3.6.13}$$

The normal component of the stress tensor reduces to equation (3.6.14) invoking continuity.

$$\tau_{xx} = -2\mu\frac{\partial v_x}{\partial x} = 2\mu\frac{\partial v_y}{\partial y} \tag{3.6.14}$$

Substituting (2.6.6) and integrating gives the normal force at the wall.

$$F_n\big|_{x=h} = -\frac{\mu V_w L^3}{h^3} \tag{3.6.15}$$

The tangential component of the stress tensor reduces to equation (3.6.16).

$$\tau_{yx} = -\mu\frac{\partial v_y}{\partial x} \tag{3.6.16}$$

Substituting (3.6.11) and integrating gives the tangential force at the wall.

$$F_t\big|_{x=h} = -\frac{3\mu V_w L^2}{2h^2} \tag{3.6.17}$$

Note that the forces at the wall are directly proportional to the viscosity and inversely proportional to the separation cubed for the normal force, squared for the tangential force.

3.7.--Physical Properties

Physical properties are needed to develop an accurate model of swallowing. The correct viscosity and density are needed for the model. The viscosity of the fluid being swallowed may or may not be easily described mathematically. If the viscosity is not a function of the rate of deformation tensor, the Navier-Stokes equations can be used to

model the fluid dynamics. If the viscosity is dependent on the rate of deformation tensor, an appropriate constitutive relation must be chosen to use with the equations of motion. Details on which constitutive relations are available for use are given in section 3.3. Since most of the data for the model will be taken from videofluoroscopic images, knowledge of the properties of barium sulfate mixtures is needed. Li, *et al.* (1992) studied the properties of various mixtures of barium sulfate using a Brookfield LVT 1115/60 concentric cylinder viscometer. The authors developed their own method for estimating the viscosity from their experimental data by deriving a relation for shear rate as a function of angular velocity assuming power law behavior. The experimental data was fit to an equation of the form shown below.

$$\mu = \mu_0 + c_0 e^{c_1 S^k} \tag{3.7.1}$$

The results for the standard mixture of e·z·hd barium sulfate (250% w/v) is given in equation (3.7.2).

$$\mu = 145 + 200e^{-1.85S^{0.6}} \pm 37 \quad \text{cP} \tag{3.7.2}$$

An equation for a diluted mixture of liquid e·z·paque (40% w/v) is given below.

$$\mu = 254 + 2530e^{-1.92S^{0.6}} \pm 83 \quad \text{cP} \tag{3.7.3}$$

Equations for mixtures of Knott's strawberry syrup mixed in different proportions with e·z·hd powder are also provided in Li, *et al.* (1992).

The rheological properties of foods have been reported extensively in the literature (Rao and Rizvi 1986; Peleg and Bagley 1983; and Jowitt, *et al.* 1987). Fluid foods exhibit a variety of rheological characteristics including Newtonian, shear thinning and thickening, thixotropic, and viscoelastic. There are no reports of rheopectic foods (Rao and Rizvi 1986). Steffe, *et al.* (1983) compiled power law data for a variety of liquid foods. Kokini and Dickie (1981) have modeled transient viscoelastic flow in foods. Rao and Rizvi (1986) review the literature encompassing all types of rheological

characteristics for liquid foods. The viscosity of saliva is about 50 mPa·s (de Bruijne, *et al.* 1993). Viscoelastic properties of saliva are reported by Van Der Reijden, *et al.* (1993). No rheological data has been reported for masticated foods to date (Steffe 1994).

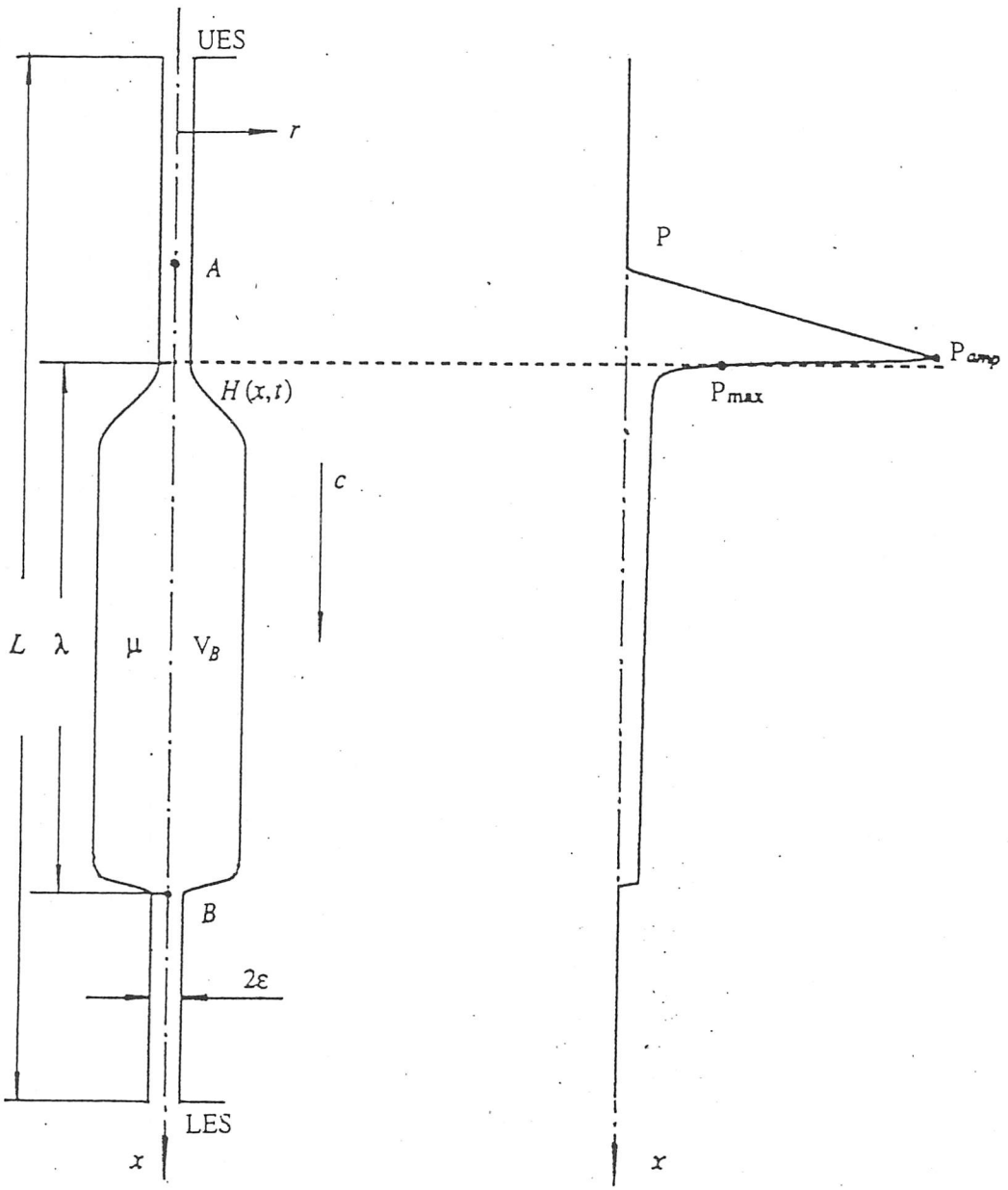

Figure 3.5.1.--Esophageal model diagram. (from Li, *et al.* 1994)

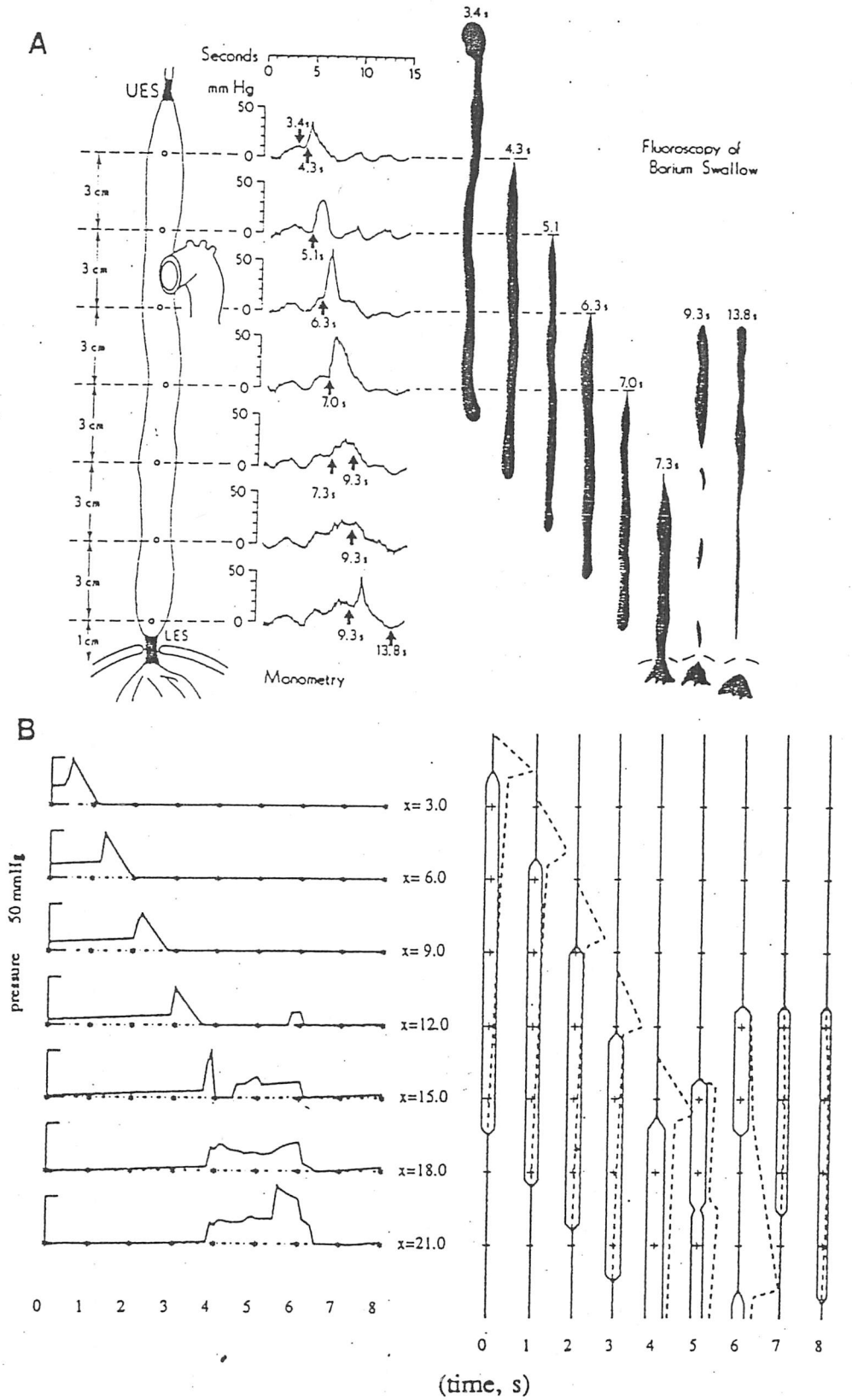

Figure 3.5.2.--Results from Li, *et al.* (1994) simulation of failed peristalsis in the esophagus compared with measured data.

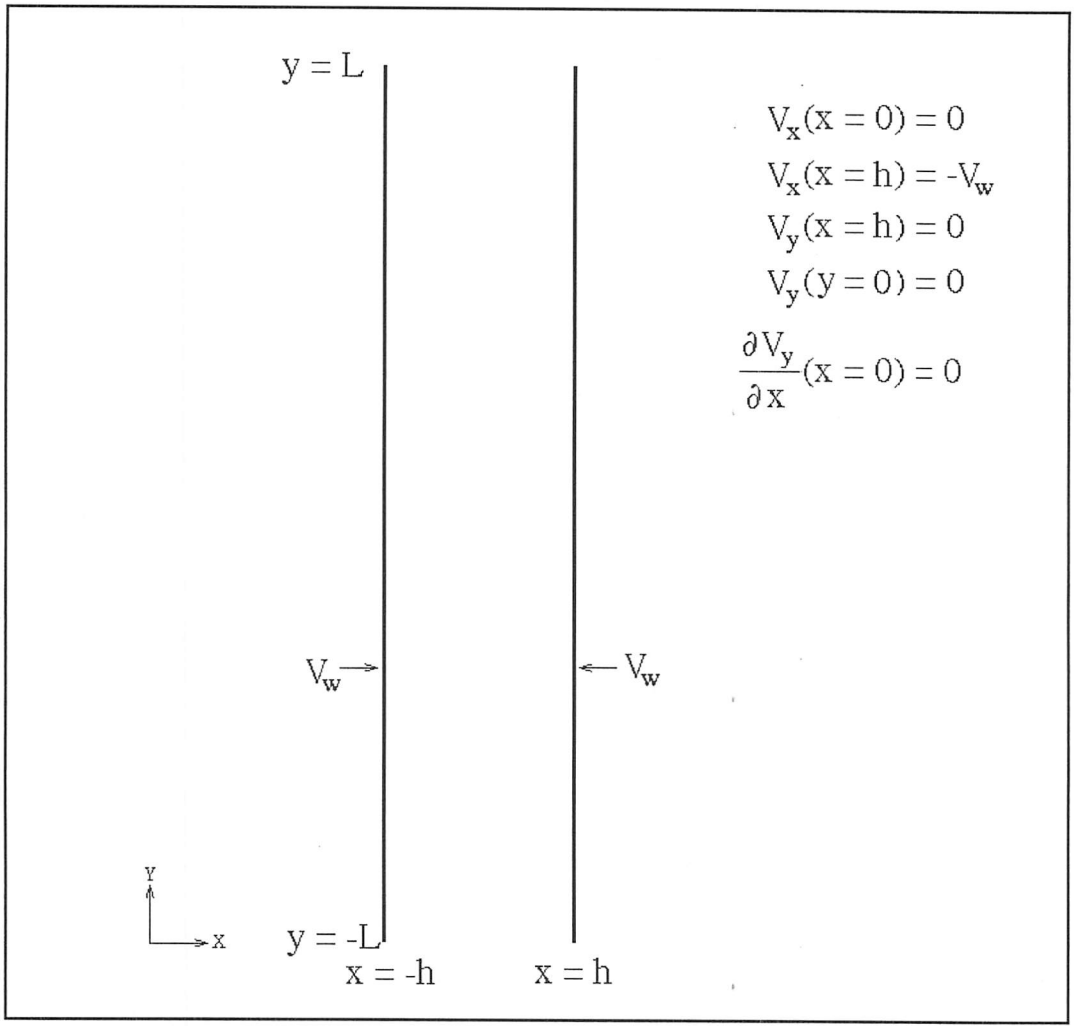

Figure 3.6.1.--Squeezing flow model diagram.

CHAPTER 4.--THE PRELIMINARY MODEL

4.1.--Introduction

Developing a generic model for the pharyngeal phase of deglutition is a very complex task. There are a great number of variables involved in the swallowing process. Many questions must be answered before the problem can be approached. First, what is being swallowed must be defined. The bolus could be a liquid, or a combination of a solid and a liquid. Once the bolus is defined, the physical properties of the bolus must be determined. Other questions involve where the bolus goes after leaving the mouth. The goal, of course, is to have the bolus transported safely to the esophagus. Other possibilities include transport to the nasopharynx , the larynx, the esophagus, or any combination of these. Part of the bolus could also remain in the mouth. In order to model such a complex process, it is often advantageous to reduce the problem to one that can be solved more readily than the complete process. This often provides insight into the more complicated problem. In this chapter, a preliminary model is generated to provide insight into what should be included in the next phase of the modeling.

4.2.--Preliminary Model

A good model for the transport of a liquid bolus from the mouth to the esophagus needs to incorporate the changing geometry of the pharynx. A model of the esophageal phase of swallowing accomplished this by assuming a certain shape of the bolus that remains constant throughout the esophagus. This assumption is acceptable in the esophagus since the geometry of the esophagus is simple; at rest, the diameter is the same at every length. While distended, the radius is also constant over the majority of the wavelength. This is not true in the pharynx. The best description of the shape of any cross-section of the pharynx is ellipsoidal. While the bolus is passing, at any length, the magnitude of either semi-axis changes rapidly with time. Kahrilas, *et al.* (1993) and

Cook, *et al.* (1989) have digitized data from bi-planar fluoroscopy studies to determine the shape of the pharynx at various locations as a function of time. Their interpolated data are shown in figure 4.2.1. The lengths noted on these graphs are shown in figure 4.2.2. The shapes of these curves vary significantly between lengths of the pharynx thus, an algebraic expression for a simple wave form cannot be accurately derived. This is where using the finite element method is advantageous. The motion of the nodes on the boundary between the bolus and the wall of the pharynx can be prescribed as a function of time. This is what is done in the preliminary model.

4.2.1.--Setup

Figure 4.2.2 is a diagram of the finite element mesh set up for the preliminary model of the pharynx. The geometry is assumed axi-symmetric with the cross-sectional area of the cylinder at any length equal to the cross-sectional area of the ellipse from the literature values. The area included in the model extends from the glossopalatal junction (GPJ) to the upper esophageal sphincter (UES). The distance between these two locations is chosen as 5 cm. This length assumes laryngeal elevation and pharyngeal shortening have completed before the initiation of the swallow. The position of the nodes on the wall boundary are at the time when the bolus is held in the mouth prior to the initiation of the oral phase. At this time, the glossopalatal junction and the UES are closed. Complete closure of any portion of the pharynx cannot be modeled; the mesh cannot collapse onto itself. The minimum radius corresponding to complete closure is chosen as 1 mm. This value can be changed in order to obtain different pressure profiles. A similar procedure was used by Li, *et al.* (1994) in their model of the esophagus.

The position of the nodes on the wall boundary are taken from literature sources for a 20 mL bolus at 4 locations shown in figure 4.2.2. The data for the UES correspond to exit of the UES. The geometry at the beginning of the UES is taken as the same as the exit, but the wall movement is started at a earlier time. This shift in time is determined

by using a velocity found by integrating the cross-sectional area at the exit over time and dividing this result into the volume of the bolus. This gives a velocity of 18.4 cm/s. Since the length of the UES is 1 cm, the shift in time is 0.0542 s. Data for the entire lumen are determined using a b-spline interpolation through these 5 data points.

A FORTRAN program interpolates the data to give cross-sectional area as a function of length at 5 ms increments in time. These data are again interpolated over the length to give the geometry at increments of 0.125 cm. This is the spacing between the nodes on the finite element mesh. The FORTRAN program calculates the velocity of the nodes at each time using three-point differentiation formulas accurate to $O(\Delta x^2)$ (Burden and Faires 1989). This information is written to a file in a format readable by FIDAP. FIDAP determines the velocity of the nodes on the surface at any time by linear interpolation within this table. FIDAP also calculates the displacement of these nodes from the velocities. Thus, the more detailed the table, the more accurate and smooth the solution.

The boundary conditions are also outlined in figure 4.2.2. A symmetry condition is applied at the centerline. The radial velocity of the nodes on the wall is prescribed as discussed above. The axial velocity of the nodes on the wall was zero (no-slip).

During the time 0 to 0.32 s, the glossopalatal junction is opening. The maximum opening is reached at 0.32 s. The glossopalatal reaches the minimum diameter again at 0.54 s. The GPJ remains closed during the rest of the simulation. The stress normal to the inlet is initially set at 30,000 dyne/cm^2 and is reduce linearly to zero at time 0.32 s (flux boundary condition). This is the oral phase of the swallow. The bolus is being transported from the mouth to the pharynx. If it is assumed that there is a constant force pushing the bolus through the GPJ, the normal stress should decrease over this time since the cross-sectional area is increasing. From time 0.32 to 0.54, the normal stress remains

zero (free boundary condition). From time 0.54 s to 1.08 s, the axial velocity is set to zero (no flow boundary condition).

From time 0 to 0.33 s, the UES is closed. It begins to open at 0.33 s and reaches the maximum opening at 0.6 s. The UES is closed again when the bolus has passed into the esophagus at time 1.04 s. The axial velocity at the outlet is zero from time 0 to 0.33 s (no flow). The UES opens at time 0.33 s. From time 0.33 to the end of the solution, the normal stress is zero at the outlet (free).

4.2.2.--Viscosity Models

As mentioned in chapter 2, the properties of the fluid can affect the geometry of the bolus during the swallow. The geometry information was obtained from two different sources that used different barium sulfate suspensions. In order to best represent what was measured in the fluoroscopy studies, the properties for the two common solutions used in these studies were used in the simulations. The two common liquids modeled are e·z·hd (250% w/v) and e·z·paque (40% w/v). Simulations were run assuming both Newtonian and non-Newtonian behavior. The shear thinning behavior given in equations (3.7.2) and (3.7.3) is fit to a model supported by FIDAP. The model supported by FIDAP that best fit the data given by equations (3.7.2) and (3.7.3) is a Carreau model shown in equation (4.2.1) (FDI 1993).

$$\mu = \mu_\infty + (\mu_0 - \mu_\infty)\left(1 + K^2 D^2\right)^{(n-1)/2} \qquad (4.2.1)$$

From equation (3.7.2), μ_0 and μ_∞ are 345 and 145 cP respectively. D is the shear rate (first invariant of the rate of deformation tensor) and is calculated by FIDAP. The parameters K and n are 8.286 s and 0.0102, respectively. These parameters were found using a least squares fit. The difference in viscosity between the two models was less than the error given for equation (3.7.2). For equation (3.7.3) μ_0 and μ_∞ are 2784 and 254 cP, K and n are 19.74 s and 0.5058, respectively.

4.2.3.--Inertial Effects

The importance of inertial effects is investigated with the preliminary model. The importance of inertial effects can be estimated by calculating the Reynolds number. As mentioned in chapter 3, if the Reynolds number for peristalsis is less than 1, the inertial terms in the equation of motion can be neglected. Since the wave form for peristalsis in the pharynx is variable, it is difficult to calculate a Reynolds number defined by equation (3.5.1). Time averaging the cross-sectional areas at various locations in the pharynx results in average radii of about 2.0 cm at the tongue base and the level of the valleculae. For a 20 mL bolus, and assuming cylindrical geometry, this gives a peristaltic wavelength of approximately 6.4 cm. The velocity of lumenal closure in the pharynx measured from fluoroscopy studies (Kahrilas, *et al.* 1988) is approximately 15 cm/s. As mentioned in chapter 3, the density and viscosity (constant at shear rates greater than 3 s^{-1}) for e·z·hd barium sulfate suspension is 1.8 g/cm^3 and 1.45 g/cm·s, respectively. Using these parameters and equation (3.5.1), the Reynolds number is approximately 12, thus inertial effects may be important.

4.2.4.--Results

The purpose of this current model is to demonstrate the ability to model swallowing in the pharynx using a boundary with a prescribed motion. The wall movement over the course of the swallow is shown in figure 4.2.3. In reality, the pharynx re-opens after the peristaltic closure wave has passed. This is not seen because the mesh represents the bolus, not the pharynx. No bolus is present in the pharynx after the peristaltic wave has passed for a normal swallow.

For the e·z·hd (250% w/v) liquid, the results for the Newtonian and Carreau models did not differ significantly. Some differences can be seen for the e·z·paque liquid. Figure 4.2.4 shows contour plots of the axial component of velocity at the point of maximum opening of the GPJ. The difference is most dramatic near the centerline. This is to be expected since the shear rate is a minimum at the centerline. To further

demonstrate this observation, figure 4.2.5 presents a contour plot of the value of the non-Newtonian viscosity at the same point in time .

Figure 4.2.6 is a time history comparison of the pressures at a node on the centerline of the UES for the Newtonian and Carreau model. The pressure tracings do not vary in form, but the magnitudes are slightly different, especially at transition times. The pressure tracings shown should not look like those measured with manometry. With manometry, both the fluid pressure and the contact pressure are measured. Here, only the fluid pressures can be reported because the fluid is being modeled, not the pharyngeal walls. Also, in manometry, the presence of the catheter disrupts the flow. A symmetry boundary condition is used at the centerline in the simulations. A no-slip boundary condition should be used to model the presence of the catheter.

Figure 4.2.7 demonstrates the difference between the simulations, with and without inertial effects. Including the inertial terms in the equation of motion has a noticeable effect on the magnitude of the axial component of the velocity. Without inertial effects, the minimum and maximum axial velocities are -6.8 cm/s and 26.5 cm/s. For the simulation including inertial effects, the minimum velocity is increased to -4.8 cm/s while the maximum velocity is decreased to 23.1 cm/s.

Figure 4.2.8 is a plot of the volumetric flow rate and the cumulative volume through the UES. A total of 18 mL of fluid passes through the UES. The geometry used for this model represents a bolus size of 20 mL. This is relatively good agreement considering the volumetric flow was not specified in this model. Also note that the maximum volumetric flow rate corresponds to maximal UES opening. A negative flow is observed when the UES initially opens. This phenomenon, called reflux, is expected in fluid dynamic models of peristaltic flow when the local radius is small. This does not occur in reality because no fluid is present in the esophagus to transport back into the

pharynx. It may be possible to reduce this effect by changing the boundary condition at this location.

4.3.--Summary

This model needs to be greatly improved in order to accurately model the pharyngeal phase of swallowing. As with most models, the key is choosing boundary conditions that best represent reality. The motion of the wall needs to be accurately represented and the inlet and outlet boundary conditions need further study. The model presented in the next chapter will address these issues.

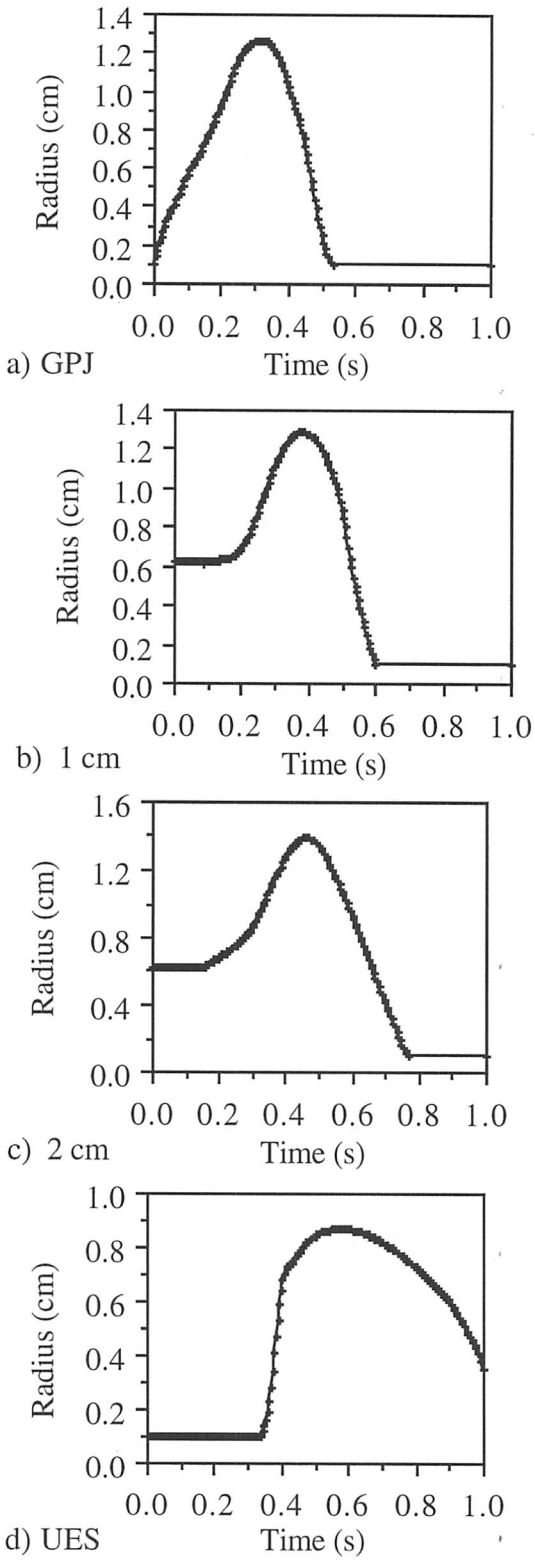

Figure 4.2.1.--B-spline data for the location of the fluid-solid interface assuming a cylindrical geometry. Data from Kahrilas, *et al.* (1993) and Cook, *et al.* (1989)

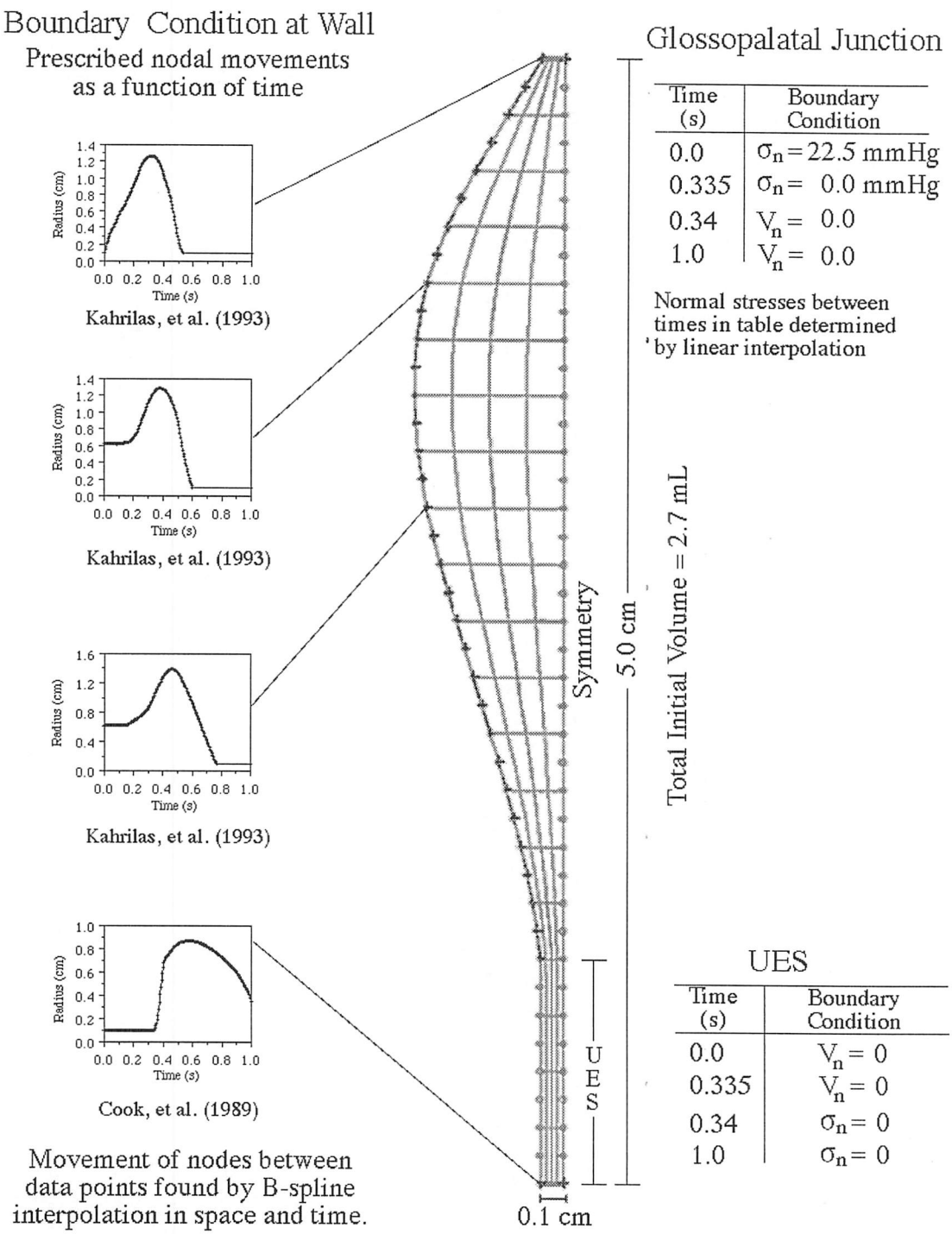

Figure 4.2.2.--Preliminary model.

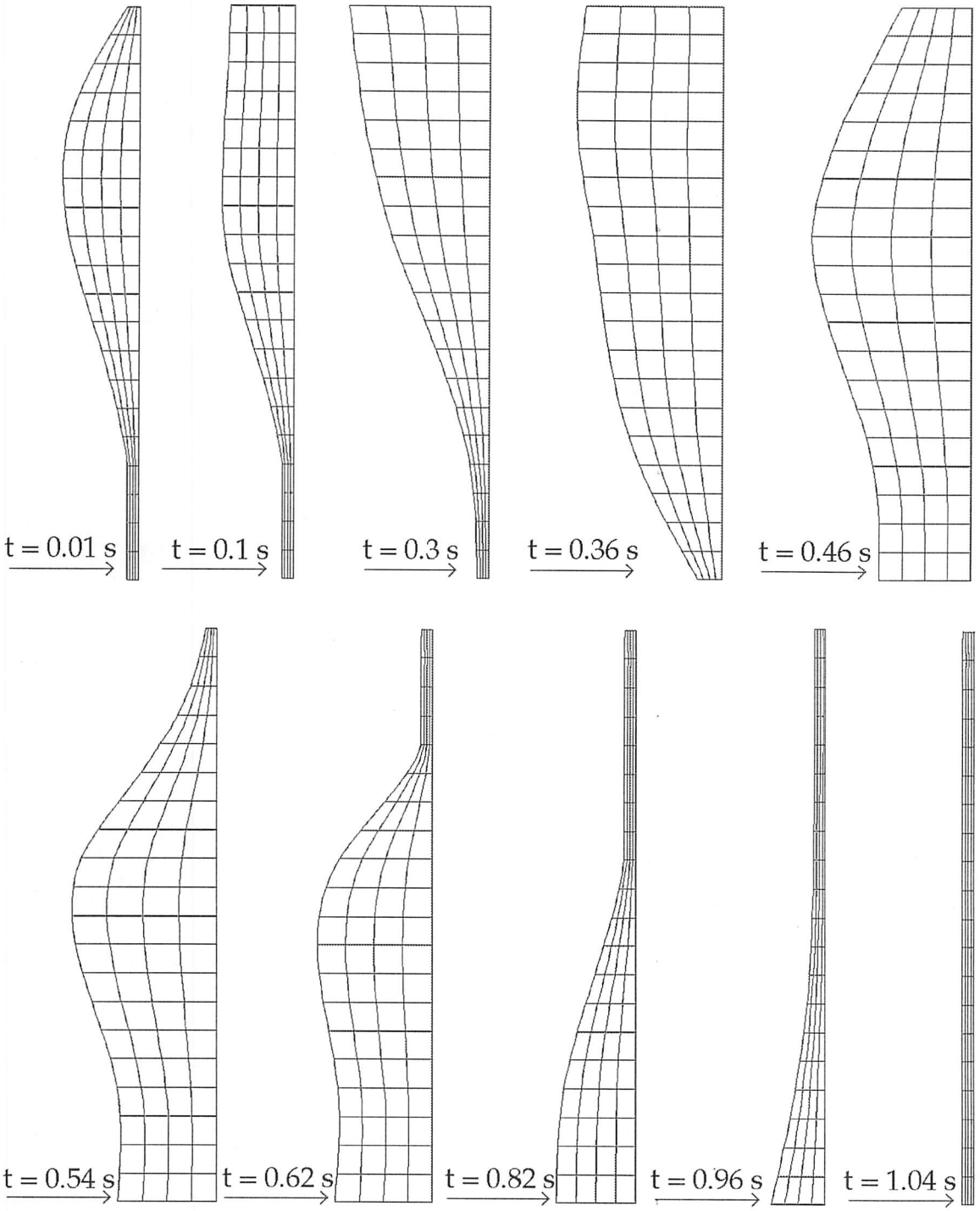

Figure 4.2.3.--Finite element mesh representing the geometry of the pharyngeal chamber at various time steps.

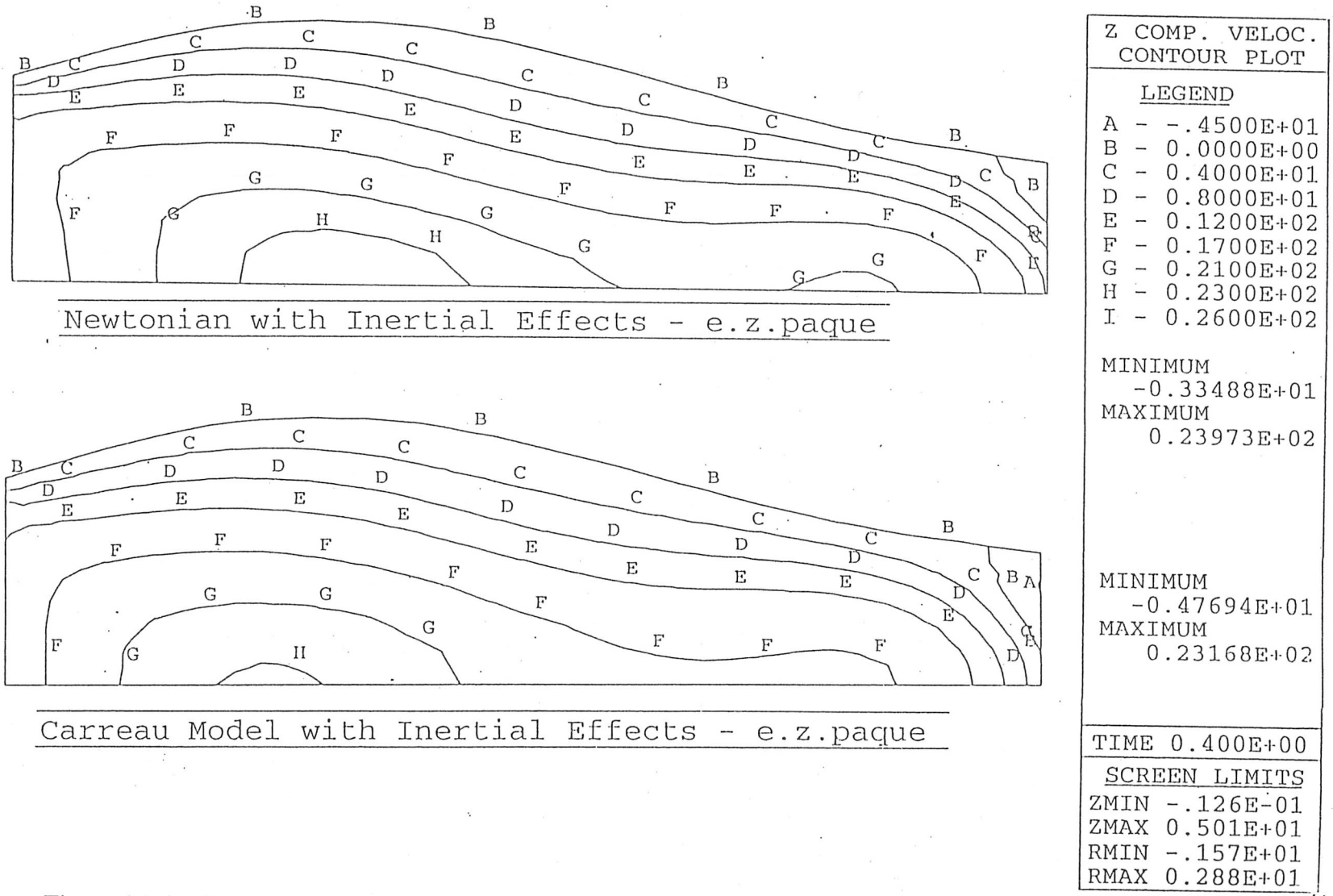

Figure 4.2.4.--Contours of the axial component of velocity comparing the Newtonian and Carreau models.

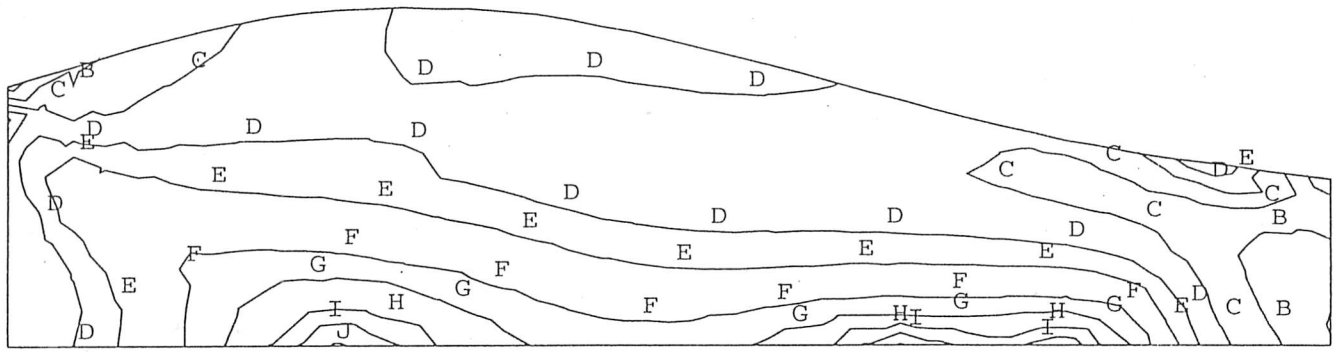

NON-NEWT. VISC
CONTOUR PLOT

LEGEND

A - 0.3200E+01
B - 0.3400E+01
C - 0.3600E+01
D - 0.3800E+01
E - 0.4000E+01
F - 0.4500E+01
G - 0.5000E+01
H - 0.6000E+01
I - 0.7000E+01
J - 0.8300E+01

MINIMUM
0.31161E+01
MAXIMUM
0.85637E+01

TIME 0.400E+00

Figure 4.2.5.--Contours of the viscosity in the Carreau model.

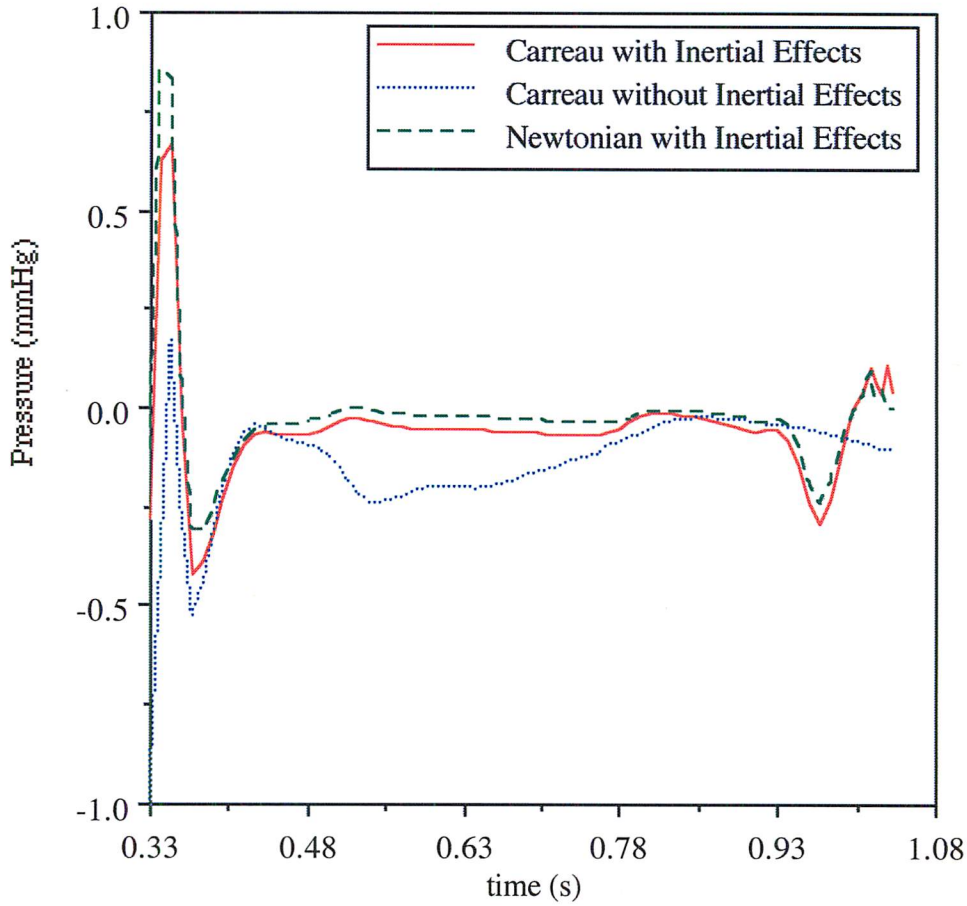

Figure 4.2.6.--Pressure histories at the UES.

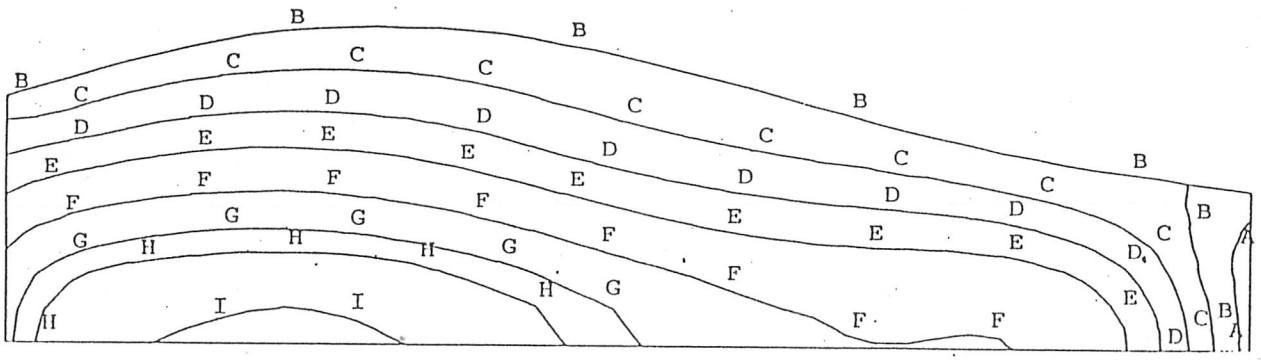

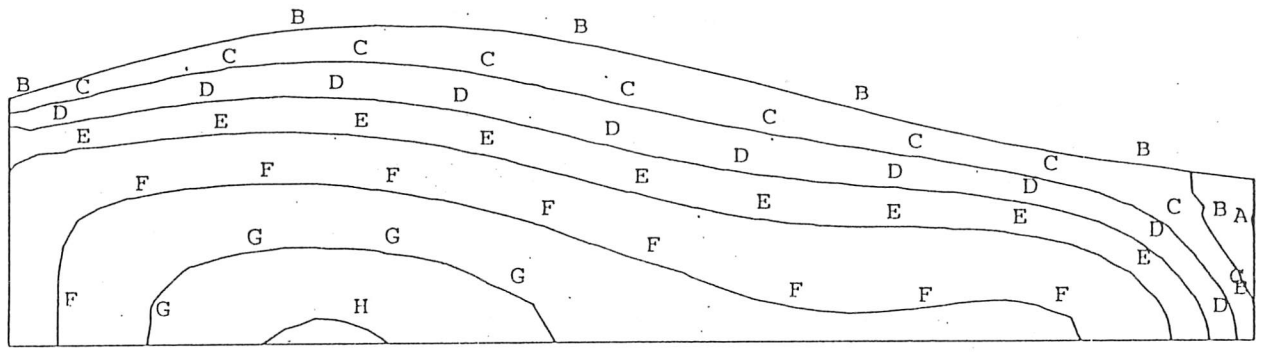

Z COMP. VELOC.
CONTOUR PLOT

LEGEND

A - -.4500E+01
B - 0.0000E+00
C - 0.4000E+01
D - 0.8000E+01
E - 0.1200E+02
F - 0.1700E+02
G - 0.2100E+02
H - 0.2300E+02
I - 0.2600E+02

MINIMUM
-0.68016E+01
MAXIMUM
0.26447E+02

MINIMUM
-0.47694E+01
MAXIMUM
0.23168E+02

TIME 0.400E+00

SCREEN LIMITS
ZMIN -.126E-01
ZMAX 0.501E+01
RMIN -.157E+01
RMAX 0.288E+01

Figure 4.2.7.--Contours of the axial component of velocity demonstrating the effect of including the inertial terms in the equations of motion.

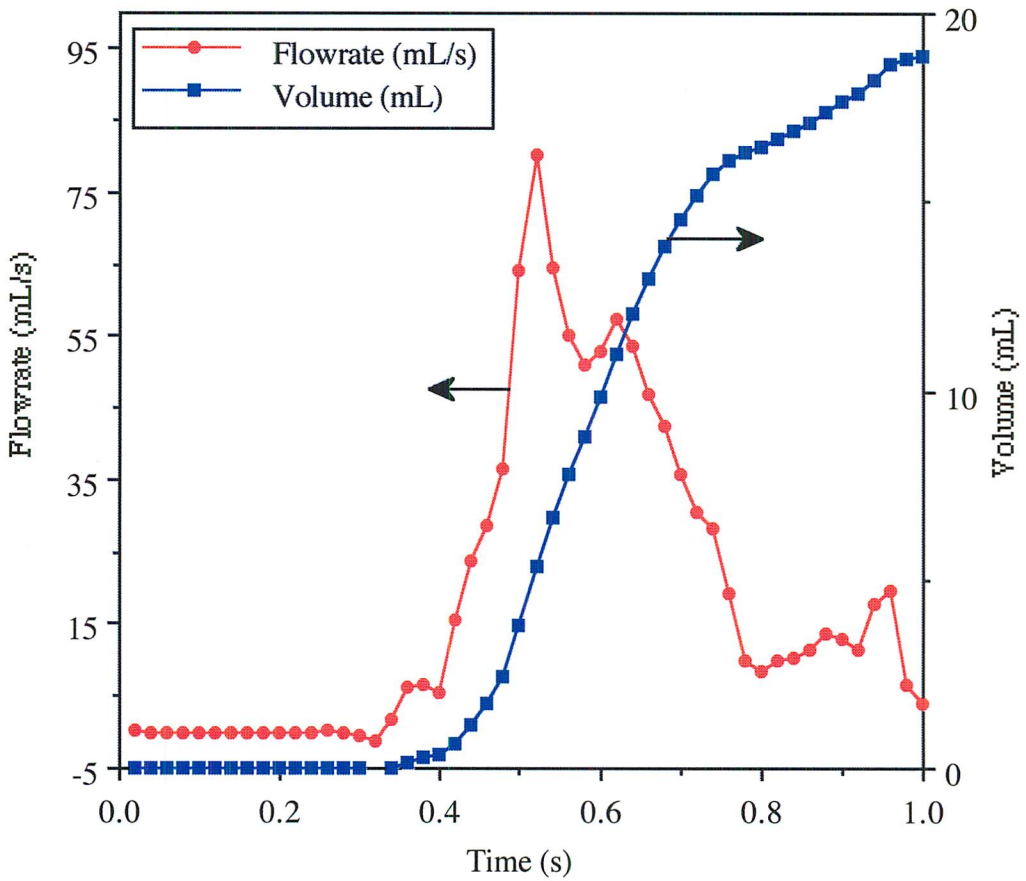

Figure 4.2.8.--Bolus transport through the UES.

CHAPTER 5.--THE MODEL

5.1.--Introduction

A two-dimensional, planar geometry in the anterior-posterior (AP) direction as seen from the lateral view of fluoroscopic images was chosen to model the pharyngeal phase of swallowing. From this view, it is possible to see the independent movements of the soft palate and the tongue base, the elevation of the larynx and UES, and the constriction of the pharyngeal muscles. The entrance to the larynx can also be included in the model. The lateral dimension, as seen from the AP view of fluoroscopic images, details only the symmetrical movement of the phayrngeal muscle with no detailed information about the movements of the other structures.

The two-dimensional, planar model is an improvement on the axi-symmetric model, like the preliminary model, because it is possible to differentiate between the various structures in the pharynx described above. The pharyngeal chamber has a very complex, three-dimensional geometry, thus, a three-dimensional model would give the most accurate information. This was not attempted for many reasons. Two-dimensional models generally provide adequate information to understand the basic physics of a flow situation. This is well demonstrated in a study by Takabatake, *et al.* (1988). They model peristaltic flow with a simple wave form for both two-dimensional, planar geometry and cylindrical geometry. They find the results are qualitatively similar between the two geometries.

To have an accurate representation of the three-dimensional geometry of the pharynx, imaging data of the cross-section of the pharynx at various levels would be required. Ultra-fast CT scans would be one way of obtaining these data (Kahrilas, *et al.* 1993). This information was not accessible. Another option would be to combine data from both the lateral and AP views from fluoroscopy. An elliptical geometry could be

assumed and these data could be interpolated around the cross-section based on data from 4 points. The gain in quantitative information from this model would be questionable with an assumption of this magnitude.

One of the goals of this project is to have a model that is relatively easy to use. The amount of image analysis required for a three-dimensional model would be at least double that of the two-dimensional model. The amount of computer time required to solve the model would increase by at least an order of magnitude. Currently, the two-dimensional model requires an minimum of 20 hours to obtain the data, analyze the data, and solve. The time for the three-dimensional model would be substantially greater. Using the current techniques, the gain in quantitative information from a full, three-dimensional model would not be worth the time investment required to generate it.

The two-dimensional, planar model can be represented with a simplified version of the continuity equation and the equations of motion presented in chapter 3. Section 5.2 will detail these equations. An appropriate constitutive model needs to be chosen in order to solve the equation of motion. Section 5.3 discusses the choice of Newton's Law. Initial and boundary conditions need to be assigned in order to solve these equations. Section 5.4 presents these conditions and how the equations are solved. The model assumptions are summarized in section 5.5.

5.2.--The Equations for a Two-Dimensional, Planar Geometry

The equations of motion are simplified by defining and making assumption about our flow situation. Choosing a two-dimensional representation in a planar geometry eliminates any dependence in the z-direction. It is also assumed that the fluid is incompressible. With these assumptions, the equation of continuity can be reduced to the equation below.

$$\frac{\partial v_x}{\partial x} + \frac{\partial v_y}{\partial y} = 0 \qquad (5.2.1)$$

For the two-dimensional, planar geometry, the z-component of the equations of motion can be eliminated. The z dependence in the x- and y-components can also be eliminated. The simplified equation for the x-component is given by equation (5.2.2) and the y-component is given by (5.2.3).

$$\rho\left(\frac{\partial v_x}{\partial t}+v_x\frac{\partial v_x}{\partial x}+v_y\frac{\partial v_x}{\partial y}\right)=-\frac{\partial p}{\partial x}-\left(\frac{\partial \tau_{xx}}{\partial x}+\frac{\partial \tau_{yx}}{\partial y}\right)+\rho g_x \qquad (5.2.2)$$

$$\rho\left(\frac{\partial v_y}{\partial t}+v_x\frac{\partial v_y}{\partial x}+v_y\frac{\partial v_y}{\partial y}\right)=-\frac{\partial p}{\partial y}-\left(\frac{\partial \tau_{xy}}{\partial x}+\frac{\partial \tau_{yy}}{\partial y}\right)+\rho g_y \qquad (5.2.3)$$

Recall that:

v_x = the velocity in the x-direction,

v_y = the velocity in the y-direction,

ρ = the density,

p = the pressure,

τ_{xx} = the normal stress exerted on a surface of constant x,

τ_{yx} = the shear stress exerted in the x-direction on a surface of constant y,

τ_{yy} = the normal stress exerted on a surface of constant y,

τ_{xy} = the shear stress exerted in the y-direction on a surface of constant x.

In order to solve these equations, an expression that describes the relationship between the stresses and the velocity gradients is needed.

5.3.--Newton's Law

Newton's Law has been chosen as the constitutive relation based on results from the preliminary model and from experimental measurements. From the preliminary model, it was found that using the Carreau model for the low-viscosity sample had an insignificant effect on the solution (see section 4.2). Experimental measurements show that the variation in viscosity between studies is greater that the variation with shear rate. Experimental results for the fluid properties can be found in section 6.2.

For two-dimensional, rectangular coordinates, Newton's Law can be written as shown in equations (5.3.1-5.3.3).

$$\tau_{xx} = -2\mu \frac{\partial v_x}{\partial x} \tag{5.3.1}$$

$$\tau_{yy} = -2\mu \frac{\partial v_y}{\partial y} \tag{5.3.2}$$

$$\tau_{xy} = \tau_{yx} = -\mu \left[\frac{\partial v_x}{\partial y} + \frac{\partial v_y}{\partial x} \right] \tag{5.3.3}$$

Simply, these equations say that the shear rate is directly proportional to the rate of deformation tensor. The constant of proportionality is the viscosity. For our model, the viscosity is assumed to be constant.

Substitution of the above into (5.2.2) and (5.2.3) gives the two-dimensional Navier-Stokes equations in rectangular coordinates. These are the equations the CFD software package, FIDAP, is directed to solve, provided with appropriate initial and boundary conditions.

5.4.--Solution Method

The simulation of the fluid bolus passing through the pharynx can be broken into two phases. The first phase is where the bolus is filling the pharyngeal cavity, before the UES opens. This phase ends when all boundaries of the bolus are in contact with the walls of the pharyngeal chamber. Whether the edges of the bolus are in contact with air or the pharyngeal chamber walls makes a difference in the type of solution method employed. Because of this, the model has been separated into two simulations, the first is known as a filling simulation, the second is known as a moving boundary simulation.

5.4.1.--Filling Simulation

The filling simulation employs a solution method known as the volume-of-fluid method. This method allows a region to be meshed that is not initially occupied by fluid. This region can then be filled with fluid. Details of how the position of the moving front

of the fluid is updated can be found in the FIDAP 7.5 Update manual (1995). It should be noted, however, that this method does not account for the presence of air in the region of the mesh not occupied by fluid. This method simply assigns zero pressure and zero velocities at the nodes where no fluid is present. Thus, air entrapment and pressure increases due to air entrapment can not be accounted for with this method. Also note that surface tension effects between the fluid and empty region are not accounted for with this method.

Mesh Generation

For the filling simulation, the geometry of the mesh is taken as the geometry when the entire bolus just comes into contact with the walls of the pharynx. This is determined by visual examination of the digitized images from fluoroscopy (see section 6.5.3 for details). Figure 5.4.1 shows an example finite element mesh generated for the low-viscosity, 10 mL swallow. Figure 5.4.2 shows the region the mesh covers on the corresponding fluoroscopic image. A metal ball is taped under the subject's chin to serve as a size reference. The size of the metal ball is 0.87 cm. The meshes for all simulations use 9-noded quadrilateral elements.

During the filling simulation, the shape of the mesh cannot change. This is a limitation of the solution method. Recall, the shape of the mesh is the shape of the bolus when all boundaries of the bolus are in visual contact with the pharyngeal walls as seen from fluoroscopy studies. While filling the pharynx, the position of the pharyngeal walls not in contact with the bolus are insignificant. The movement of the bolus cannot be affected by the wall if the wall is not in contact with the bolus. In this situation, the assumption of a mesh of constant geometry is valid. However, at the GPJ, the bolus is always in contact with the pharyngeal walls and these walls move during the filling simulation. This assumption is accounted for in the model by adjusting the boundary

condition at the GPJ accordingly. This compensation is discussed in this and later sections.

Initial Condition

In order to solve the above equations, initial and boundary conditions must be assigned. The initial condition prescribes the initial state of the system. For the initial condition, at time zero, the mesh contains no bolus except for a small amount just penetrating the GPJ (see figure 5.4.1). It is necessary to have some elements full initially to avoid convergence problems. At time zero, the bolus has a velocity in the x-direction of 2-5 cm/s. The y-velocity is zero. The velocity at any node where no bolus is present is zero. The pressure is also zero in every location where no bolus is present. Gravity is acting in the negative y-direction.

Boundary Conditions

Boundary conditions must also be assigned to solve the equations presented in section 5.2. Boundary conditions prescribe how the fluid behaves at the edges of the flow domain. For the filling simulation, the x-velocity at the GPJ is prescribed as a function of time. It is determined by trial and error by visually comparing the rate of fill on the simulations with the rate of fill on digitized images from fluoroscopy (see figure 6.5.1). The y-velocity at the GPJ is zero throughout the simulation.

The velocity at the UES is set to zero during the filling simulation since it does not open until after the pharynx fills.

For the anterior and posterior walls, the velocity is set to zero for the filling simulation corresponding to a no-slip boundary condition. This assumes that the walls of the pharynx do not move during the filling simulation. This assumption is valid for most of pharynx except in the region near the GPJ, as mentioned above. The width of the GPJ changes during this time. Assuming the dimension of the GPJ is constant during this time is accounted for by the variable velocity boundary condition at the GPJ. If the width

of the GPJ is actually less than represented by the mesh, the velocity is reduced to produce the correct flow rate through the GPJ. The flow rate passing through the GPJ in the simulations must corresponds to the actual flow rate since the rate of fill in the simulation matches the rate of fill seen on the images.

5.4.2.--Moving Boundary Simulation

The moving boundary simulation uses a solution method known as the method of spines. The shape of the mesh can change using this method. The position of the nodes on each spine (see figure 5.4.1) is an additional variable in the discrete problem. This variable is determined through analysis of the fluoroscopic images. Details about this procedure can be found in section 6.5.5. The geometry of the mesh at the beginning of the moving boundary simulation is the same as the mesh in the filling simulation.

Initial Condition

The moving boundary simulation is a continuation of the filling simulation thus, there is no initial condition in a physical sense. To start the CFD simulation, an initial condition must be given. This is accomplished by reading the results of the filling database at the last time step. The initial values of the velocities at each node are assigned as the velocities at the end of the filling simulation.

Two-phase flow cannot be modeled in the moving boundary simulation. This is a limitation of the solution method; modeling multiple free boundaries is a very difficult problem. Because of this limitation, any region from the filling simulation that is not occupied by bolus becomes so at the beginning of the moving boundary simulation. This is a major assumption. The ramifications of this assumption are discussed at length in chapter 7.

Boundary Conditions

Continuing from the filling simulation, the x-velocity is specified as a function of time at the GPJ. The y-velocity is zero. When the GPJ closes, the velocity at this boundary is set to zero.

From the start of the moving boundary simulation, the condition at the UES corresponds to zero applied external forces. This is a common boundary condition for an outflow of a truncated domain. This condition arises naturally from the application of the finite element method to the equations of motion and, accordingly, is known as the natural outflow boundary condition. This corresponds to setting the normal component of the surface stress vector to zero, in a weighted sense, over the boundary. This implies when the viscous contribution to the normal stress is small, the pressure at the boundary is zero. This assumes that the UES is open. Flow is not seen through the UES on the images at the start of the moving boundary simulation. It has to be assumed that there is a small opening at the UES in order to mesh the region. Because of this assumption, results from the simulations during this short period of time that the UES is closed are questionable. After the UES opens, this boundary condition is appropriate.

The anterior and posterior boundaries move to imitate the peristaltic action of the pharynx during this part of the simulation. The velocity at the anterior and posterior boundaries are prescribed to move at the rate seen on the digitized images. The movement is simulated by displacing the nodes on the boundary of the mesh in the direction of the spine at the velocity prescribed. The location of the nodes on the interior of the mesh are automatically updated by the program by adjusting the distance between nodes to the new normalized length of the spine. Details of how these velocities are obtained and assigned can be found in section 6.5.5.

The anterior and posterior boundaries do not come together completely to simulate the closer of the pharynx behind the bolus. The mesh cannot collapse onto

itself. This would result in infinite forces causing the computer simulation to crash. This can be seen from equation (3.6.17); as h approaches zero, the force approaches infinity. In order to avoid this difficulty, the minimum distance between the anterior and posterior boundary is chosen as approximately 0.2 cm.

5.5.--Summary

This chapter specifies the mathematical model developed for the pharyngeal phase of swallowing. Table 5.5.1 summarizes the assumptions used in this model. The procedure for obtaining these data for the assignment of the boundary conditions is detailed in the next chapter. Ramifications of the assumptions are discussed with the analysis of the results in chapters 7 and 8. Chapter 9 presents recommendations for improvement of this model.

Table 5.5.1.--Model Assumptions

• Two-dimensional, planar geometry
• Incompressible, Newtonian fluid
• Pressure of the air is constant during filling simulation
• No air is present during the moving boundary simulation
• Geometry of mesh doesn't change during filling simulation
• Small amount of bolus present at GPJ initially
• No-slip at pharyngeal walls
• UES open after point of fill
• Small amount of bolus present at end of simulation

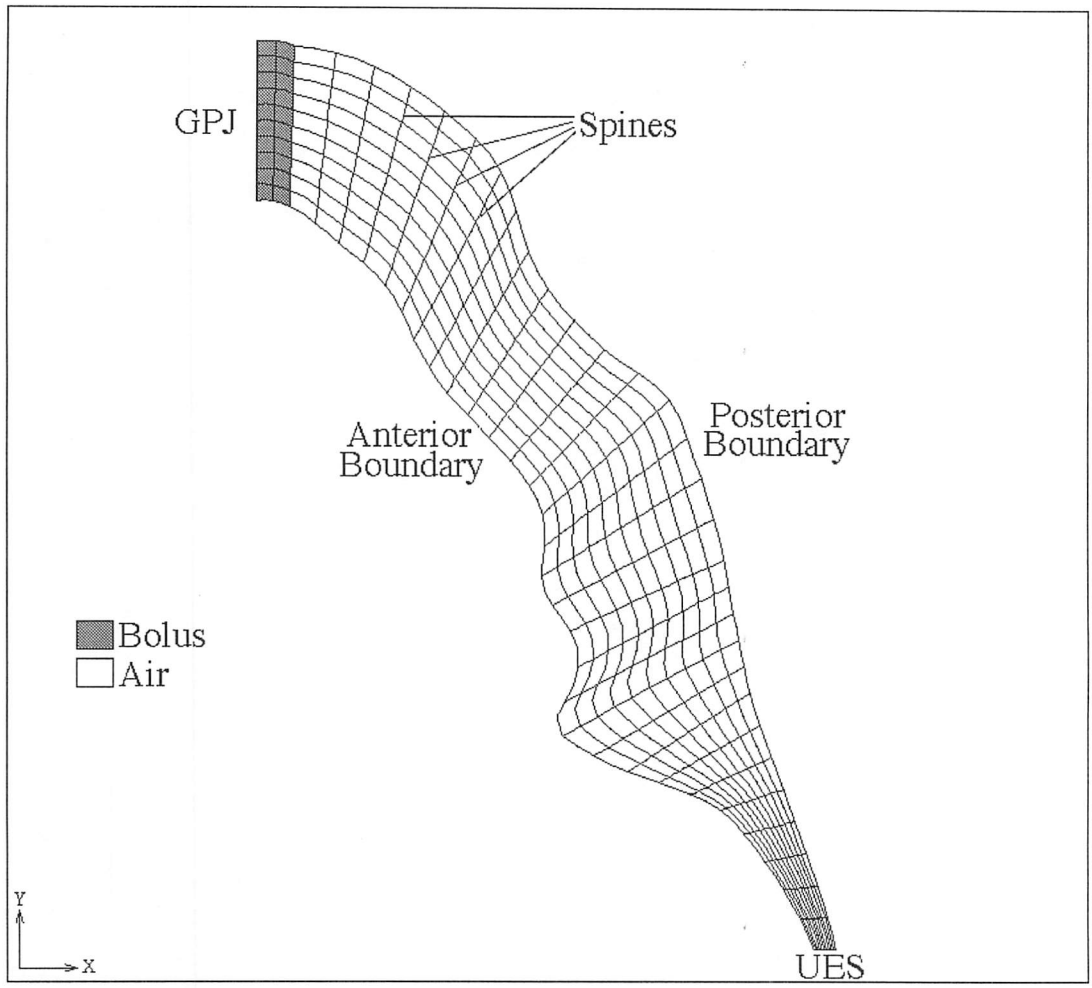

Figure 5.4.1.--Representative finite element mesh demonstrating the initial condition.

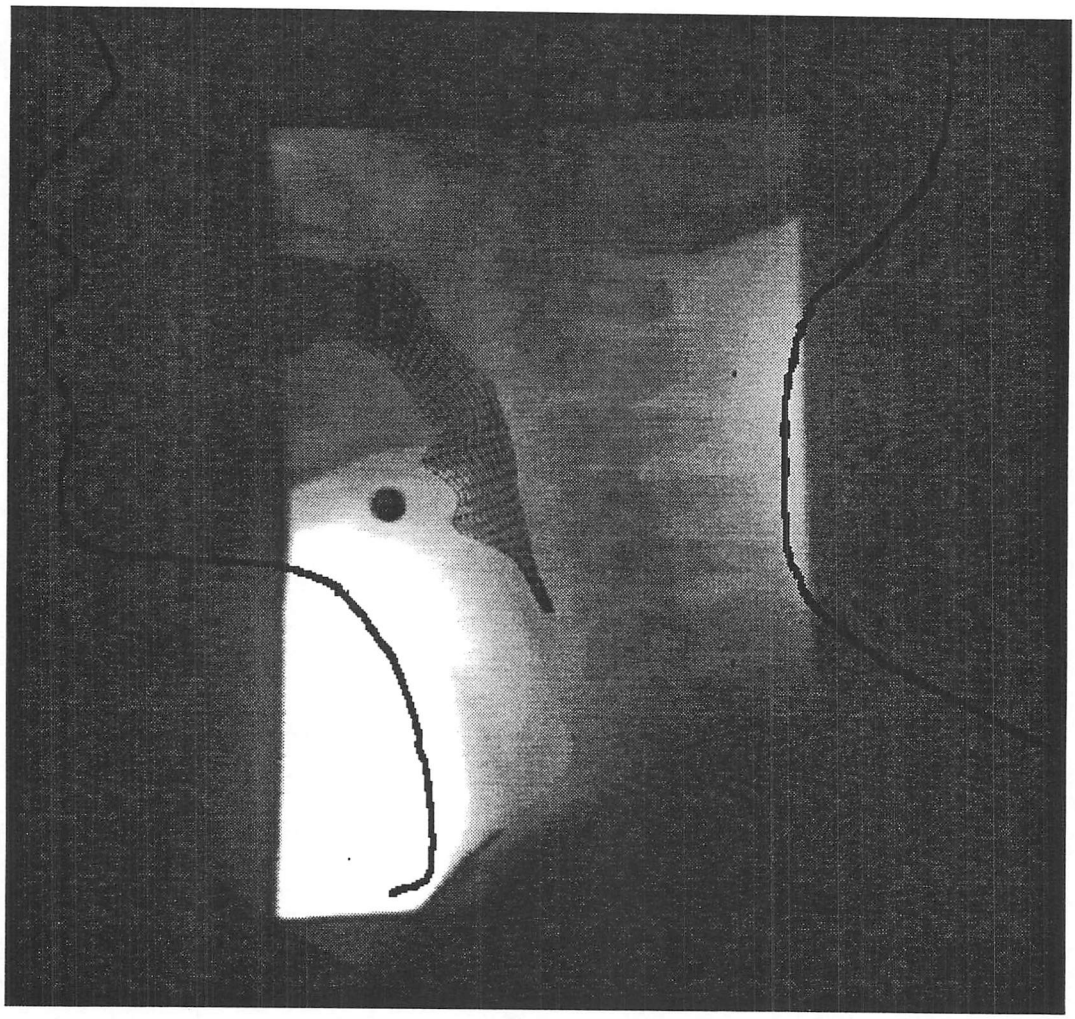

Figure 5.4.2.--Finite element mesh overlaid onto fluoroscopy image.

CHAPTER 6.--OBTAINING THE DATA

6.1.--Introduction

The mathematical model developed for the pharyngeal phase of swallowing was covered in the previous chapter. This chapter presents how the data required to solve the mathematical model with the computational fluid dynamics program, FIDAP, are generated. First, we need the properties of the fluid bolus in order to solve the model. Previous chapters discussed how the shape of the bolus changes during swallowing. In order to have a representative model, this shape needs to be characterized accurately. This can be accomplished by computer analysis of videofluoroscopic images. Each frame of the videotape can be digitized for geometric analysis with the use of a personal computer equipped with a special video card. Once the position of the boundary as a function of time is determined, this information can be converted to velocities for input into FIDAP. This chapter discusses in detail how these data, along with the data for other boundary conditions, are obtained.

The experimental values for the properties of the fluids used in the study are presented in the next section. Section 6.3 covers the protocol used for the human subjects fluoroscopy studies. These studies are stored on videotape. The process of converting the data on videotape into digital information for computer analysis is discussed in section 6.4. Section 6.5 explains how the digitized data are analyzed to provide the information required to run the CFD simulations.

6.2.--Fluid Properties

It is necessary to know the properties of what is swallowed for the mathematical model. Only substances with known or measurable properties should be used in these studies. Three fluids with viscosities differing by an order of magnitude were used in our studies. They are the mixtures recommended by Li, *et al.* (1992) in their test kit for

motility studies. Li, *et al.* (1992) have documented the properties of these samples and give detailed instructions on how to mix them. The low-viscosity sample is a standard e·z·hd barium sulfate suspension (250% w/v). The mid-viscosity sample is a mixture of 300 mL of Knott's strawberry syrup with 680 g of e·z·hd powder. The high-viscosity sample is 170 mL of Knott's strawberry syrup with 680 g of e·z·hd powder. They recommend that the samples should be used at room temperature for the reported properties to be accurate. They suggest mixing the samples at least an hour prior to the study to allow the temperature to equilibrate. Significant variations in viscosity were found as the samples aged. They also noticed large changes in viscosity with small changes in the amount of syrup.

In order to verify the properties of these fluids, we measured the viscosity and density of these fluids on multiple occasions. The viscosity of these samples were measured with a Wells-Brookfield Cone and Plate Viscometer, Model RVT equipped with cone CP-52. The viscometer was calibrated using Brookfield viscosity standards (100 cP, 5,000 cP, and 60,000 cP). The density of these fluids was measured using a graduated cylinder and a balance.

Plots of the viscosity versus shear rate can be found for these three mixtures in figures 6.2.1-6.2.3. The average of all experiments is also plotted in these figures. Note the variation of the 95% confidence interval based on the Student's t-distribution is greater than the variation due to shear rate for all samples. Also note that our measured values differ significantly from those reported by Li, *et al.* (1992). These results are not surprising. It would be unrealistic to expect the viscosity of Knott's strawberry syrup to be constant between samples.

Our data also indicates that the viscosity varies significantly as the samples aged for the mid- and high-viscosity samples. Figures 6.2.2 and 6.2.3 show viscosity data for

the same sample measured 6 hours apart. This extreme variation with time also indicates that the assumption of constant viscosity is reasonable.

Density values for the three samples are presented in figure 6.2.4. The density was measured on three separate occasions. The density did not vary significantly between samples or with time.

6.3.--Protocol for Fluoroscopy Studies

As discussed in chapter 2, many fluoroscopy studies have been presented in the literature. Many investigators suggest a protocol that involves varied volume and viscosity swallows for the study of dysphagia (Li, *et al.* 1992; Dantas, *et al.* 1990; Palmer, *et al.* 1993). Our protocol, detailed in table 6.3.1, is designed to study the effects of volume, viscosity, and head position for the normal swallow.

During the study, the subject should be sitting upright in a normal position of comfort. The subject should try to move as little as possible during the swallow to ease in the image processing. If there is measurable movement during the swallow, the digitized images will have to be re-aligned before analysis.

A spherical metallic ball of known diameter is taped under the subjects chin to give a reference length on the images. The ball needs to be positioned so that it does not interfere with the view of the oral cavity, pharynx, or upper esophagus. It should not be moved between lateral and anterior-posterior (AP) views. The position of the ball can be used as a reference in the processing of AP and lateral views for future models.

Three different volumes (5, 10, and 20 mL) and viscosities (low, mid, and high) are swallowed for each view. This results in a total of 16 swallowing sequences (see table 6.3.1). X-ray "on-time" for thorough videofluorographic studies can range from 4-10 minutes (Palmer, *et al.* 1993). Those studies include mastication and swallowing of solid foods. Our study does not. Thus, an estimate of 4-6 minutes of "on time" is reasonable for this protocol. This results in radiation exposure range of 38.8 to 58.2

mrem to the lung, 48.6 to 72.9 mrem to active bone marrow, and 82.0 to 123.0 mrem to the thyroid (Beck and Gayler 1990). These data are an estimate for a 70 Kg adult with the fluoroscope operated at 110 kVp.

6.4.--Digitization

The fluoroscopy studies are stored on videotape. The video format used to record the studies is super-VHS (S-VHS). This requires play-back on a VCR with the S-VHS format. Our computer system is equipped with a Mitsubishi HS-U770 S-VHS VCR with jog/shuttle control. The jog/shuttle control allows us to advance the tape one frame at a time. This aids in positioning the tape for the frame-grabbing procedure.

The pharyngeal phase of the swallow lasts about 1 second. The standard video rate is 30 frames/second with odd-number scan lines displayed in 1/60 of a second and even displayed the next 1/60 of a second. The analog signal from the VCR can be converted to digital information for computer analysis. Our Apple Macintosh Power PC 7100/80av is equipped with a Precision Digital Images IMAXX Video Capture Board. This board allows us to capture every frame on the videotape directly to memory for about 50 consecutive frames. Expansion of the computer's random access memory (RAM) would increase the number of frames that can be grabbed at once. Precision Digital Images provides the software package, MAXXGrab, to perform the frame-grabbing operation.

The process of digitization converts the analog signal into digital information by converting the scan lines into square picture elements (pixels) based on the brightness value. The fluoroscopic images are black and white so the brightness value for each pixel ranges between 0 and 256 (8 bits/pixel). From the S-VHS fluoroscopic image, 480 scan lines were digitized. Each scan line is broken into 512 pixels. After these images are pulled into memory, they can be saved in TIFF format for analysis with the National Institute of Health's free-ware software package, NIH Image.

6.5.--Image Analysis and Setting up the Simulations

The free software package, NIH Image, is used to analyze the digitized images. With this software, all images can be converted into a "stack" that can be easily paged through using the greater than and less than keys on the keyboard. This feature aids in the image analysis greatly by allowing the user to compare the frame before and after with the current frame readily. The image analysis is done in a specified manner to ease in the setup of the computation fluid dynamics simulations. Thus, it is most easily understood if both the set up and image analysis are explained together.

6.5.1.--Obtaining the Timing Information

After creating the stack with NIH Image, the first step is to identify the frames where the GPJ opens, the pharynx fills, the UES opens, the GPJ closes, and the UES closes. This determines the timing of the swallow. Each frame is 1/30th of a second, so the timing of the swallow can be calculated by labeling where each of these events occur. We set time zero at the start of the filling simulation as the first frame where fluid starts to pass into the GPJ from the oral cavity. The frame at the point of fill is set as the time where the filling simulation ends and the moving boundary simulation begins. This also specifies the time where the boundary condition at the UES changes from a no-flow condition to a free (natural) condition (see section 5.4). The frame at which the GPJ closes specifies the time where the boundary condition changes from a flow to a no-flow condition. The moving boundary simulation ends when the UES closes.

6.5.2.--Setting the Scale

The dimensions on the images are determined by measuring the number of pixels in the metal ball taped to the subjects chin during the fluoroscopy study. The size of the metal ball is 0.87 cm. The scale is chosen in units of centimeters within NIH Image based on this information.

6.5.3.--Generating the Mesh

The next step is to generate the finite element mesh. The mesh is based on data from the image at fill. This image is where the entire bolus has come into contact with the walls of the pharynx. Using NIH Image, the pixels at the boundary of the bolus are identified. Each pixel has an x- and y-dimensional value that is written to a data file when selected with the computer mouse. These values are adjusted to have x = 0 at the GPJ and y = 0 at the UES. These data are used to specify the boundaries of the finite element mesh. The UES is not filled with bolus at the point of fill, so we assume a small opening exists (approximately 2 mm) in the area of the UES. This is required for the moving boundary simulation. The region must be meshed initially in order to move the boundary of that region. Since the moving boundary continues from the filling simulation, the mesh at the start of the moving boundary simulation must be identical to the mesh in the filling simulation. Once the mesh has been generated, the filling simulation can be started after an initial guess for the velocity at the GPJ is obtained.

6.5.4.--Boundary Condition at the GPJ

By close inspection of the images while the GPJ is open, an initial guess for the velocity at the GPJ is obtained. When this is obtained, the filling simulation can be started. To check if the boundary condition at the GPJ is correct, each fluoroscopy image between the GPJ opening and the point of fill is compared with the results of the simulation. If the amount of fill in the simulation visually matches the amount of fill on the image, the boundary condition is satisfactory for the filling simulation (see figure 6.5.1). Note, this boundary condition during the moving boundary simulation must also be checked.

At the beginning of the moving boundary simulation, the GPJ is still open but the UES is closed. This duration varies between volume and viscosity of boluses, but generally lasts for about 2-3 frames (1/15-1/10 of a second). During this time period, any volume of fluid entering the GPJ must be compensated for by the expansion of the

pharyngeal chamber. Recall, however, the condition at the UES is free during the moving boundary simulation. To compensate for this assumption, the boundary condition at the GPJ is adjusted during this part of the simulation so that there is a small, but positive outward flow through the UES. Changing the GPJ boundary condition in the moving boundary simulation requires re-iteration of the filling simulation if the velocity is changed at the beginning of the moving boundary simulation since it corresponds to the same point in time as the end of the filling simulation. The boundary condition at the GPJ is iterated upon until satisfactory results are obtained from both the filling and moving boundary simulations. Figure 6.5.2 outlines how the boundary condition at the GPJ is obtained.

6.5.5.--Specifying the Moving Boundary

The movement of the boundary is specified by assigning a velocity to each node on the boundary as a function of time. The nodes move along the direction of the spine that it lies upon (see figure 5.4.1). Since only two of the spines are oriented in the x=0 or y=0 planes (spines passing through GPJ and UES), both a velocity in the x-direction and y-direction must be assigned for each node.

The data used to calculate these velocities are obtained by analysis of the digitized fluoroscopic images. This is accomplished by overlaying the spines on each of the fluoroscopy images from the point of fill until the UES closes. To do this, the locations of the boundary nodes are imported into an Microsoft Excel spreadsheet from FIDAP. The slope of each spine is calculated. The x-pixel values from the digitized images are entered into the spreadsheet to determine a corresponding y-pixel value on the spine. Once the spine location is defined by 2 pixels, it is drawn onto one of the images. When all spines have been drawn on one image, the file is saved. The software package Adobe Photoshop is used to convert this file to an image that displays only the spines in black. This file is copied and overlaid onto each image using the layers tool between the point of

fill and the closure of the UES. The resulting image is a multiplication of the two images with the opacity of the spines at 20% so they do not obscure information in the fluoroscopy image. The combined images are saved in TIFF format to be opened by NIH Image, converted to a stack, and analyzed.

The images are analyzed by marking the intersection of the bolus boundary with every spine for each frame. Note, the bolus will intersect each spine in two locations, the anterior boundary and the posterior boundary. Figure 6.5.3 shows representative images.

Data files containing the locations of these intersections are read by a FORTRAN program that interpolates the locations exactly onto the spine. Since a pixel represents a small area, it is not necessarily located exactly on the spine. Care must be taken when generating the finite element mesh so that two nodes on the boundary are not within a pixel distance of each other and will not come within a pixel distance of each other during any part of the swallow. If the nodes do come within a pixel distance of each other, the FORTRAN program could assign velocities that would result in two spines intersecting. This would force the CFD program to fail.

Once the location of these intersections are interpolated back onto each spine for each frame, the FORTRAN program calculates displacements in the x- and y-directions and the corresponding velocities. These data are written to a file in a format readable by the CFD program, FIDAP. FIDAP reads an ASCII input file with the problem specifications, including tables of time versus velocity data for each node on the moving boundary.

6.6.--Summary

The procedures outlined above provide all the data required to specify the initial and boundary conditions for the CFD simulations. These simulations were run on our Silicon Graphics Indigo R4000 workstation. A satisfactory boundary condition for the

GPJ could take anywhere from 1 to 20 iterations. It requires about 1-2 hours to run the filling simulation and 3-6 hours to run the moving boundary simulations.

Many simulations were run to investigate the effects of viscosity, volume, head position, and gravitational forces. The filling simulations are also modified to study the effect of volume, viscosity, and gravitational forces on laryngeal penetration. A moving boundary simulation was set up using data from a dysphagic patient. A single swallow from a second normal subject was modeled to verify the method. The mesh is refined for one swallow to confirm the accuracy of the model. The results for these studies are presented in the following chapters.

Table 6.3.1.--Sequence of Swallows

Swallow #	VIEW	VISCOSITY	VOLUME
1	Lateral	Low	5 mL
2	Lateral	Low	10 mL
3	Lateral	Low	20 mL
4	Lateral	High	5 mL
5	Lateral	High	10 mL
6	Lateral	Mid	10 mL
7	Lateral 20° back	Mid	10 mL
8	Lateral 20° forward	Mid	10 mL
9	PA	Low	5 mL
10	PA	Low	10 mL
11	PA	Low	20 mL
12	PA	High	5 mL
13	PA	High	10 mL
14	PA	Mid	10 mL
15	PA 20° back	Mid	10 mL
16	PA 20° forward	Mid	10 mL

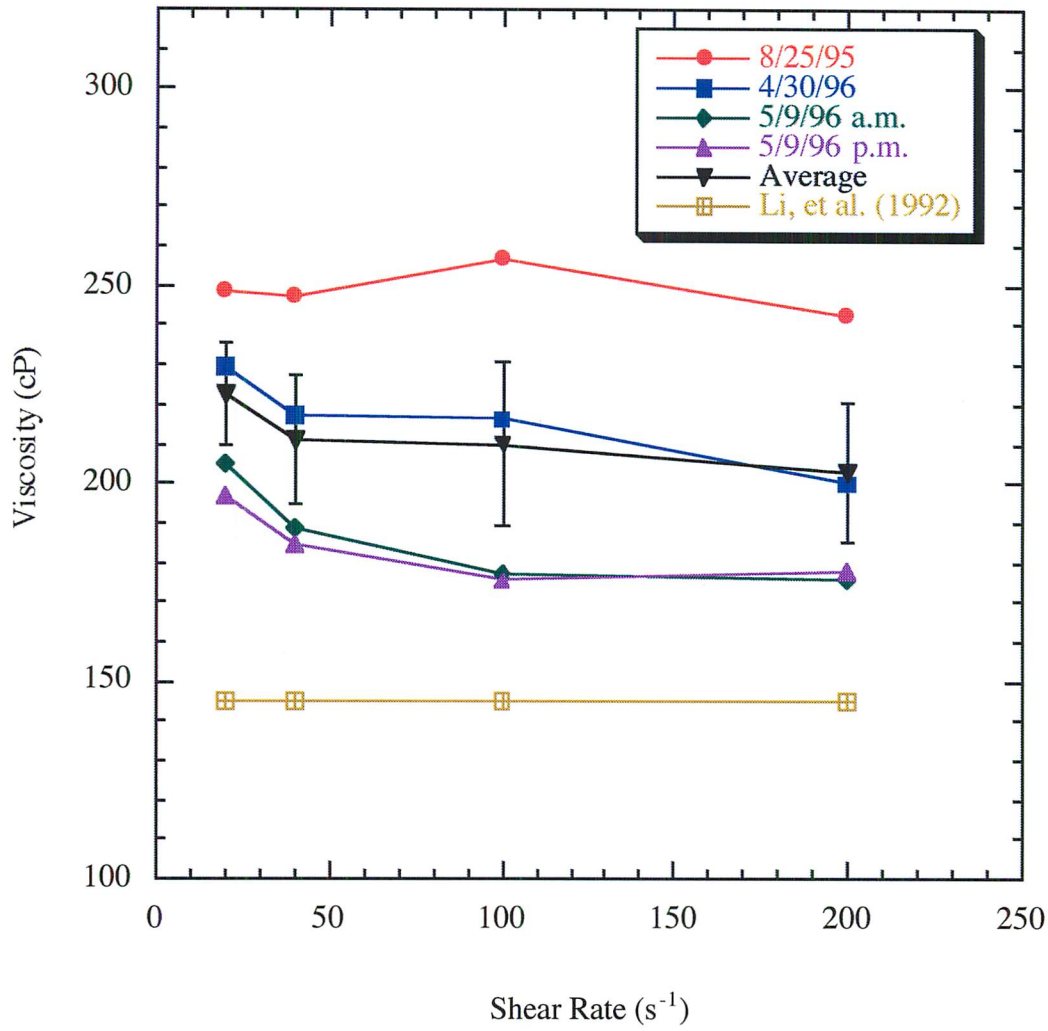

Figure 6.2.1.--Viscosity measurements for the low-viscosity sample demonstrating the variation between studies. The 5/9/96 data is from the same sample measure 6 hours apart. Error bars represent 95% confidence intervals based on the Student's t-distribution.

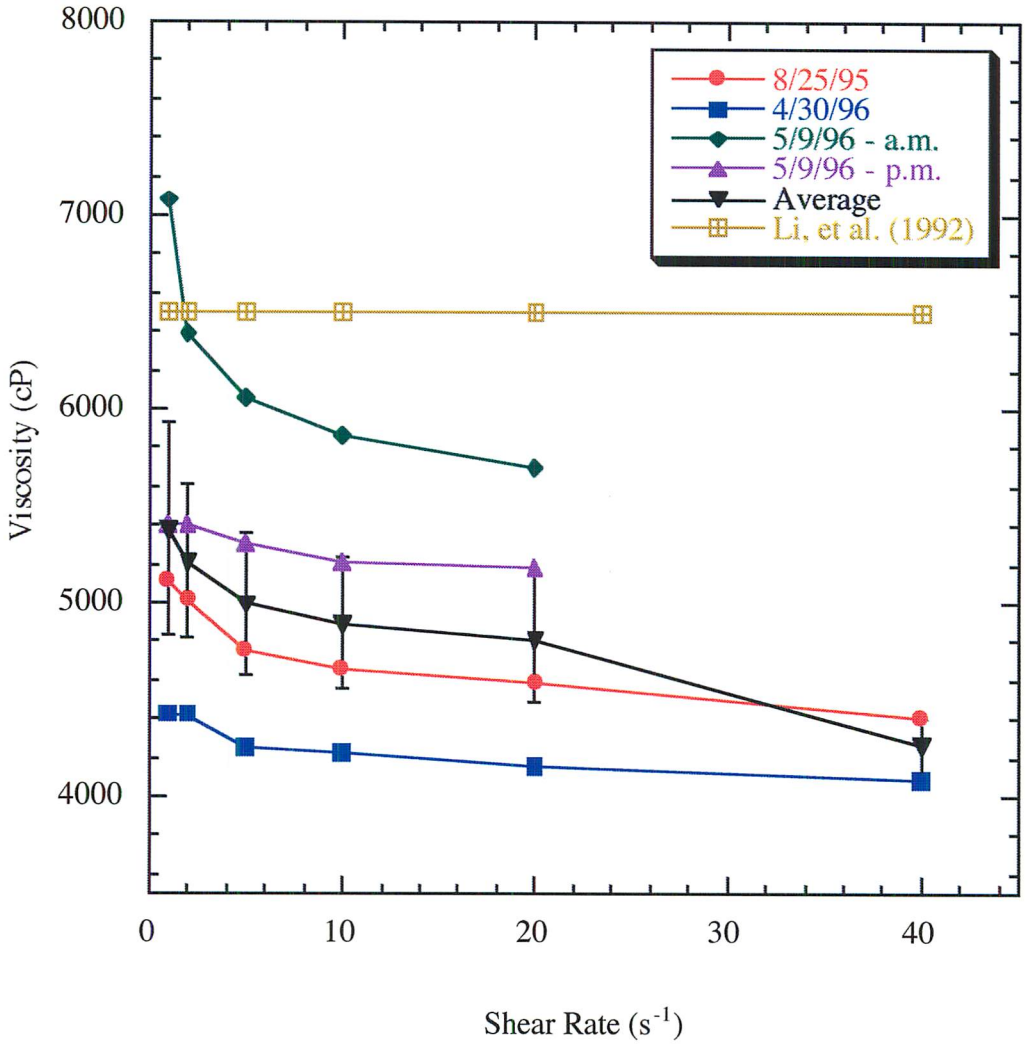

Figure 6.2.2.--Viscosity measurements for the mid-viscosity sample demonstrating the variation between studies. The 5/9/96 data is from the same sample measure 6 hours apart. Error bars represent 95% confidence intervals based on the Student's t-distribution.

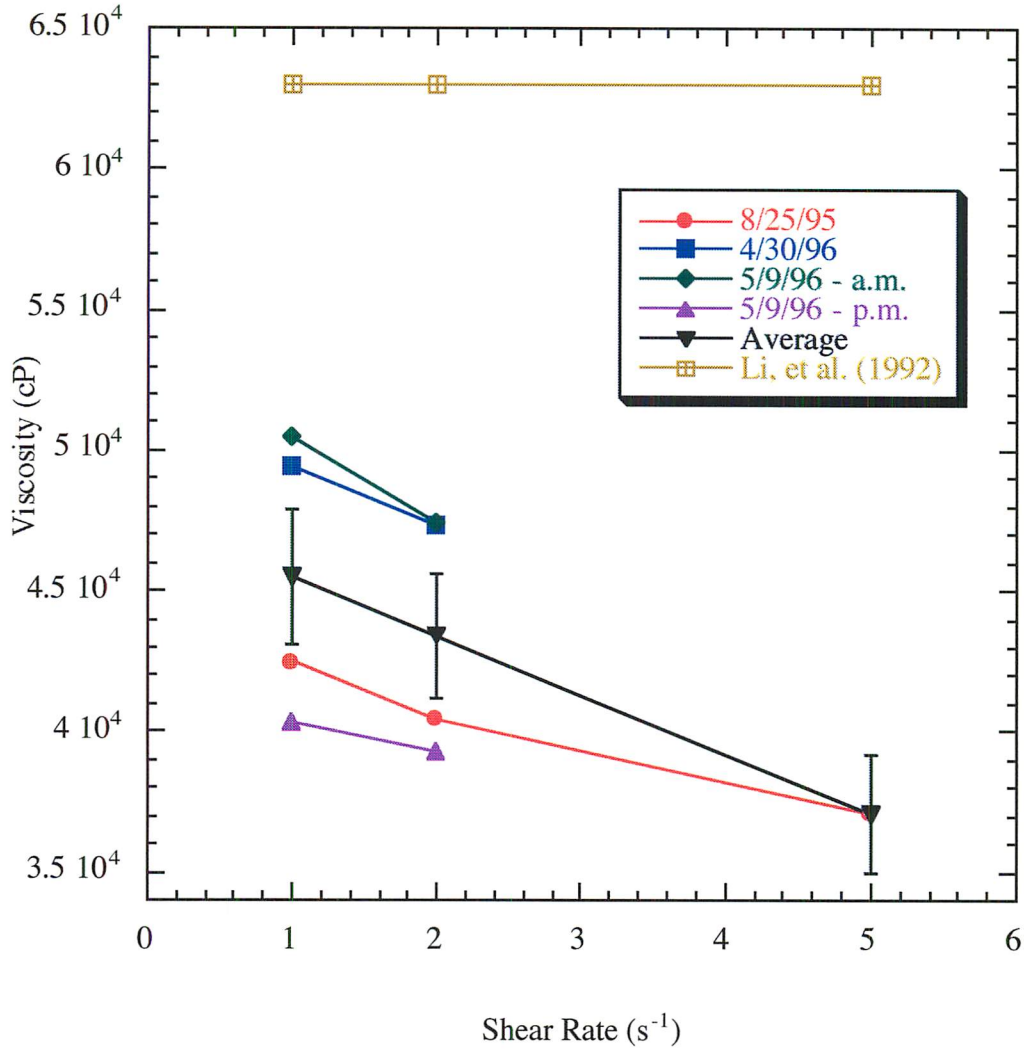

Figure 6.2.3.--Viscosity measurements for the high-viscosity sample demonstrating the variation between studies. The 5/9/96 data is from the same sample measure 6 hours apart. Error bars represent 95% confidence intervals based on the Student's t-distribution.

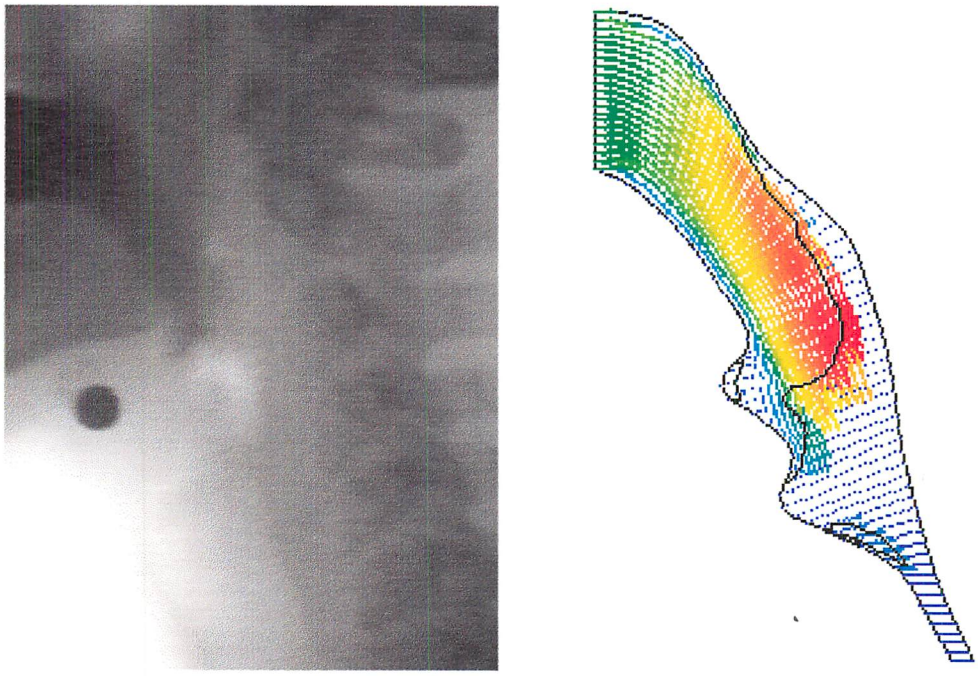

Figure 6.5.1.--Representative images from the fluoroscopy study and the simulation at the same point in time demonstrating how the boundary condition at the GPJ is obtained during the filling simulation.

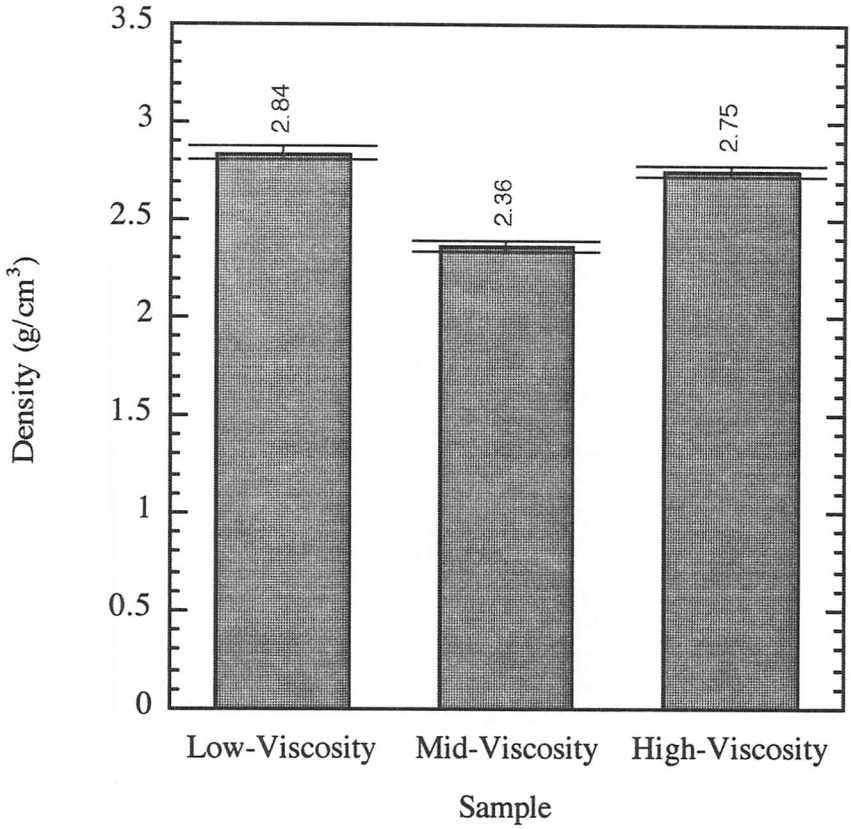

Figure 6.2.4.--Density of the three samples used in the fluoroscopy studies.

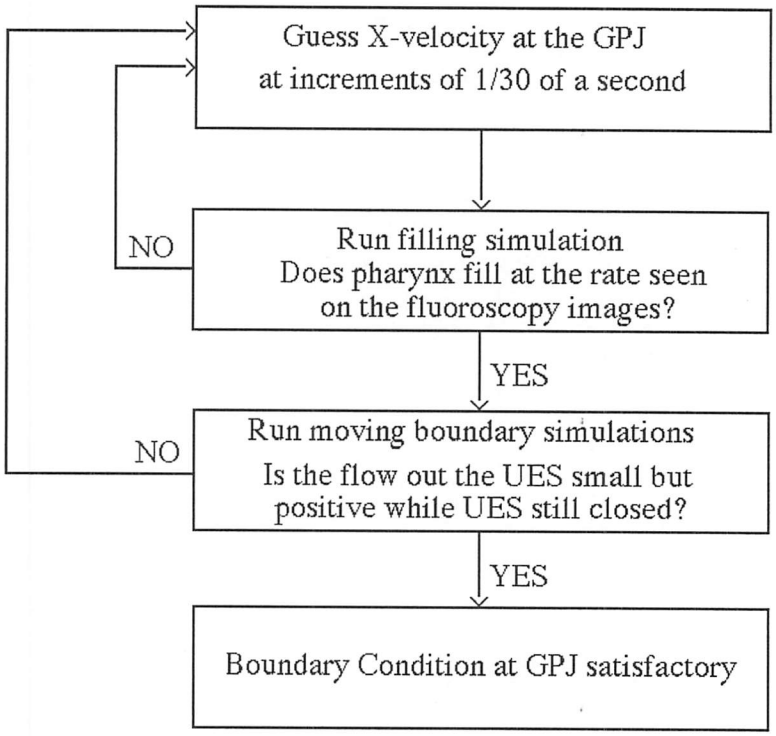

Figure 6.5.2.--Flowchart outlining how the boundary condition at the GPJ is determined.

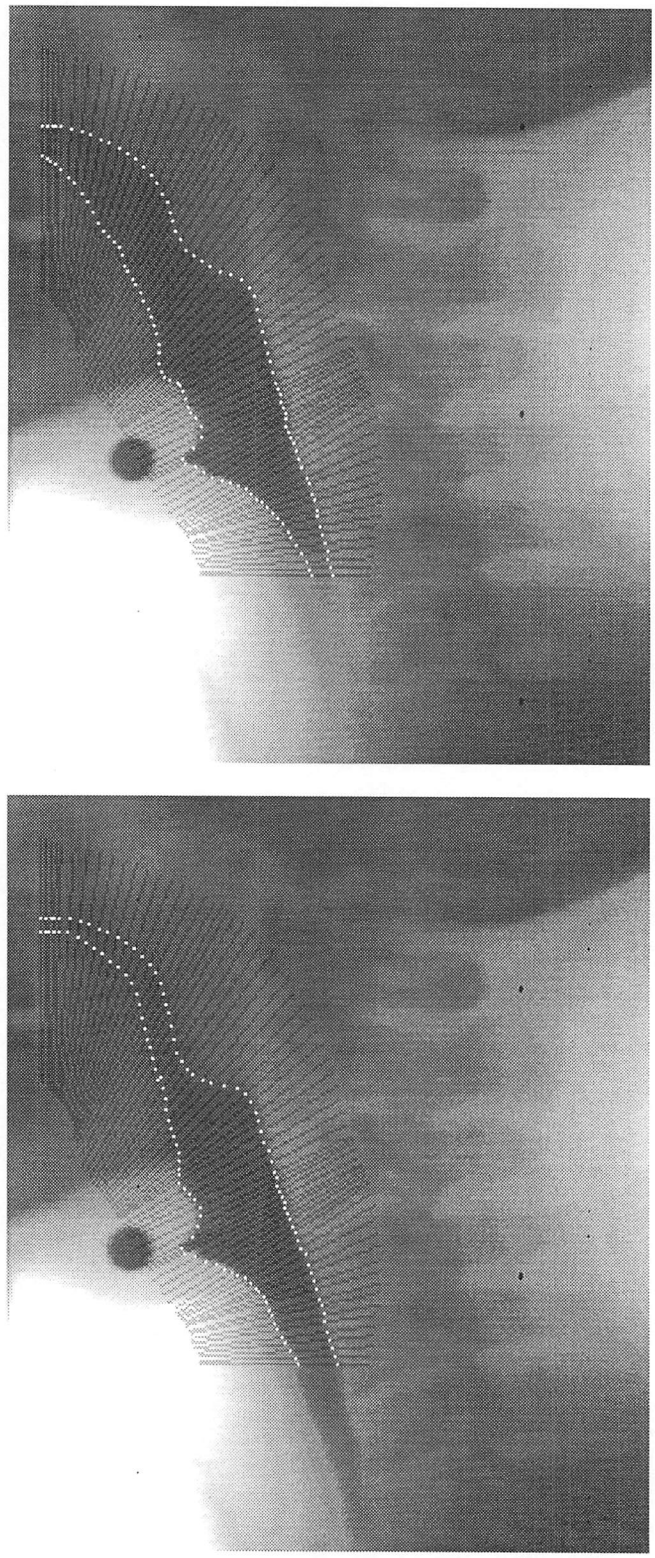

Figure 6.5.3.--Representative frames from the image analysis procedure.

CHAPTER 7.--THE NORMAL SWALLOW

7.1.--Introduction

The procedure discussed in the previous chapter was applied to a single normal subject (subject 4) for 8 swallows. We chose to apply the model to the fourth videofluoroscopy study based on information gained in the previous studies. Subject 4 moved the least during swallowing. All relevant anatomic features were present on the image during the entire course of each swallow. The contrast between the bolus and the pharyngeal chamber was also well defined for this subject.

This chapter presents the results of the model applied to the normal subject. Recall that our protocol is designed to study the effects of bolus volume, viscosity, and head positioning on the pharyngeal phase of swallowing. Section 7.2 discusses the effect of bolus volume. The effect of viscosity is presented in section 7.3. Head positioning is discussed in section 7.4. The results of a normal subject are also used to study the role of gravitational forces. These results are presented in section 7.5. The numerical accuracy of the model is verified by refining the mesh to show that the results do not change. Section 7.6 present these results. The same modeling techniques were applied to a second normal subject to investigate the reproducibility of the model. The reproducibility is discussed in section 7.7. The chapter is summarized in section 7.8.

7.2.--Bolus Volume

As discussed in chapter 2, many studies have investigated the effect of bolus volume. These investigations have studied the effect of bolus volume on the pharyngeal geometry, timing of the swallow, and manometry measurements. With our protocol, we can make similar measurements as in the literature with the exception of manometry. We did not have a system in place for combined fluoroscopic and manometric measurements at the time of our studies.

In this section, the measurements reported in the literature are compared with measurements from our studies. These data are complimented with results from the mathematical model. Pressures calculated in the computer simulations can be compared with manometry measurements from the literature, but we must keep in mind that the literature data include pressures induced by the walls of the pharynx compressing the catheter. Also keep in mind that the manometric assembly moves during the swallow and this movement is not in coordination with the movements of the pharynx. The limitations of manometry data are discussed at length in this and later sections.

7.2.1.--Timing and Geometry

The effect bolus volume on the geometry of the bolus and the timing of the swallow is well demonstrated by viewing the bolus boundary as a function of time. MPEG movies, low5.mpg, low10.mpg, and low20.mpg, of the simulations for the 5, 10, and 20 mL swallows can be found on the compact disk (CD) included with this dissertation. These movies show the magnitude of the velocity vectors at 0.01 second increments. These movies further demonstrate the effects discussed below.

One the most significant effects of bolus volume on the pharyngeal swallow is the timing of events. Table 7.2.1 presents the timing data for the three different volumes swallowed by subject 4 compared with data from literature (Kahrilas, *et al.* 1993). The data from literature are based on averaged data from eight subjects. Error values in the literature data shown in table 7.2.1 range from 0.01 to 0.05 seconds. The values for our study agree with the literature data within the error limits except for the data for GPJ and UES closure for the 5 mL swallow. There could be many reasons why the timing for our 5 mL data disagree with the literature. The most likely is that subject 4 just varies a great deal from the 8 subjects investigated in the literature. Table 7.2.2 presents these timing data in terms of duration of events. The discussion of the effect of volume on the pharyngeal phase of swallowing will be based on the events in this table.

Time to open GPJ

The time to open the GPJ begins when the bolus is first seen exiting the oral cavity and finishes when the GPJ is fully open. Recall that the GPJ is formed by the tongue base and soft palate coming together to prevent the bolus from escaping into the pharynx before initiation of the pharyngeal swallow. As the tongue tip pushes the bolus back towards the pharynx, the anterior portion of the GPJ begins to open. The GPJ continues to open over a small period of time until the bolus can be seen falling freely into the pharyngeal chamber. Our data indicate that this time increases in duration with swallow volume. This effect is most likely a measure of the coordination of the initiation time of the oral and pharyngeal phases. This assumes that after the initiation of the oral swallow, the GPJ fully opens after the same time period for all swallows. The larger volume bolus requires more area towards the posterior oral cavity to be contained on top of the tongue. It is going to be seen crossing into the GPJ earlier than the smaller volume boluses. The smaller volumes require more time to be seen exiting the oral cavity after the initiation of the swallow than the larger volumes. Data reporting timing values for this phenomenon have not been found in the literature. Whether or not this is a significant result requires the analysis of more swallows and more subjects.

GPJ Opening Duration

The GPJ opening duration begins when the bolus is first seen exiting the oral cavity and ends when the tongue base contacts the posterior pharyngeal wall. This duration increases significantly with bolus volume. These data agree with values reported in the literature within error of the literature values except, again, for the 5 mL swallow. The volume effect here is partly due to the same argument as above along with mass conservation requirements. Figure 7.2.1 is a plot of the volumetric flow rate through, the width of, and the velocity through the GPJ. Time equal to zero is when the bolus is first seen exiting the oral cavity. Note that the volumetric flow rate is in units of

area/time since it is a two-dimensional simulation. The volumetric flow rate is the product of the velocity and the width of the opening.

The maximum volumetric flow rate increased dramatically from the 5 mL swallow to the 10 mL swallow. The 10 and 20 mL swallows have similar maximums. This may indicate that there is a maximum volumetric flow rate for any swallow volume. This could be verified with further studies including swallows of larger volumes. The steep upward climb of the volumetric flow rate and velocity occurs when the GPJ fully opens. As shown in table 7.2.1, the time to fully open the GPJ increases with swallow volume. These plots also demonstrate the GPJ opening duration increases with swallow volume.

Recall, the velocity as a function of time is prescribed at the GPJ in the mathematical model. These plots summarize the boundary condition at this location. The velocities were chosen by trial and error to match the bolus movement seen on the fluoroscopic images. The width of the GPJ opening is shown as a constant during the time to fill the pharynx because we cannot model the moving boundary and the filling at the same time. This is a limitation of the software used to solve the mathematical model. In reality, the width of the GPJ and the bolus are changing while the pharynx is filling. The width of the GPJ during the filling is taken as the width at the point of fill. This assumption is compensated for by choosing the velocity to be slower than actual in order to have a correct volumetric flow rate (see sections 5.4.1 and 6.5.4). Since the bolus is incompressible, in order for the rate of fill in the simulation to match the rate of fill on the videofluoroscopic images, the volumetric flow rate prescribed must be correct due to conservation of mass.

Notice that the maximum velocity decreases with increasing swallow volume. This effect is actually more profound than shown in figure 7.2.1 due to the assumption of constant width at the GPJ early in the swallow. Assuming the volumetric flow rates are

accurate, the velocities before the point of fill would actually be greater than shown since the width of the GPJ is always less than the width at the point of fill with one exception. The maximum width of the GPJ for the 5 mL swallow occurs at the frame (0.033s) before the point of fill. This would reduce the velocity at time 0.133 s for the 5 mL data.

The timing of the maximum opening of the GPJ is also a function of swallow volume. The maximum width of the GPJ for the 10 mL swallow occurs at the point of fill. The maximum width for the 20 mL swallow occurs at the frame after (0.033s) the point of fill. Note that the maximum width does not correspond to the maximum flow rate or velocity at the GPJ.

Time to Fill

The time to fill begins with the bolus passing into the GPJ and ends when the bolus just comes into contact with the walls of the pharynx (when the pharynx is filled with bolus). This time increases with swallow volume due to the time to open the GPJ. The time between the GPJ being fully open and fill is constant among swallow volumes.

Time Between GPJ Closure and UES Opening

Another significant timing measure is the time between UES opening and GPJ closure. In our study, the GPJ closes before the UES opens for the 5 mL swallow. This is not observed in the literature. This again suggests variability among subjects. Note that the data for the 10 and 20 mL swallows do not agree with the literature data very well either. The volume effect on this timing measure is much more pronounced in our study than reported in the literature. This could be due to many factors, including differences among subjects and even differences in interpreting when these events occur. Recall that we only have data from fluoroscopy studies at every 1/30 of a second.

Pharyngeal Clearance

Here we see that the time for pharyngeal clearance (time between UES and GPJ closure), which is an indicator of peristaltic velocity, is constant among swallow volumes

in the literature. The values for our study agree within error, again, except for the 5 mL swallow. The peristaltic velocity has been reported to be constant by many investigators in the literature (see section 2.4.3).

UES Opening Duration

The duration of UES opening also increases with swallow volume. Our data agree relatively well with literature data except for the 5 mL swallow. Table 7.2.3 compares the duration of UES opening with studies from the literature. The differences between these studies further demonstrate a significant variation between subjects.

The UES does open wider for larger volume boluses, but this effect is not great enough to transport the different volume boluses over the same time period through the UES. This is demonstrated in figure 7.2.2. Figure 7.2.2 shows the volumetric flow rate, width of the UES, and velocity through the UES as a function of time for the three volumes.

The volumetric flow rate and velocity are artificially high at the beginning of the flow through the UES for all swallows modeled. This is because we have to assume the UES is open at all times in order to mesh the region. We must have the region meshed in order to move the nodes on the boundary of the UES (see section 5.4.2). We compensate for this assumption by allowing no flow out the UES during the filling simulation and by keeping the opening very narrow (~2 mm) until the UES begins to open. At the point where the UES begins to open, the nodes on the posterior and anterior boundary move to open the UES to the dimensions seen on the fluoroscopic images. Shortly after this point in time, the flow rates represents reality.

The dimension of the UES as a function of time and bolus volume is shown in figure 7.2.2B. Table 7.2.4 compares these dimensions with studies in the literature. The literature values form Cook, *et al.* (1989) represent average ± SD maximal parasagittal UES sphincter diameter for 8 male subjects. The data from Jacob, *et al.* (1989) are

average ± SEM maximal UES PA diameter for 8 male subjects. Both studies included concurrent manometry. The large deviation on these literature values and the large difference with the data for subject 4 further demonstrates the variation between subjects.

Total Time

The GPJ, pharynx, and UES do compensate for larger bolus volumes by opening wider but not enough to transport the boluses through the pharynx in the same amount of time. This is demonstrated by the large difference in the total time required to transport the bolus from the oral cavity to the esophagus. The major events that compensate for increasing bolus volumes are the duration of GPJ and UES opening. Both these events increase in duration with bolus volume as discussed above. Note also the coordination of these events is affected by bolus volume. This is demonstrated by the difference between GPJ closure and UES opening. The UES doesn't have to be open at the same time as the GPJ for the low volume swallows since the pharyngeal chamber can contain these volumes. When the volume of the bolus is larger than the pharyngeal chamber, the UES has to open to allow the rest of the bolus to be transported from the mouth into the pharynx. This also can indicate the difference between subjects. Some subjects have a larger pharyngeal chamber than others. A smaller chamber will require the GPJ and UES to be open concurrently for smaller bolus volumes.

7.2.2.--Pressures and Stresses

Figure 7.2.3A is a plot of the pressure at the center node near the level of the laryngeal entrance over the entire course of the swallow for the three volumes. In this figure, the pressure is relative to the pressure at the UES. In both the filling and moving boundary simulations, the pressure is zero at the UES. In the filling simulation, this is because the pressure in the air phase is zero. In the moving boundary simulation, the pressure is zero at the UES due to the stress-free boundary condition. The pressures reported in manometry studies are relative to atmospheric pressure. The pressures

measured with manometry can be compared directly with the filling simulation because both measurements are relative to atmospheric pressure. We cannot say with certainty that the pressures from the moving boundary simulation are directly comparable because we do not know what the pressure at the UES is relative to atmospheric pressure.

Cerenko, *et al.* (1989) show the pressure to be negative early in the bolus flow through the UES. They state that when the bolus completely fills the UES, the pressure immediately rises to zero mmHg. Jacob, *et al.* (1989) report that the UES pressure increases steeply to zero mmHg at the time of the first video frame showing sphincter opening. The pressure then increases to a maximum value which is dependent on bolus volume. Figure 7.2.4 shows the intrabolus pressure within the UES as a function of time during bolus flow and bolus volume from Jacob, *et al.* (1989). The final time in this plot represents the time of maximal UES opening. Note that the maximum intrabolus pressure does not occur at maximum opening. Cook, *et al.* (1989) also report bolus pressure within the UES, 1 cm upstream, and 1 cm downstream at maximal UES opening. These data are reported in table 7.2.5. The data from these studies indicate that the UES pressure is not constant during bolus passage. As mentioned previously, we cannot expect the pressures within the bolus predicted by the model to look like pressures measured using manometry as in figure 2.4.1. There are many reasons for this including limitations of manometry and limitations of the model.

Limitations of manometry include, 1) the pressure transducers measure the squeeze of the pharyngeal lumen when no bolus is present, 2) the pressure transducers move during the course of the swallow due to the lifting of the soft palate causing traction on the manometry assembly, and 3) the presence of the catheter disrupts the flow of the bolus.

The uncertainty of whether or not the pressures measured are due to the bolus passing or due to the squeeze of the lumen on the catheter can be resolved with

concurrent videofluoroscopy. Concurrent videofluoroscopy makes it possible to distinguish when the bolus is passing the sensor. The exact timing of when the bolus is passing the sensor cannot be pinpointed accurately due to limitations of videofluoroscopy. The time resolution of standard videofluoroscopy is only 1/30 of a second. The pressure can change as rapidly as 4000 mmHg/s in the pharynx (Kahrilas, *et al.* 1994).

The movement of the catheter is a significant limitation since the location of the pressure measurements cannot be specified. The best example of this limitation is measuring the pressure within the UES. In this situation, both the catheter and the UES elevate during the course of the swallow. The catheter rises due to the elevation of the soft palate. The UES elevates in coordination with the larynx. The onset of these movements is not synchronous (Isberg, *et al.* 1985). The soft palate rises before the UES which moves the catheter from the UES into the pharynx. As the UES rises, the catheter moves back into the UES and continues moving into the cervical esophagus (Ravich 1995). In this example, correct interpretation of the pressure within the UES is impossible.

The presence of the catheter in the pharynx inherently disrupts the flow by changing the geometry. The catheter could also effect the muscle contraction. Brasseur and Dodds (1991) present a thorough discussion of these effects. They estimate that the intrabolus pressure could be affected by as much as 20% due to the presence of the catheter. Other studies have shown that the diameter of the catheter affects the pressures measured (Castell and Castell 1993).

Limitations of the model produce the large peaks shown in figure 7.2.3A. These large pressures are not seen in manometric studies. These peaks occur in the model when the simulation switches to the moving boundary simulation. These are due to the artificially high flow rates through the UES discussed above along with the assumption

that the bolus is homogeneous at the start of the moving boundary simulation.

In all simulations, about 10-20% of the area is air at the point of fill. At the start of the moving boundary simulation, this area is assumed to be bolus with zero velocity. We have to make this assumption because we cannot model a two-phase moving boundary problem (see section 5.4.2). This is a limitation of the software; modeling multiple free boundaries is a very difficult problem. Assuming the bolus is homogeneous during the moving boundary simulation is the largest flaw of the model. This causes a sharp increase in pressure due to the fact that the density is increased by replacing the air with bolus. The effect of this assumption on the pressure is alleviated when the UES begins to widen. This also explains the artificially high flow rates discussed above.

Having air present at the point of fill is actually a valid assumption. The pharynx, being part of the airway, is filled with air prior to the swallow. As the bolus begins to enter the pharyngeal chamber, the passageway to the nasopharynx is sealed. The larynx completes elevation shortly after the bolus begins filling the pharynx. The air has no way to escape. Videofluoroscopy cannot clarify what portion of the passing bolus is actually air. There is some indication by the intensity of the bolus, but we cannot quantify how much air is present. Ergun, *et al.* (1993) have shown via ultrafast CT scans that at any time while the bolus is passing, a substantial portion of the cross-sectional area is occupied by air. A recent study in the esophagus also confirms that a substantial portion of the swallowed bolus is made up of air (Pouderoux, *et al.* 1996); thus, we know that the air is transported through the UES. Due to these limitations of the model, the data from the point of fill to the opening of the UES cannot be significantly interpreted.

Figures 7.2.3B and C present the pressure data for the period before fill and after UES opening, respectively. Figure 7.2.3B shows the pressure history over the course of the filling simulations for the 5, 10, and 20 mL swallows. All three volumes show the same behavior in that the pressure increases to about 20 mmHg when the bolus arrives at

that location. These data can be compared to literature since they are both relative to atmospheric pressure. Maddock and Gilbert (1993) report the maximal pressure amplitude early in the swallow near the level of the entrance to the larynx to be ~16.5 mmHg for the 5 mL swallow, ~18.5 mmHg for the 10 mL swallow, and ~20.5 mmHg for the 20 mL swallow. These pressures are comparable to our data in figure 7.2.3B although we show no correlation with volume.

Figure 7.2.3C shows the pressure histories for the three volumes after the UES has opened. Again, all three volumes show similar trends in that the pressures are about the same in magnitude with variations due to peristaltic action at different levels of the pharynx. The walls of the pharynx come together at varying rates at different levels. As shown in the analysis for squeezing flow in section 3.6, the pressure is directly proportional to the velocity of the walls coming together.

Figure 7.2.5 is a plot of the total normal force acting in the region of the laryngeal entrance divided by the length of this region. These forces are calculated over element edges. Since the length of the elements can change during the simulation due to the moving boundary, we must normalize the data for comparison by dividing by the length of the elements. A negative stress acts in the negative x-direction, towards the larynx. Notice the large negative stresses act just as the bolus arrives in this location during the filling simulation. The stresses become positive as the anterior wall moves towards the posterior wall as peristalsis occurs. Notice, these plots suggest the magnitude of the negative stresses are less for increasing bolus volume. This is counter-intuitive. Since the magnitude of these values are relatively small and the variation with time is great, it cannot be concluded that there is a significant volume effect.

7.3.--Viscosity

Many studies in the literature have investigated the effect of different consistency boluses on the pharyngeal swallow, but few report the viscosity of these boluses. Our

study was designed to investigate the effect of three different viscosity boluses on the pharyngeal swallow. These three fluids include standard e·z·hd barium sulfate suspension as a low-viscosity fluid (~185 cP), standard e·z·hd powder mixed with 300 mL of Knott's strawberry syrup for the mid-viscosity fluid (~5,000 cP), and standard e·z·hd powder mixed with 170 mL of Knott's strawberry syrup for the high-viscosity sample (~45,000 cP). In this section, the effect of viscosity on the timing of the swallow, geometry of the bolus, flow pattern within the bolus, and pressures and stresses calculated with the model will be discussed.

7.3.1.--Timing and Geometry

The effect of viscosity on the timing of pharyngeal swallow is not as dramatic as the effect of volume. Table 7.3.1 details the timing of events for the three fluids. Recall that each of these swallows were 10 mL in volume. Table 7.3.2 presents the timing in terms of duration of events. Notice the time to open the GPJ, GPJ opening duration, and UES opening duration are not a function of viscosity, but are dependent on bolus volume as discussed above. There are no data in the literature that can be quantitatively compared to our data. Qualitative comparisons of our results with literature data are discussed below.

Time to Open the GPJ

According to our data, the time between when the bolus is first seen exiting the oral cavity and the GPJ being fully open is not dependent on bolus viscosity. Dantas, *et al.* (1990) report bolus lengths in the mouth as a function of volume and viscosity. They compare a liquid barium bolus to a paste barium bolus. The viscosity of their liquid bolus is similar to our low-viscosity sample. The paste bolus is the same mixture as our high-viscosity sample. They find that the bolus length in the oral cavity increases with bolus volume, supporting our statement that larger bolus volumes require more area towards the posterior oral cavity. They find no significant viscosity effect on bolus length within the

oral cavity. Based on the argument in section 7.2.1 explaining why larger bolus volumes require less time to be seen crossing the GPJ, we should expect that the viscosity would have no effect on the time to open the GPJ if it has no effect on the bolus position within the oral cavity.

Opening Duration of the GPJ

The data from subject 4 suggest that GPJ opening duration is not dependent on bolus viscosity. This contradicts with data from Dantas, *et al.* (1990). They found that the oral transit time, which is not defined but intuitively should be similar, increased with increasing viscosity. The oral transit time for their 10 mL, low- and high-viscosity bolus was 0.38 ± 0.05 s and 0.52 ± 0.09 s. From table 7.3.2, the opening duration for our study was 0.33 s for all 10 mL swallows. It is difficult to speculate about this discrepancy without knowledge of the definition of their measurement. Hamlet, *et al.* (1996) studied the effect of viscosity on the oral and pharyngeal phases of swallowing using scintigraphy. Their data also contradict the data from Dantas, *et al.* (1990). Hamlet, *et al.* (1996) compare the oral discharge time, defined as the interval from the start of rapid bolus movement past the mandibular marker (near the GPJ) until the tail of the bolus passes the same point, for water and a fluid with a viscosity of about 1,100 cP. The oral discharge time for water (1 cP) and thickened apple juice (1,100 cP) was 0.366 ± 0.043 s and 0.338 ± 0.066 s, respectively. These data compare with our data, suggesting no connection between bolus viscosity and GPJ opening duration.

Figure 7.3.1 is a plot of the volumetric flowrate through, the width of, and the velocity at the GPJ for the three fluids. Notice that these plots seem to indicate that the GPJ closes earlier for the low-viscosity fluid. The GPJ reaches the minimum width earlier for the low-viscosity bolus, but there is still a small amount of flow at that time. The flowrate through the GPJ is very similar for the higher viscosity fluids.

Figure 7.3.1B shows the width of the GPJ. Again, the width is assumed to be

constant prior to the point of fill for the same reasons discussed in section 7.2.1. From this plot, it is hard to conclude whether or not the width is a function of viscosity. As mentioned previously, the maximum width of the GPJ is 14.5 mm and occurs at the point of fill (0.2 s) for the low-viscosity, 10 mL data. For the mid-viscosity swallow, the maximum width (15.4 mm) is measured over two frames at times 0.167 and 0.2 seconds prior to fill (0.23 s). The maximum width for the high-viscosity swallow also occurs over two frames at 0.133 and 0.167 seconds, also prior to the point of fill (0.23 s), at a value of 16.4 mm. These data indicate the maximum width of the GPJ increase slightly and occurs earlier with increasing viscosity.

Figure 7.3.1C shows the velocity through the GPJ decreases with increasing viscosity. This effect is actually more profound than shown due to the assumption of constant width at the GPJ prior to fill. The maximum widths for the mid- and high-viscosity swallows are greater prior to the point of fill as discussed above. Recall that these velocities are prescribed at the GPJ in the model in order to match the rate of fill shown on the images.

Time to Fill

Recall, the time to fill was only a function of bolus volume because of the time required to open the GPJ. The viscosity effect on the time to fill is not dependent on the time to open the GPJ. The increase in time required for the higher viscosity fluids to fill the pharynx occurs between the GPJ being fully open and the point of fill. This suggests the velocity of the bolus head is greater for the lower viscosity fluid. The increased volumetric flow rate and velocity for the lower viscosity fluid at the GPJ supports this observation. More of the bolus is transported early in the swallow for the low viscosity bolus. This effect is largely due to inertial effects; inertial effects become more significant for fluids with lower viscosity. Low viscosity fluids require much less force to transport than higher viscosity fluids.

Time Between GPJ Closure and UES Opening

Our data show that the time between the closure of the GPJ and opening of the UES is a function of bolus volume and viscosity. This is essentially a measure of bolus length, or the wavelength of peristalsis. As the viscosity of the bolus increases, the duration between GPJ closure and UES opening decreases, hence, more viscous boluses do not spread out as much as lower viscosity boluses. This observation is supported by Dantas, *et al.* (1990). As mentioned above, they measured bolus length in the mouth and pharynx for two fluids similar to our low- and high-viscosity samples. They found the length of the bolus in the pharyngeal chamber to be 62.9 ± 2.5 mm and 56.5 ± 1.8 mm for the low- and high-viscosity fluids, respectively. This effect is also due to the increased significance of viscous terms in the equations of motion.

Pharyngeal Clearance

The pharyngeal clearance is a measure of the peristaltic velocity. It is the time between GPJ closure and UES closure. This duration increases with increasing viscosity indicating that the velocity of peristalsis decreases with increasing viscosity. Literature data reporting peristaltic velocity for different viscosity boluses have not been found. Dantas, *et al.* (1990) report that there is a delay in UES opening for the higher viscosity bolus. They also report a significant increase in the duration of peristaltic pressure wave for higher viscosity boluses. Both of these effects could indicate a decreased peristaltic velocity, although the delay in UES opening is also due to the reduced bolus length discussed above. This effect, again, can be attributed to the increase in the significance of viscous forces. The increased stresses at the boundary between the bolus and pharyngeal constrictors due to the increased viscous forces could be slowing the response of the muscle action.

UES Opening Duration

The data from subject 4 indicate that the duration of UES opening is not

dependent on the viscosity of the bolus. Dantas, *et al.* (1990) find a significant increase in manometric UES relaxation duration for higher viscosity boluses. Their study used combined manometry and fluoroscopy to study the effects of bolus volume and viscosity. Each subject had two manometric probes placed in the pharynx of 1.5 mm OD each. As discussed previously, the presence of a catheter will effect the fluid flow. Two catheters will have an even greater effect. This measurement is based on manometric data, not fluoroscopy data. Hamlet, *et al.* (1996) also find that their timing data do not compare with the data from Dantas, *et al.* (1990). No manometric catheters were present in more recent study.

As stated above, the length of the bolus is shorter for the higher viscosity boluses. From this observation we would expect the duration of UES opening to decrease with increasing viscosity. This effect could be negated by the reduction in peristaltic velocity with increasing viscosity.

Figure 7.3.2 is a plot of the volumetric flowrate through, width of, and velocity through the UES for the three boluses. Again we see the effect of the assumptions made in the model. The flowrate through the UES is high before flow is seen on the fluoroscopic images. Recall the timing data discussed are based on the image analysis, not the model due to limitation in the model. After UES opening, we see similar flowrates for the three boluses. We do see that the UES opens wider for the higher viscosity fluids. This is to be expected in order to conserve mass since the bolus length is decreased for the higher viscosity fluid and the transport times are equal. The velocity through the UES is greater for the lower viscosity fluids near the period of maximum opening.

Total Time

The total time to complete the pharyngeal swallow increases with increasing viscosity. Unlike the effect of bolus volume, this is not due to increase GPJ or UES

opening duration. This effect can be attributed to the increase in time to fill and the increase in pharyngeal clearance. Both of these effects can be attributed to the greater significance of viscous forces in the equations of motion. This effect is demonstrated beautifully in the MPEG movies, low10.mpg, mid10.mpg, and high10.mpg, for the low-, mid- and high-viscosity fluids included on the CD with this dissertation. Figures 7.3.3 and 7.3.4 show representative frames from the low-, mid-, and high-viscosity simulations. We see that the recirculations in the fluid disappear in the mid- and high-viscosity simulations. Recirculations are an indication of the significance of inertial forces. Inertial forces dominate over viscous forces for lower viscosity fluids (see section 3.4).

Recall from section 3.5 that the Reynolds number can be calculated to estimate the importance of inertial effects. The Reynolds number is estimated in section 4.2.3 to be approximately 12 using data reported by Li, *et al.* (1992). Viscosity and density data for the fluids used in our studies were presented in section 6.2. Using the data for these fluids give Reynolds numbers of 14.4, 0.44, and 0.057 for the low-, mid-, and high-viscosity swallows, respectively. Section 3.4 discussed why the inertial terms in the equations of motion cannot be ignored for Reynolds numbers greater than one. For Reynolds numbers less than one, the viscous forces become more important. The Reynolds numbers calculated above show that the viscous forces outweigh the inertial forces for the mid- and high-viscosity boluses. For our low-viscosity sample, the inertial effect contribute significantly and the viscous forces become less important.

7.3.2.--Pressures and Stresses

Figure 7.3.5 is a plot of the pressure history at the center node near the level of the entrance to the larynx over the entire course of the swallow. The pressure for the high-viscosity bolus is dramatically higher than the low-viscosity bolus. The largest peak can be attributed to the effect of switching from the filling simulation to the moving boundary simulation. In the moving boundary simulation, the boundary condition at the UES is

free. The initial condition in the moving boundary is to read the velocity and pressure at every node from the last time step of the filling simulation. In addition to the effects of this assumption discussed in section 7.2.2, large velocities in the narrow region of the UES at this time will produce a large pressure drop. As mentioned previously, the large pressures and velocities at this point are reduced when the nodes on the boundary of the UES begin to move widening the opening.

Figure 7.3.5B and C show the pressure profiles during the filling simulation and moving boundary simulation after the UES opens, respectively. These plots show that the pressure is strong function of the fluid viscosity. In fact, the pressure is directly proportional to the viscosity. This is to be expected from a mathematical standpoint. Many analytical solutions for simple flow problems demonstrate this functionality including flow through a cylinder (Hagen-Poiseuille law), flow in an annulus, peristaltic flows, and squeezing flow (see section 3.6). Recall that the analysis for squeezing flow also showed the pressure to be inversely proportional to the separation to the third power. This predicts that the pressure will increase dramatically as the walls come together at a significant velocity. This explains the various larger peaks during the moving boundary simulation. The peaks can be attributed to the closure of the pharyngeal lumen at differing velocities at various levels. The greater the velocity of the walls coming together, the more profound the effect on the pressure profile.

There have been limited studies on the effect of viscosity on manometry measurements. As mentioned previously, Dantas, *et al.* (1990) did a combined videofluoroscopy and manometry study on boluses with similar properties to our low- and high-viscosity samples. They report pressures measured 1 cm upstream from the UES during trans-sphincter flow. For their 10 mL, low-viscosity bolus, they measure a pressure of about 8 mmHg. The pressures from the computer simulations near the entrance of the larynx while the UES is open is the closest comparable data. The results

from the low-viscosity, 10 mL simulation around zero mmHg between about -15 to 15 mmHg. The pressure measured for the 10 mL, high-viscosity bolus by Dantas, *et al.* (1990) is about 23 mmHg. The data from the simulations fluctuate greatly between 0 and 1,600 mmHg, averaging about 220 mmHg, for the high-viscosity sample while the UES is open at the level of the laryngeal entrance. The data from Dantas, *et al.* (1990) do not show a direct dependence on the viscosity of the bolus. Limitations of manometry measurements cannot fully explain this large of a discrepancy. There must be some physical reason not accounted for in the model for this large of a difference. Two possible explanations are considered. One explanation is the presence of air. The second could be due to the effect of a lubrication layer within the pharynx.

Our model and the analytical solutions discussed above assume incompressible flow (constant density). Air is compressible; as the pressure increases, the volume decreases. Two studies investigate what happens to the air in the pharyngeal chamber during swallowing. Ergun, *et al.* (1993) applied ultrafast computerized tomography to visualize the cross-section of the pharyngeal chamber during swallowing. They estimate the amount of dead space (air) just as the nasopharynx and larynx seal prior to bolus propulsion to be 14.0 ± 3.0 mL. This value was averaged over data from 7 male subjects and is reported to be highly variable between subjects. They conclude that approximately 15 mL of air is transported into the esophagus with each swallow. It could be suggested that the air is transported to the esophagus in this study because the subjects were in the supine position during this study. One could argue that in the upright position, the air rises above the bolus and is not swallowed due to density differences. This argument is invalid for two reasons. First, the pharyngeal constrictors completely obliterate the pharynx at every level to ensure complete bolus transport. Second, Gramiak, *et al.* (1967) measure nasal pressure changes during swallowing and find that the pressure decreases significantly when the passageway to the nasal cavity reopens after pharyngeal

peristalsis. This indicates that the air present in the pharyngeal chamber prior to the swallow is transported to the esophagus. If the air is not transported to the esophagus, this pressure decrease would not be seen. The negative pressure measured is due to the re-expansion of the pharyngeal chamber. The maximum negative nasal pressure measured during oropharyngeal relaxation was on the order of 10 mmHg and did not vary significantly between bolus volume, consistency, or body position (supine vs. upright). Pouderoux, *et al.* (1996) also investigate what happens to the air during swallowing via ultrafast CT scans in the esophagus. They find that and average of 17.7 mL of air is swallowed with a 10 mL liquid bolus.

The presence of air in the pharynx would result in pressures less than predicted with the mathematical model. Increased stresses within the fluid could be relieved by compression of the air. We can show through analysis of the data in the literature that the air does relieve some of the pressure. Ergun, *et al.* (1993) show that the fraction of the area integrated over time taken up by air is reduced with increasing bolus volumes. Dantas, *et al.* (1990) show that the intrabolus pressure becomes a much stronger function of viscosity as the bolus volume increases. As the relative volume of bolus to air increases, the less able the air is to relieve the pressures within the bolus. The air is reducing the bolus pressures during the pharyngeal phase of the swallow more for the lower volume boluses than the higher volume boluses. This also explains why much of the data in the literature show that the pressure increases with increasing bolus volume, yet the model does not predict this behavior.

Although our protocol does not investigate the viscosity effect for different volume boluses, we can show that the pressures are not directly proportional to the viscosity when air in present by comparing the pressures during the filling simulation. In figure 7.3.6B the pressure at the level of the larynx during fill does not show a direct proportionality to viscosity. The closest comparable literature data are from Shaker, *et al.*

(1993). They measured the intrabolus pressure amplitude near the level of the larynx for 10 mL water and 10 mL mashed potato swallows. The maximum amplitude prior to the large upstroke indicating peristalsis for the water and potato are reported as 5.7 ± 1.3 mmHg and 16.8 ± 3.1 mmHg, respectively. This is the pressure wave seen as the bolus begins to pass the manometric sensor and thus, is comparable to pressures calculated during the filling simulation. Although the properties of the mashed potatoes is unknown, we know the viscosity of water is about 1 cP and that mashed potatoes are much more viscous than water.

A second possible explanation for the discrepancy between the pressures predicted by the model and pressures measured with manometry could be due to a thin lubrication layer coating the walls of the pharynx. Brasseur, *et al.* (1987) derive an analytical solution for peristaltic flow including a peripheral layer with a different viscosity assuming the lubrication approximation. They show that the pressure drop is not as strong a function of viscosity when the viscosity of the lubrication layer is greater than the interior fluid. This effect is probably not as great the effect of the air compressing during the swallow.

The stresses near the entrance to the larynx (figure 7.3.6) show a similar behavior as the pressure data. Recall that these stresses are the normal force normalized over the length of the elements near the laryngeal entrance. The magnitude of the normal force can be entirely attributed to the pressure forces for Newtonian fluids, thus, the same analysis applies as given above. Literature data show that the squeeze of the pharyngeal lumen on the catheter does increase in magnitude and duration with higher viscosity swallows (Shaker, *et al.* 1993; Dantas, *et al.* 1993) suggesting the muscles do respond to the higher stresses within the bolus.

7.4.--Head Position

Our protocol is designed to investigate the effect of head position on the normal

pharyngeal swallow. It has been documented in the literature that flexion of the head (head tilted forward) helps to protect against laryngeal penetration. Welch, *et al.* (1993) measured changes in the dimensions of the pharynx due to head flexion. They hypothesize that the airway is protected more in the chin-tuck position due to the posterior shift of anterior pharyngeal structures. The effect is to narrow the opening of the larynx. The tongue base is also positioned back further over the entrance of the larynx. It has also been observed that the vallecular space is widened with head flexion (Logemann 1983). This increased area in the valleculae can hold more of the bolus giving the larynx additional time to close before penetration can occur. It is also suggested that head extension (head tilted back) increases the risk of aspiration. With the head in this position, the pharyngeal passageway is aligned with the airway. Defective closure of the larynx has been observed with the head extended (Ekberg 1986).

Based on the theory of the effect of head position on swallowing, we cannot expect our mathematical model to provide us with any new insight on why aspiration may occur. The main feature described that we may be able to investigate further with our mathematical model is the effect of the widening of the vallecular space. The time it takes to fill the pharynx could be affected by the change in geometry. This effect will be more profound for lower viscosity fluids as discussed above. Our study used 10 mL of the mid-viscosity fluid to study head position. Because of the dominance of the viscous forces in this flow situation, large differences in the rate of fill were not seen with head position. The protocol has since been modified to use the lower viscosity fluid to study this effect.

Table 7.4.1 details the timing data for the three head positions. We can see that the time to fill is only dependent on the time to open the GPJ. The UES opens earlier compared to the GPJ being fully open for the forward position. This is most likely due to the decreased distance between the GPJ and UES in this position. The geometric

differences due to head position are easily observed in the MPEG movies, for10.mpg, mid10.mpg, and back10.mpg, included on the CD version of this dissertation. Representative frames are shown in figure 7.4.1. Due to the geometric changes between the head positions, we cannot provide a comparative analysis of the duration of events.

Pressures calculated at the level of the entrance to the larynx are shown in figure 7.4.2. The pressure is greater for the head tilted back than in the forward or neutral positions while the UES is open. Figure 7.4.3 shows the normalized normal force near the entrance to the larynx. This plot also suggests the forces are reduced for the neutral and chin-tuck positions. More investigation is needed to determine the significance and reproducibility of these results.

7.5.--Gravity

Many studies have investigated the effect of body position on swallowing. Our protocol did not investigate subjects in the supine position; however, we can investigate the significance of gravitational forces easily with the mathematical model. In the model presented in chapter 5, we include the forces of gravity in the equations of motion. We can see whether or not the gravitational forces are significant just by solving the model without these terms in the equations.

Figure 7.5.1 shows the pressure histories at the level of the entrance to the larynx for the low-, mid-, and high-viscosity 10 mL swallows. These show the gravitational forces are more significant for the lower viscosity fluids. The difference in pressure can be attributed to the increased significance of the gravitational term in the equations of motion relative to the viscous terms. The question that needs to be answered is whether or not this has any significance on the flow field.

Figure 7.5.2 is a plot of the flowrate through the UES for the low-, mid-, and high-viscosity 10 mL boluses. The inclusion of the gravitation terms in the equations of motion has no effect on the flow through the UES. Recall, this reflects the solution of the

moving boundary simulation only; the UES is not open during the filling simulation. This is because we specify the flow situation with velocity boundary conditions in the moving boundary simulation. The only effect including gravity has is in the pressure profile; hence,

$$\frac{\partial p}{\partial z} - \rho g_z = \text{constant} \tag{7.5.1}$$

for the moving boundary problem. This is not true for the filling simulation. The flow situation is not specified because the position of the interface between the bolus and air is unknown. This position has the potential to be affected by gravitational forces.

Figure 7.5.3 shows the position of the interface at t = 0.11 seconds for the low-viscosity, 10 mL swallow during the filling simulation with and without gravitational forces included in the equations of motion. As can be seen from this figure, gravity has an effect on the rate at which the front advances. Figure 7.5.4 is a similar plot for the mid-viscosity, 10 mL swallow. Including gravitational forces in this simulations seems to have no effect on the advancement of the front. This effect can also be attributed to the increasing significance of the viscous forces with higher viscosity fluids. The same effect is seen for the high-viscosity, 10 mL swallow. In short, gravitational forces are significant for the lower viscosity fluids. The effect is to increase the rate of fill and reduce the static pressure within the bolus.

Ingervall and Lantz (1973) found that the time required for the bolus to pass through the pharynx for lower viscosity fluids is shorter in the upright position than in the supine position. Viscous fluids (barium paste) showed no effect of body position on transport time. These results agree with what is predicted by the mathematical model.

Dejaeger, *et al.* (1994) used manofluorography to study the effect of body position. They found that the integral of the pressure profile over time near the tongue base, entrance of the larynx, and UES increase in the supine position. These values increased further in the upside down position. The amplitude of the pressure did not

change significantly between positions. Since the pressure amplitudes did not vary but the integral of the pressures over time did, one would have to assume that the duration of the pressure waves increased. They do report an increase in pharyngeal transit time from upright, to supine, to inverted, but do not report this as significant. The properties of the bolus are not reported; it is only stated as 10 mL of liquid barium. These data could indicate a difference in the response of the musculature involved due to position. If the response is different, the movement of the bolus boundaries would change and thus, the boundary conditions in the mathematical model should change. This could be verified by including having the subject swallow in the protocol for fluoroscopy studies.

Significant results from Johnsson, *et al.* (1995) include changes in UES opening duration and size, and intrabolus pressure with body position. The UES opened wider for a shorter time period in the supine and inverted positions. The intrabolus pressure measured above the UES increased dramatically from the erect to the supine position, and even further for the inverted position. These results suggest the bolus holds together better in the supine and inverted position. The sensor will measure a greater pressure if it is in contact with the bolus only and not air. The duration of bolus passing through the UES will be shorter for a bolus that holds together better. A shorter bolus of the same volume will require the UES to open wider in order to transport in the same or less amount of time. They also report that the body position has no significant effect on bolus length, velocity of the bolus head and tail, oral transit time, pharyngeal transit time, or the amplitude or duration of the contraction waves. No variation of bolus length disagrees with their data on UES transport. If the UES opens wider for a shorter period of time, the length must be reduced. These data also support the above analysis. The mathematical model shows that not including gravity in the simulation results in a shorter bolus. The influence of gravity should be studied further to verify these theories by applying the model to fluoroscopy data from supine and inverted positions.

7.6.--Mesh Refinement

It is common practice to check the accuracy of a numerical solution by refining the mesh to see if the solution changes. If the solution changes, then the model is inaccurate and more nodes should be added to the mesh. This procedure can be repeated until there is no longer any variability between mesh refinements.

Our model uses 9 noded-quadrilateral elements. In each simulation, the anterior and posterior boundaries have 65 nodes each (32 elements). The GPJ and UES have 21 nodes (10 elements). We are somewhat limited to the number of nodes by the software. Each node on the anterior and posterior boundary has a prescribed x- and y-velocity assigned to it. These velocities vary between nodes and with time. We prescribe these velocities using the time function command. There is a maximum 300 time functions allowed in each simulation. This results in a maximum of 75 nodes on each side. Since the boundary condition at the inlet is also a function of time, we are limited to 73 nodes on each side. The velocities could be prescribed with a user-defined subroutine, but this would be very involved since there is no simple functionality that describes the movement of these nodes with time.

We chose to verify the numerical accuracy with the low-viscosity, 10 mL filling simulation. This is the most difficult simulation from a numerical standpoint due to the free surface and the increased importance of the non-linearity due to inertial effects. Also, since there is no prescribed movement in the filling simulation, we are not limited to the number of nodes in the mesh. For the simulation using a refined mesh, the number of nodes at the GPJ and UES is increased to 31. The number of nodes on the anterior and posterior sides is increased from 73 to 107. This more than doubles the number of nodes in the mesh from 1365 for the regular mesh, to 3317 for the refined mesh. Velocity vector plots for the same point in time late in the simulation are shown in figure 7.6.1. These plots show that the front of the bolus has advanced to the same position for both

the regular and refined meshes. Also notice the maximum velocities are the same. Figure 7.6.2 shows the pressure profile at the level of the laryngeal entrance for the regular and refined meshes. Notice that the pressure peaks at a slightly greater value for the refined mesh, but other than this small discrepancy, the profiles are similar. This plot also indicates that there are no significant variations in the movement of the front since the pressure rises when the fluid arrives at this location at the same time for both simulations. From the results demonstrated in these figures, it can be concluded that 32 by 10 elements results in an accurate solution for all simulations.

7.7.--Reproducibility

The results of the model discussed in this chapter are from a single human subject. To lend validity to the model, we need to know how it will vary between subjects. Can we expect the same results from all normal subjects? Should we not since we know there is a great deal of variability between subjects? To answer these questions, we applied the same techniques used on subject 4 to another study (subject 6).

Table 7.7.1 and 7.7.2 detail the timing of the low-viscosity, 10 mL swallow for subject 4 and subject 6. These data demonstrate the variability between subjects. Specifically, notice the difference between the point of fill and the GPJ fully open; filling the pharynx requires more time for subject 6. Also notice the difference in timing of the UES opening and the duration between GPJ close and UES opening. The UES opens earlier for subject 4. The GPJ and UES have to be open at the same time for a longer duration for subject 4. All of these data suggest that the pharyngeal volume of subject 6 is greater than subject 4. Table 7.7.3 shows the difference in dimensions for the two subjects. Notice that the height between the GPJ and UES is much greater for subject 6 than subject 4. The maximum dimension of the GPJ is also greater for subject 6. The UES dimension is essentially the same between the subjects. These data confirm the pharyngeal chamber is larger for subject 6 and therefore explains the differences in the

timing data.

Figure 7.7.1 is a plot of the volumetric flowrate through, width of, and velocity at the GPJ for the two subjects. Again note that figure 7.7.1B indicates the GPJ closes before stated in table 7.7.1 for subject 4, but flow can still be seen even though the GPJ has reached the minimum width. This figure also shows the width of the GPJ is greater for subject 6. Notice that the flowrate and velocity show similar behavior at the GPJ between the two subject except both are higher for subject 4. Figure 7.7.2 is a plot of the volumetric flowrate through, width of, and velocity at the UES. Notice the opening of the UES is very similar between the two subjects except the UES opens earlier for subject 4. The velocity and flowrate show similar behavior also ignoring the time where the UES is assumed open when no flow is seen on the fluoroscopic images.

Figure 7.7.3 shows the pressure histories for both subjects for the entire time (A), during filling (B), and while the UES is open (C). The pressure magnitudes are quite comparable between subjects. The magnitudes of the stresses near the entrance to the larynx are also quite similar (see figure 7.7.4). These pressure and stresses demonstrate that the mathematical model can predict similar behavior between subjects. The timing, flow and geometrical data show the flexibility of the model between subjects.

7.8.--Summary

Applying the mathematical model to data from a normal subject has provided additional insight on the effects of bolus volume and viscosity, head positioning, and gravity on the pharyngeal phase of swallowing. The accuracy of the model is verified by refining the mesh and applying the same modeling techniques to a second normal subject. This section highlights what has been learned from the model.

A great deal of information has been published on the effect of bolus volume on the pharyngeal swallow. Data from this study agree with much of the literature data with a few exceptions. Differences in the timing data can be attributed to differences in

pharyngeal geometry between subjects. The pressures predicted with the model show no correlation with bolus volume. The pressures measured with manometry increase with increasing volumes because the relative ratio of bolus to air is reduced. Our model does not include the air during the moving boundary simulation, thus we should not expect to see any effect of volume on the pressures measured. The major effect of bolus volume is to increase the duration of GPJ and UES opening. The pharyngeal phase of swallowing takes longer for larger volumes simply because there is more fluid to transport. The GPJ, pharynx, and UES do open wider for larger volume boluses, but not enough to transport these boluses in the same amount of time.

The model predicts the pressures within the bolus to be directly proportional to the viscosity. Analytical solutions of similar flow situations predict the same behavior. Manometry measurements do not. This is because a substantial volume of air is swallowed with every bolus. This volume of air is roughly equal to the volume of the pharyngeal chamber prior to swallowing (Pouderoux 1996). The air has the effect of reducing pressures within the bolus by compressing.

The major effect of viscosity on the pharyngeal swallow is to reduce the transport time by reducing the rate of fill and pharyngeal clearance. This can be attributed to the increased significance of viscous forces. The viscous forces dominate over inertial forces for Reynolds numbers less than 1. For pharyngeal peristalsis, this occurs at a kinematic viscosity of 9 cm^2/s or less for a 20 mL bolus using the parameters discussed in section 4.2.3.

Changing the position of the head during swallowing results in geometrical modifications that influence the filling of the pharynx. Literature shows that the entrance to the larynx is better protected in the chin-tuck position and less protected in the extended position. With our protocol, we were unable to predict any significant differences between head positions because we used the mid-viscosity fluid. With this

fluid, no significant change in the rate of fill was observed due to the dominance of viscous forces. The model would be best applied to flow situations where inertial effects are important. This would correspond to studies using the low-viscosity fluid.

While our protocol did not investigate subjects in the supine position, we were still able to study the effect of gravity on the pharyngeal phase of swallowing with the mathematical model. By doing so, it was determined that the effect of gravity is significant for the lower viscosity fluids only. The effect is to increase the rate of fill and reduce the static pressure within the bolus. These results concur with investigations reported in the literature.

The accuracy of the numerical method was verified by solving the most difficult simulation with a refined mesh and showing that the results did not change significantly. It was also demonstrated that the mathematical model is able to predict similar results in a second normal subject while having the flexibility to account for the geometric differences between subjects. The largest limitation of the model was determined to be the inability to move the boundary with two-phase flow. This limitation could be eliminated if we could move boundaries during the filling simulation. The result of this limitation is inaccurate predictions of the pressures and stresses within the pharyngeal chamber. It has also been discussed why the pressures measured manometrically have to be interpreted carefully due to the movement of the catheter and the presence of air throughout the phayrngeal phase of swallowing.

The next chapter discusses how the model can be applied to gain insight on swallowing disorders. Recommendations for improvements will be discussed in chapter 9.

Table 7.2.1.--Timing of Events Demonstrating the Effect of Bolus Volume.
Literature data from Kahrilas, *et al.* (1993).

EVENT	5 mL		10 mL		20 mL	
Time (s)	**Subject 4**	**Literature**	**Subject 4**	**Literature**	**Subject 4**	**Literature**
GPJ Opening	0.0	0.0	0.0	0.0	0.0	0.0
GPJ Fully Open	0.10	-	0.13	-	0.17	-
Fill	0.17	-	0.20	-	0.23	-
UES Open	0.30	0.26	0.27	0.27	0.3	0.28
GPJ Closed	0.27	0.34	0.33	0.38	0.47	0.42
UES Closed	0.67	0.85	0.83	0.88	0.93	0.93

Table 7.2.2.--Duration of Events Demonstrating the Effect of Bolus Volume

EVENT	5 mL		10 mL		20 mL	
Time (s)	Subject 4	Literature	Subject 4	Literature	Subject 4	Literature
Time to Open GPJ	0.10	-	0.13	-	0.17	-
GPJ Opening Duration	0.27	0.34	0.33	0.38	0.47	0.42
Time to Fill	0.17	-	0.20	-	0.23	-
GPJ Close - UES Open	-0.03	0.08	0.07	0.11	0.17	0.14
Pharyngeal Clearance	0.4	0.51	0.50	0.50	0.47	0.51
UES Opening Duration	0.37	0.59	0.57	0.61	0.63	0.65
Total Time	0.67	0.85	0.83	0.88	0.93	0.93

Table 7.2.3.--Comparison of UES Flow Duration

units (s)	5 mL	10 mL	20 mL
Subject 4	0.36	0.57	0.67
Kahrilas, *et al.* (1993)	0.59 ± 0.01	0.61 ± 0.02	0.65 ± 0.02
Cook, *et al.* (1989)	0.48 ± 0.05	0.55 ± 0.05	0.62 ± 0.07
Jacob, *et al.* (1989)	0.45 ± 0.01	0.50 ± 0.02	0.54 ± 0.03

Table 7.2.4.--Comparison of UES Dimension at Maximum Opening

units (cm)	Subject 4	Cook, *et al.* (1989)	Jacob, *et al.* (1989)
5 mL	7.0	11.0 ± 1.9	8.5 ± 0.5
10 mL	8.6	11.8 ± 1.6	10.5 ± 0.5
20 mL	13.2	13.3 ± 2.0	11.8 ± 0.4

Table 7.2.5.--Bolus Pressure at Maximal UES Opening
(from Cook, *et al.* 1989)

units (mmHg)	Upstream	UES	Downstream
5 mL	7.9 ± 2.1	3.8 ± 4.4	2.6 ± 2.5
10 mL	7.8 ± 2.1	5.1 ± 4.0	2.4 ± 3.0
20 mL	13.8 ± 2.1	13.8 ± 5.2	11.3 ± 2.1

Table 7.3.1.--Timing of Events Demonstrating the Effect of Bolus Viscosity

Time (s)	Low	Mid	High
GPJ Opening	0.0	0.0	0.0
GPJ Fully Open	0.13	0.13	0.13
Fill	0.20	0.23	0.23
UES Open	0.27	0.3	0.33
GPJ Closed	0.33	0.33	0.33
UES Closed	0.83	0.87	0.9

Table 7.3.2.--Duration of Events Demonstrating the Effect of Bolus Viscosity

Time (s)	Low	Mid	High
Time to Open GPJ	0.13	0.13	0.13
GPJ Opening Duration	0.33	0.33	0.33
Time to Fill	0.20	0.23	0.23
GPJ Close - UES Open	0.07	0.03	0.00
Pharyngeal Clearance	0.5	0.53	0.57
UES Opening Duration	0.57	0.57	0.57
Total Time	0.83	0.87	0.9

Table 7.4.1.--Timing of Events Demonstrating the Effect of Head Position on the 10 mL, low-viscosity swallow

Time (s)	Back	Neutral	Forward
GPJ Opening	0.0	0.0	0.0
GPJ Fully Open	0.10	0.13	0.10
Fill	0.20	0.23	0.20
UES Open	0.27	0.30	0.30
GPJ Closed	0.33	0.33	0.33
UES Closed	0.73	0.87	0.8

Table 7.7.1.--Timing of Events for the 10 mL, Low-Viscosity Swallow Demonstrating the Variability between Subjects

Time (s)	Subject 4	Subject 6
GPJ Opening	0.0	0.0
GPJ Fully Open	0.13	0.10
Fill	0.20	0.20
UES Open	0.27	0.30
GPJ Closed	0.33	0.33
UES Closed	0.83	0.83

Table 7.7.2.--Duration of Events for the 10 mL, Low-Viscosity Swallow Demonstrating the Variability between Subjects

Time (s)	Subject 4	Subject 6
Time to Open GPJ	0.13	0.1
GPJ Opening Duration	0.33	0.33
Time to Fill	0.20	0.20
GPJ Close - UES Open	0.07	0.03
Pharyngeal Clearance	0.50	0.50
UES Opening Duration	0.57	0.53
Total Time	0.83	0.83

Table 7.7.3.--Dimensions of Pharyngeal Chamber Demonstrating the Variability between Subjects

Length (cm)	**Subject 4**	**Subject 6**
Height of GPJ at fill	7.56	9.44
Width of GPJ at fill	1.45	1.80
Maximum width of UES	0.86	0.87

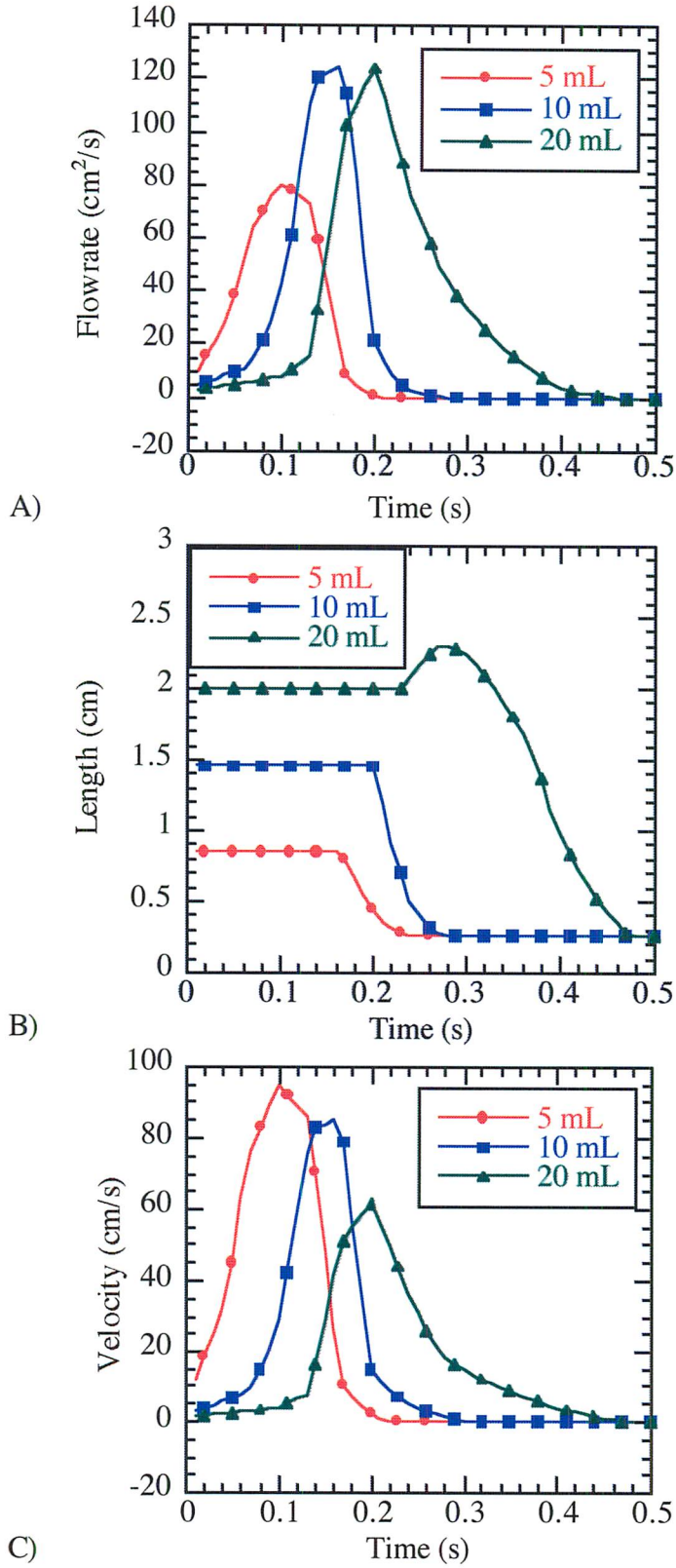

Figure 7.2.1.--Volumetric flowrate (A), width (B), and velocity (C) at the GPJ demonstrating the effect of bolus volume.

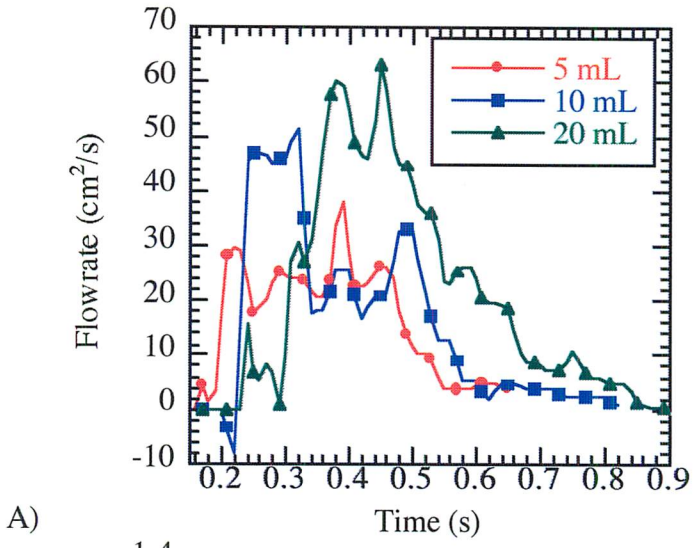

A)

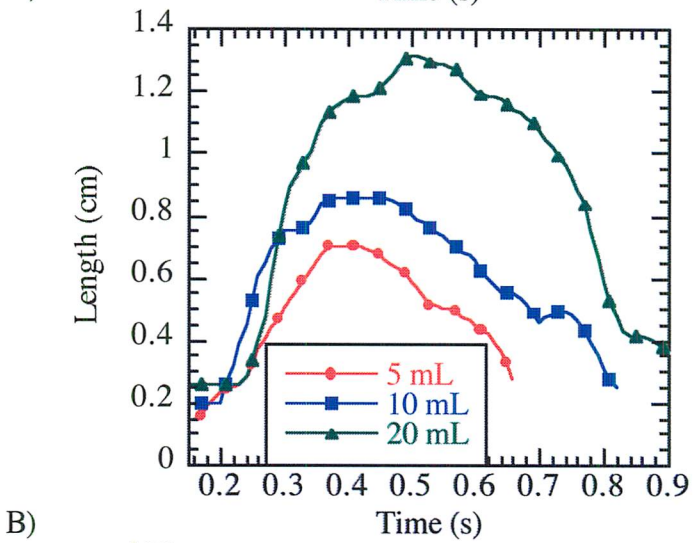

B)

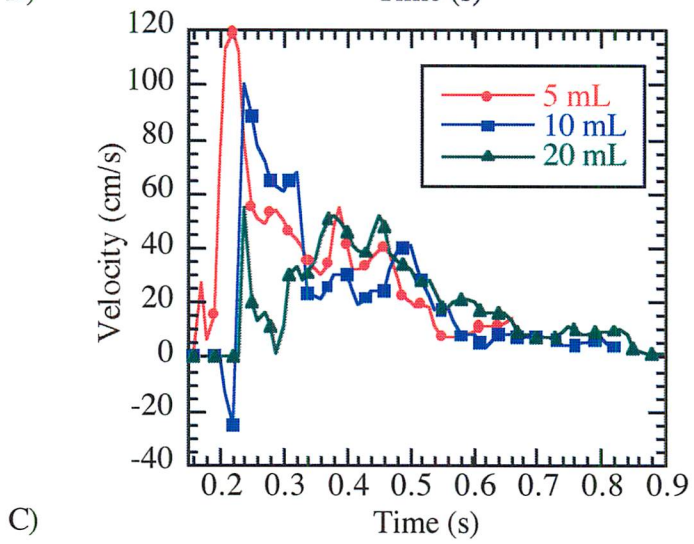

C)

Figure 7.2.2.--Volumetric flowrate (A), width (B), and velocity (C) at the UES demonstrating the effect of bolus volume.

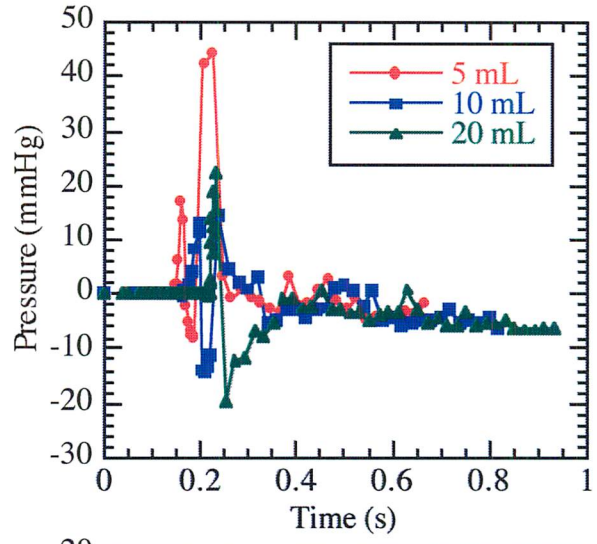

A)

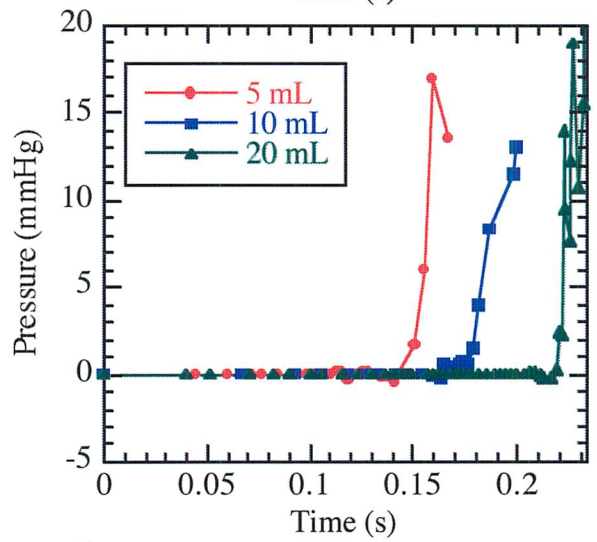

B)

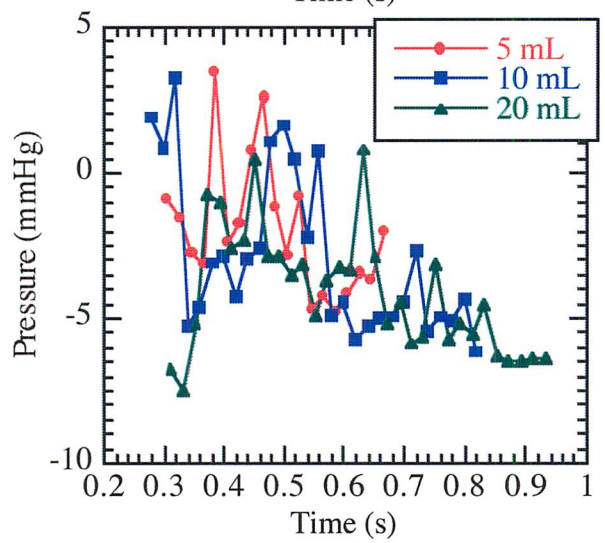

C)

Figure 7.2.3.--Pressure histories at the level of the larynx demonstrating the effect of bolus volume. (A) Total time, (B) Filling, (C) UES open.

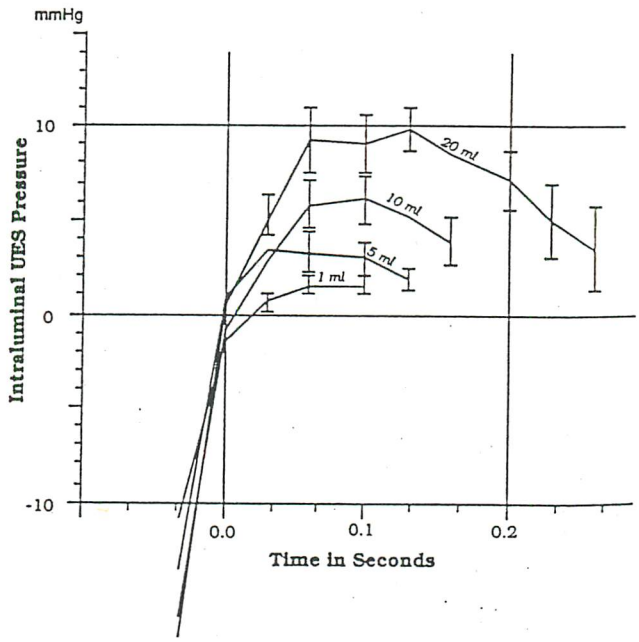

Figure 7.2.4.--Intrabolus pressure in the UES while sphincter area is increasing. (from Jacob, *et al.* 1989)

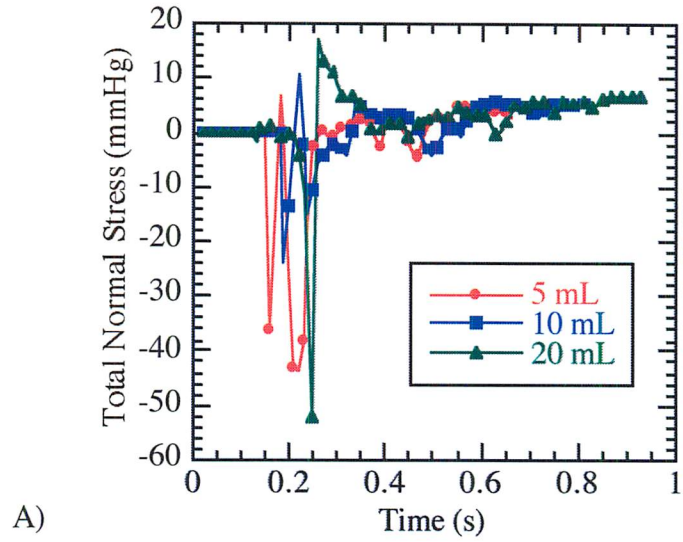

A)

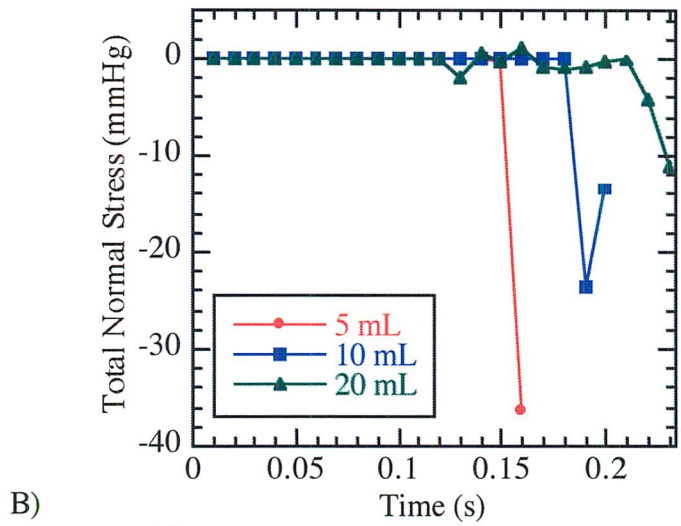

B)

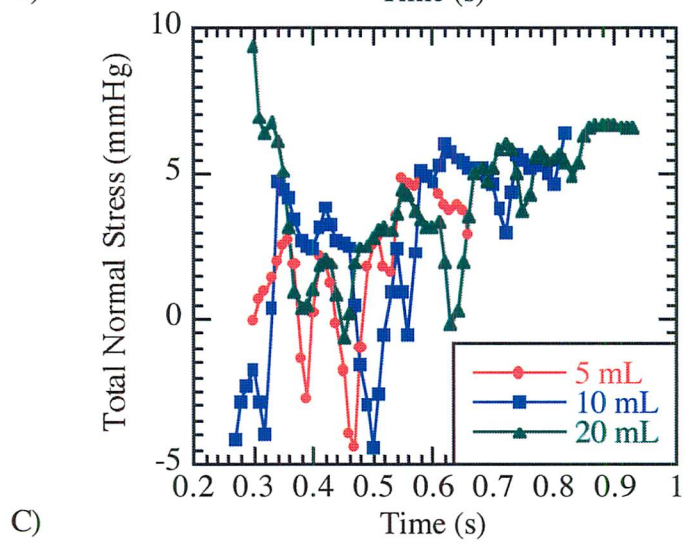

C)

Figure 7.2.5.--Total normal stresses at the entrance of the larynx demonstrating the effect of bolus volume. (A) Total time, (B) Filling, (C) UES open.

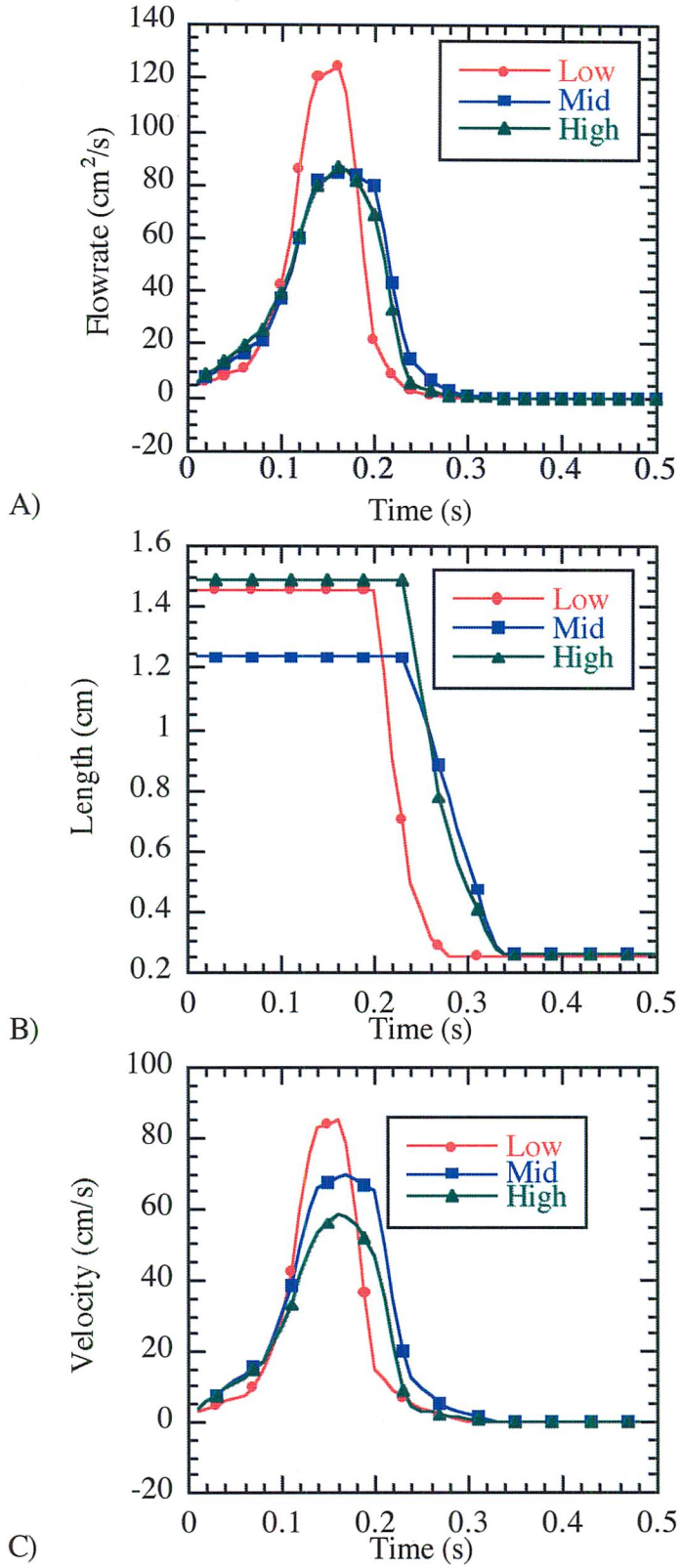

Figure 7.3.1.--Volumetric flowrate (A), width (B), and velocity (C) at the GPJ demonstrating the effect of bolus viscosity.

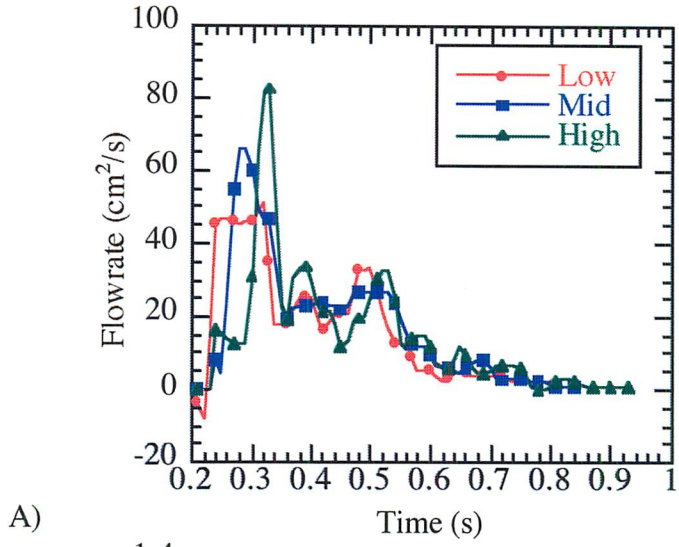

A)

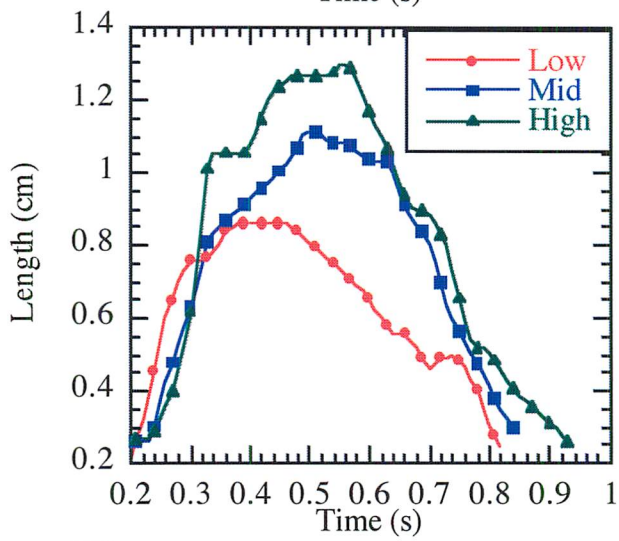

B)

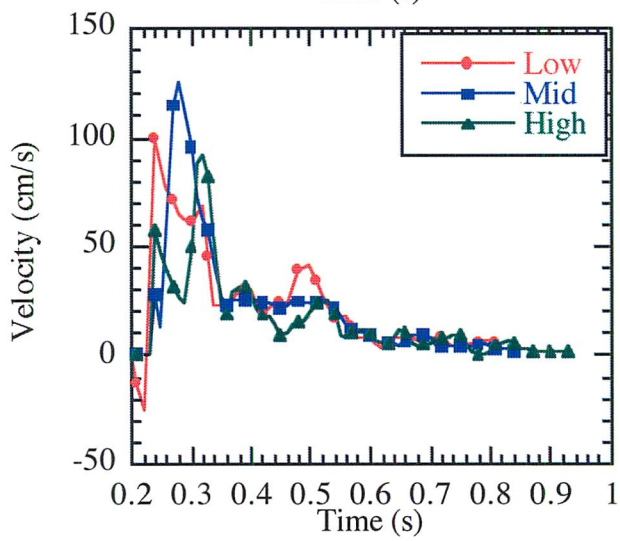

C)

Figure 7.3.2.--Volumetric flowrate (A), width (B), and velocity (C) at the UES demonstrating the effect of bolus viscosity.

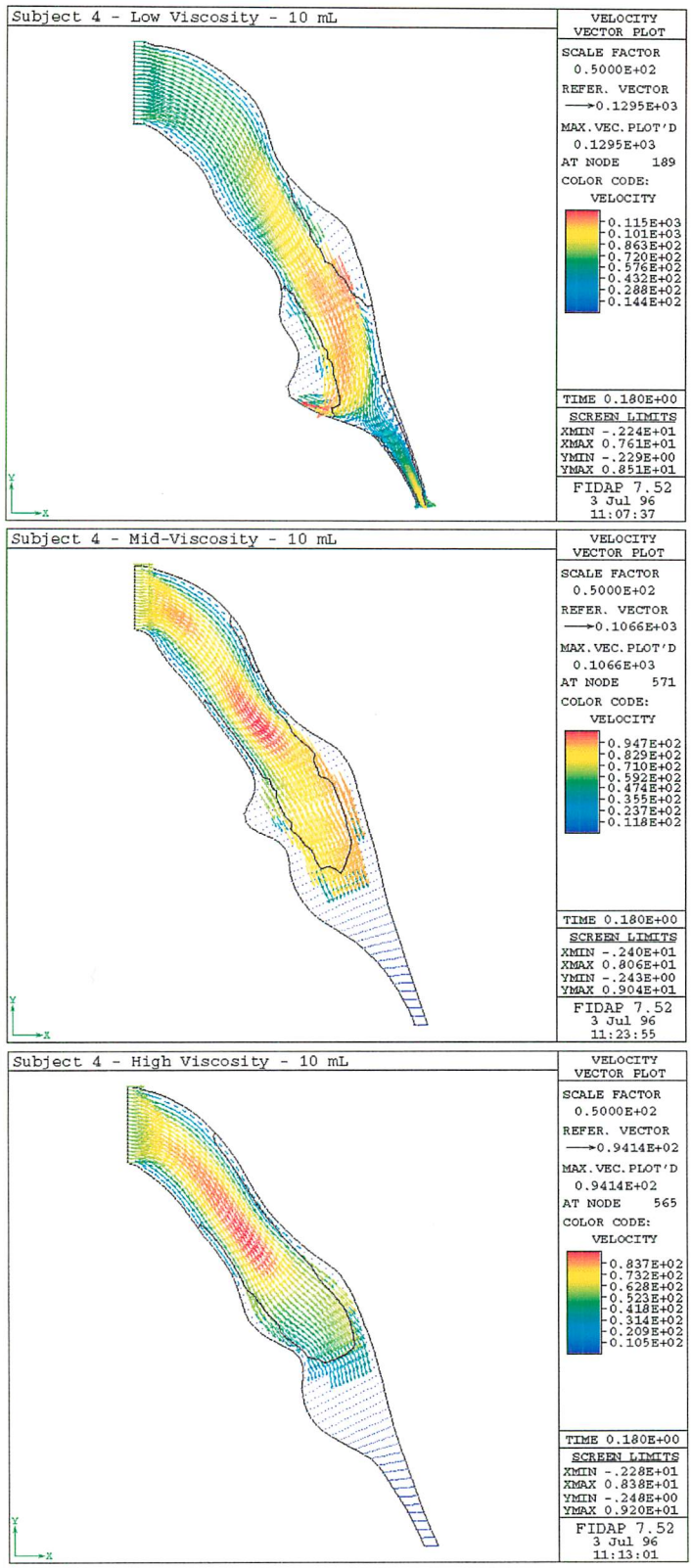

Figure 7.3.3.--Velocity vector plots at 0.18 seconds after GPJ opening for the low-, mid-, and high-viscosity fluids for 10 mL boluses demonstrating the effect of viscosity.

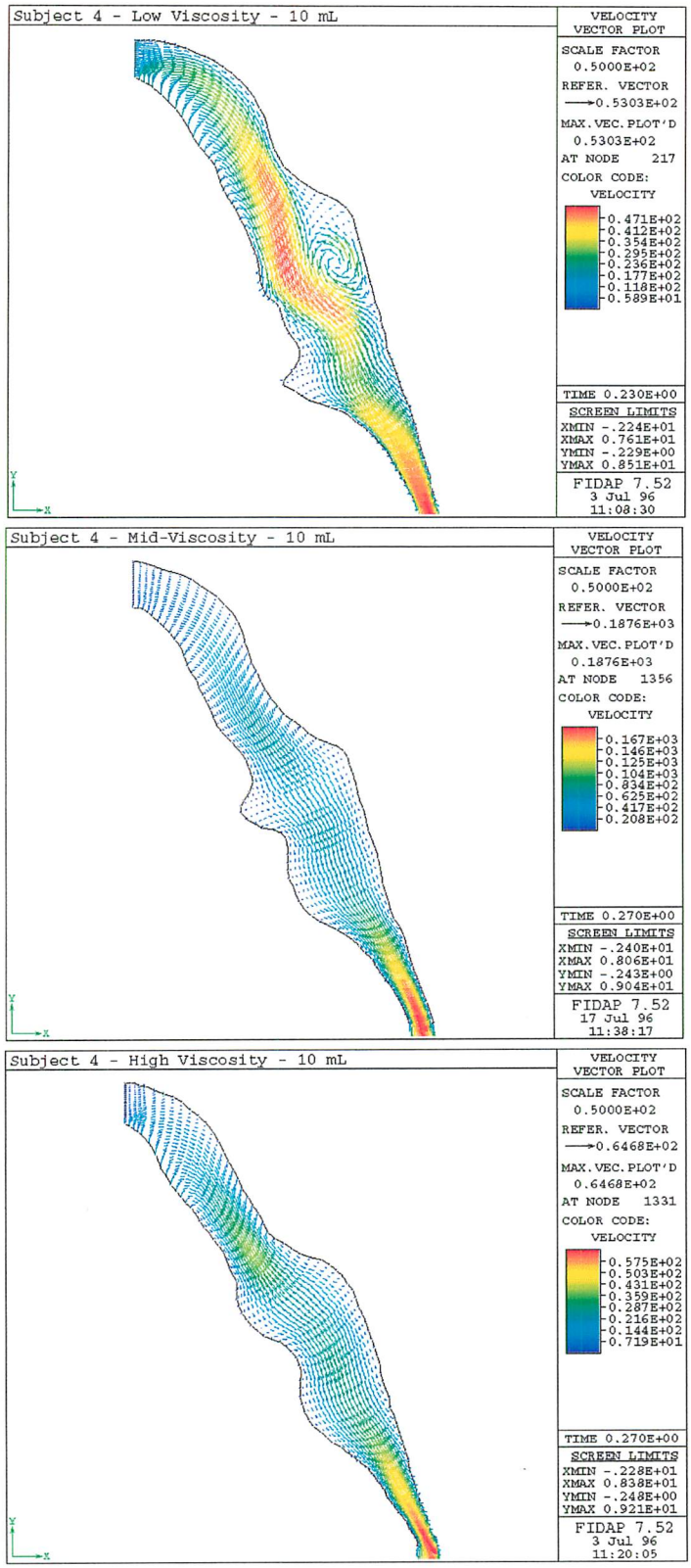

Figure 7.3.4.--Velocity vector plots at similar periods during peristalsis for the low-, mid-, and high-viscosity fluids for 10 mL boluses demonstrating the effect of viscosity.

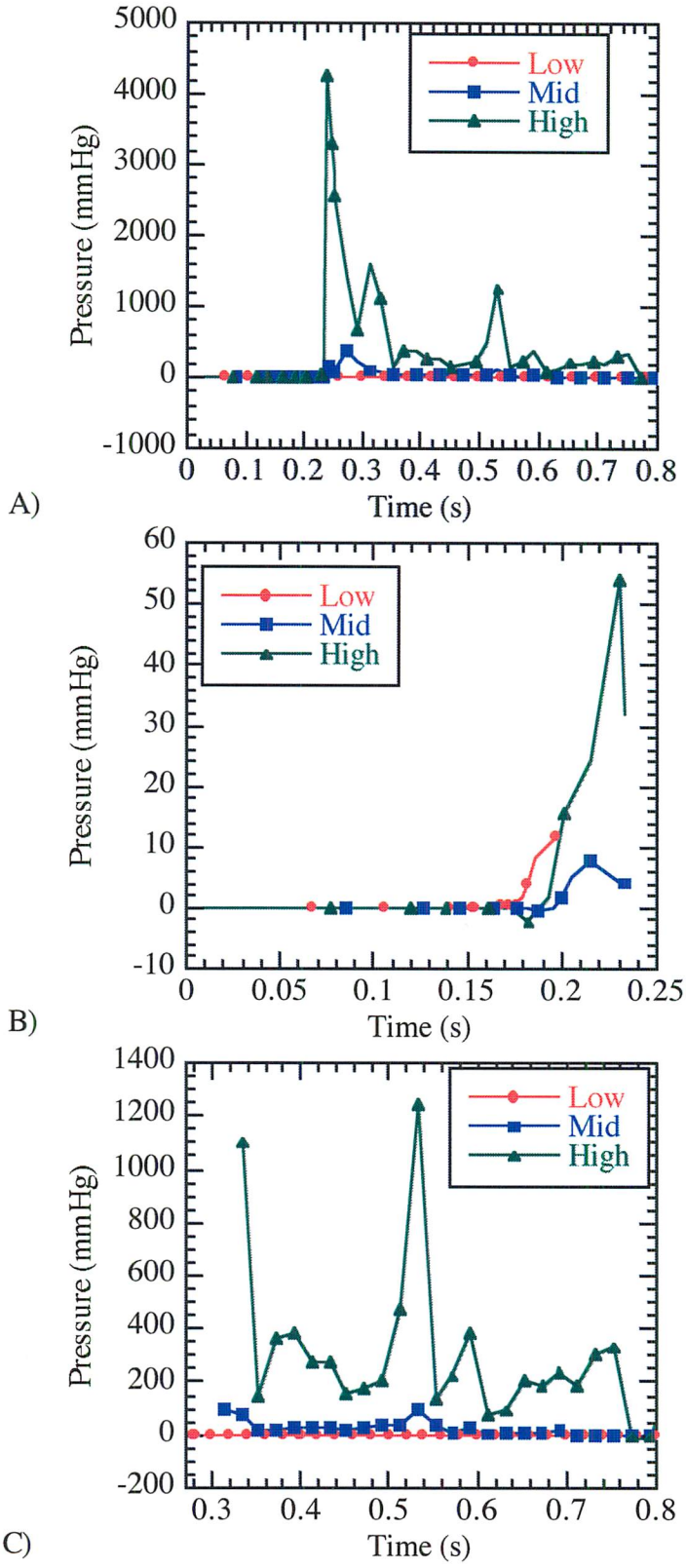

Figure 7.3.5.--Pressure histories at the level of the larynx demonstrating the effect of bolus viscosity. (A) Total time, (B) Filling, (C) UES open.

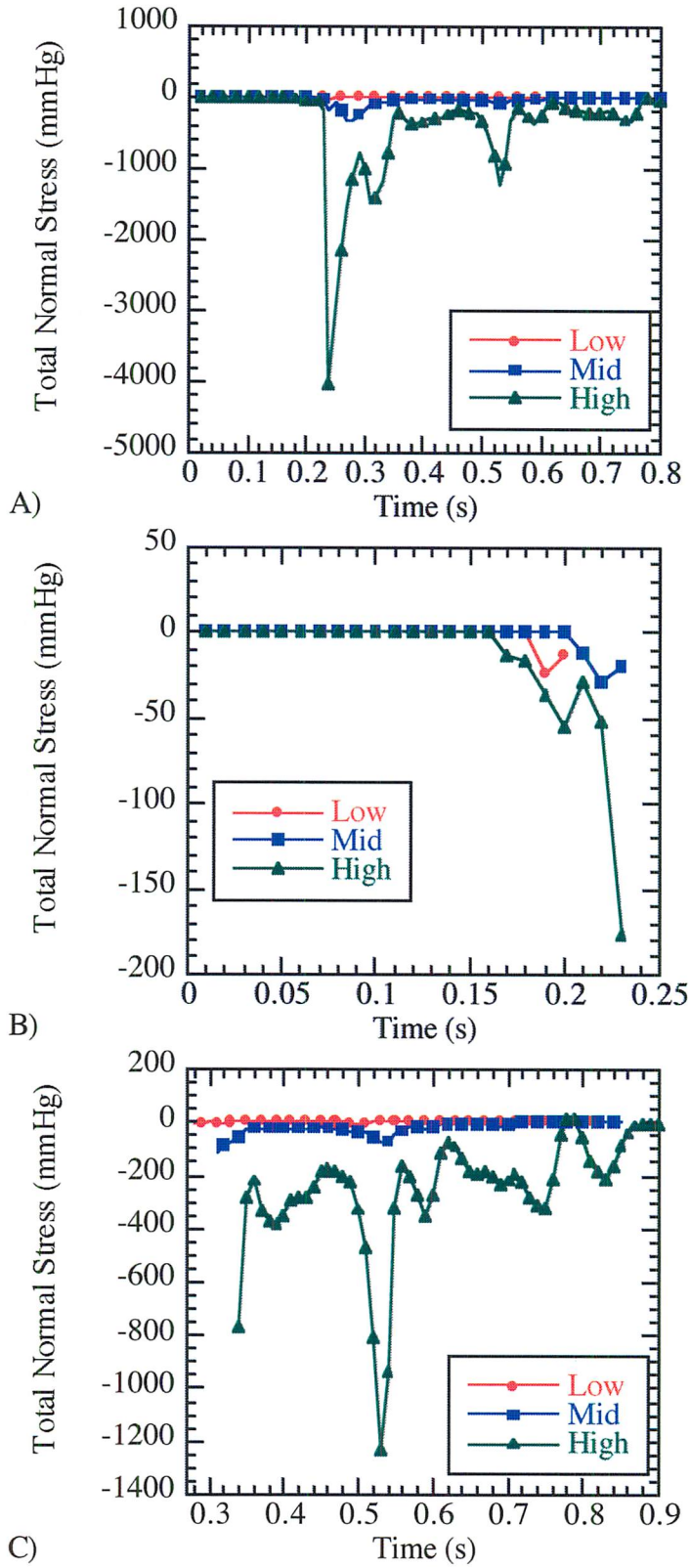

Figure 7.3.6.--Total normal stresses at the entrance of the larynx demonstrating the effect of bolus volume. (A) Total time, (B) Filling, (C) UES open.

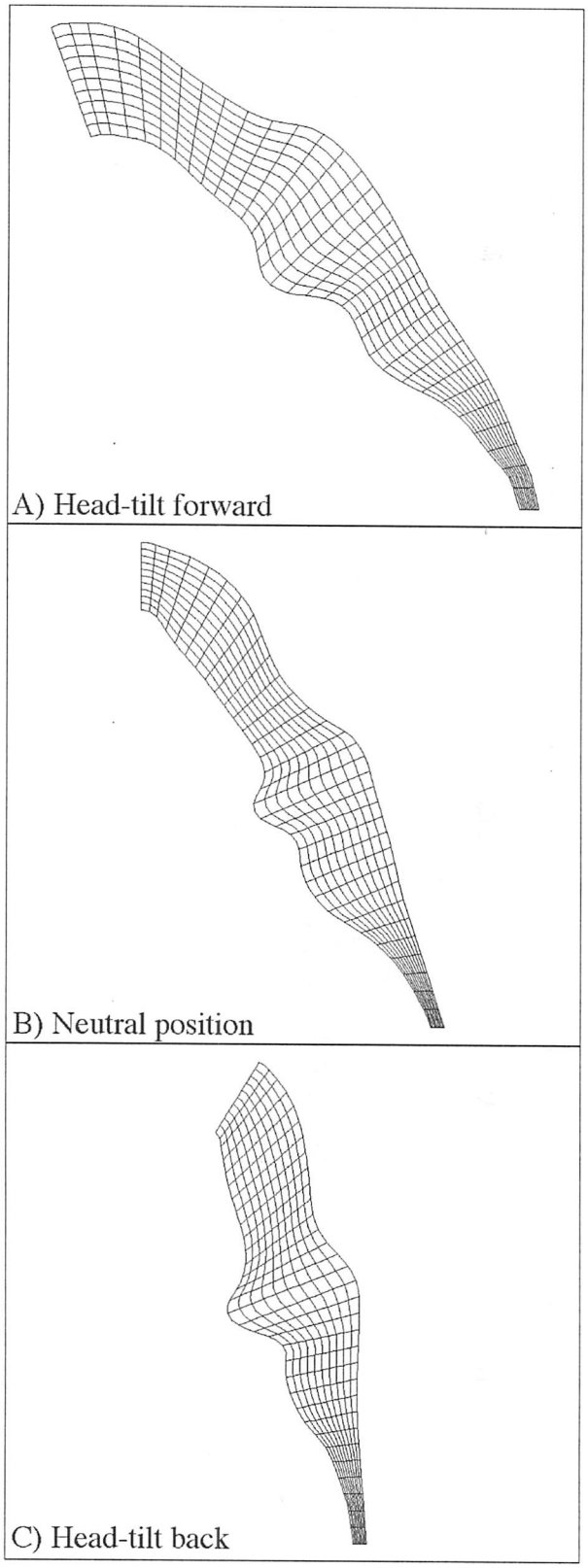

Figure 7.4.1.--Finite element meshes for the A) head-tilt forward, B) neutral, and C) head-tilt back positions demonstrating the geometrical differences at the point of fill.

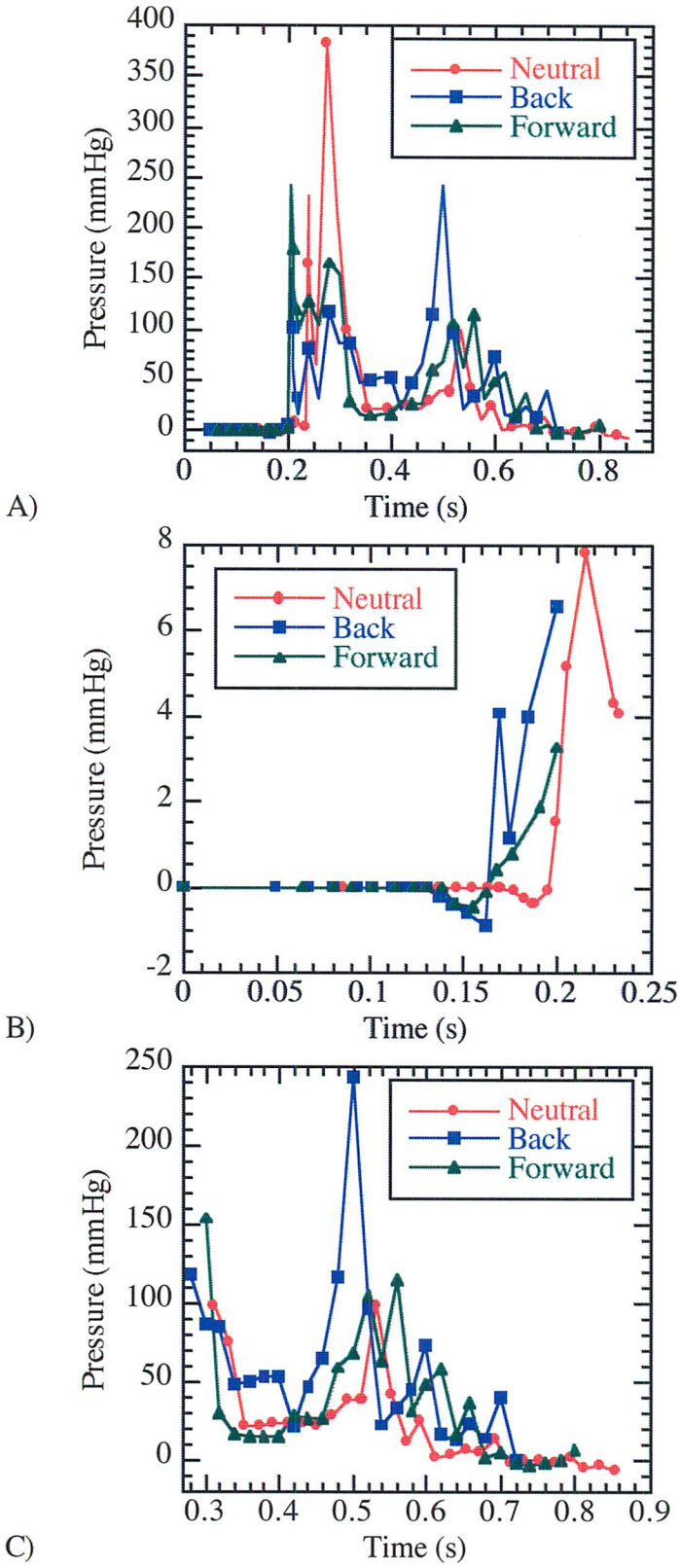

Figure 7.4.2.--Pressure histories at the level of the larynx demonstrating the effect of head position. (A) Total time, (B) Filling, (C) UES open.

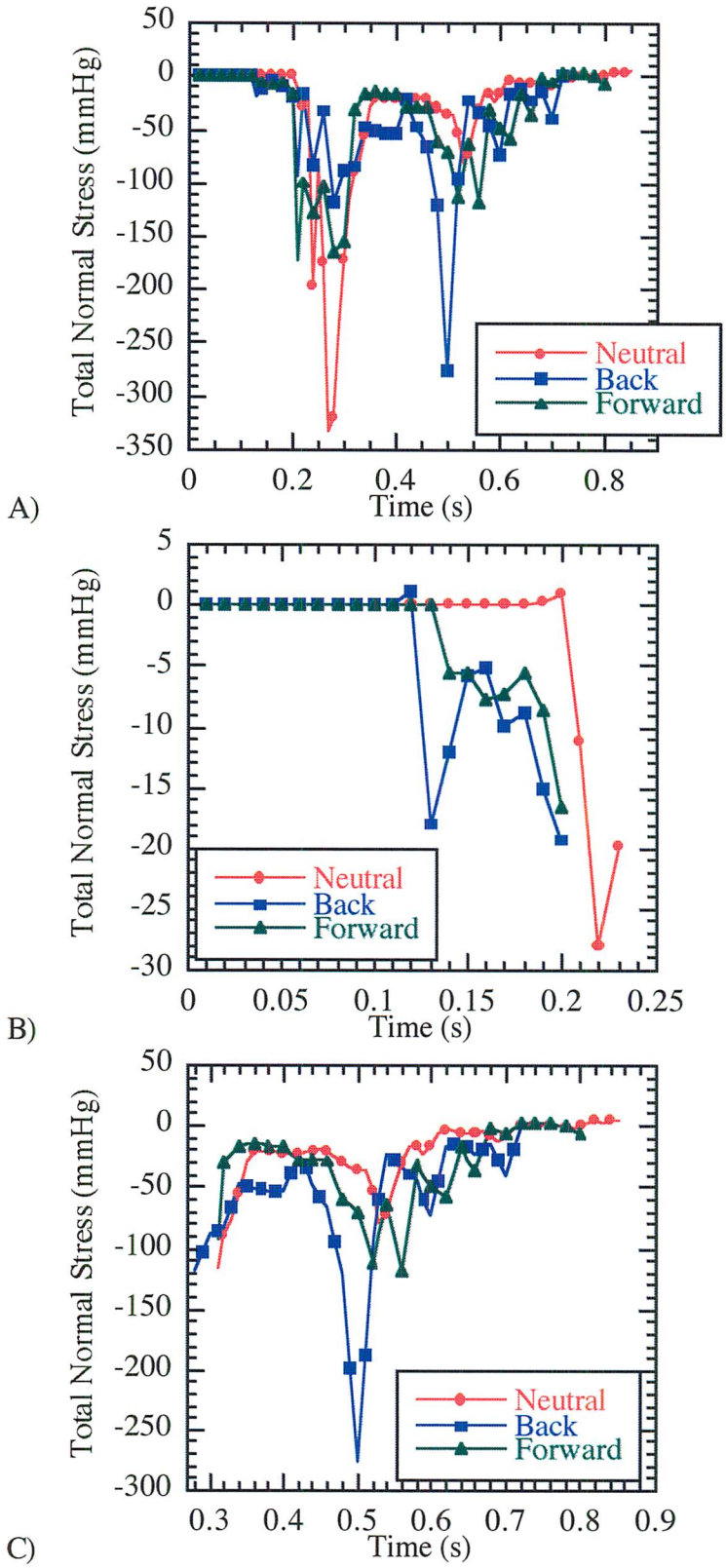

Figure 7.4.3.--Total normal stresses at the entrance of the larynx demonstrating the effect of head position. (A) Total time, (B) Filling, (C) UES open.

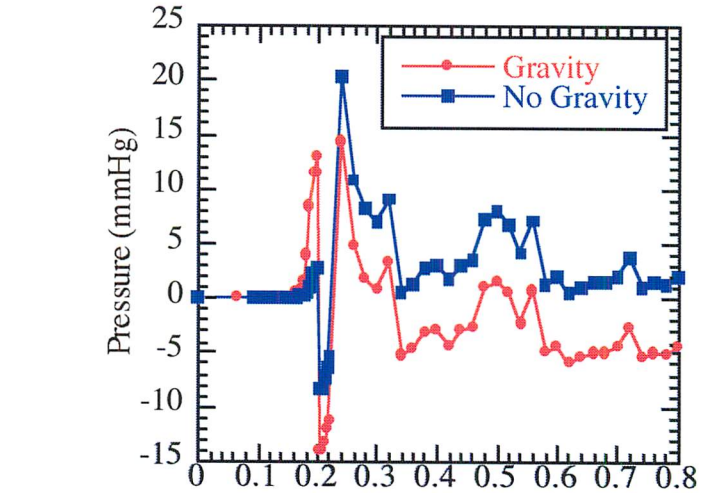

A) Low-Viscosity

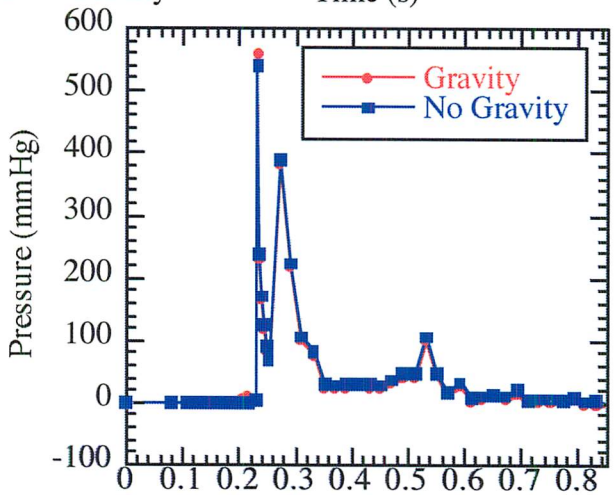

B) Mid-Viscosity

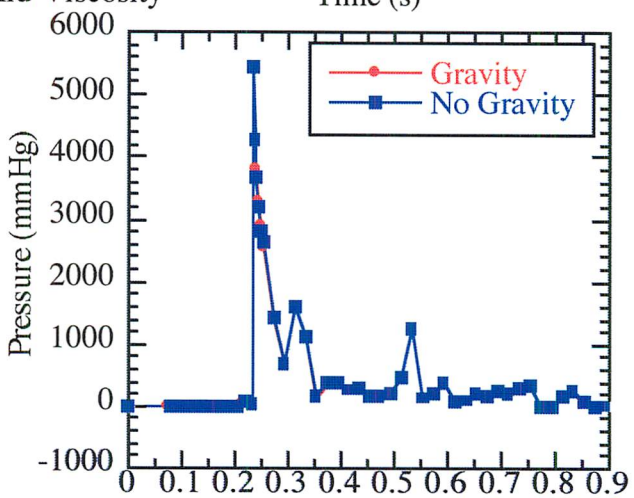

C) High-Viscosity

Figure 7.5.1.--Pressure histories near the entrance to the larynx for the 10 mL swallows demonstrating the effect of gravity on the different viscosity boluses.

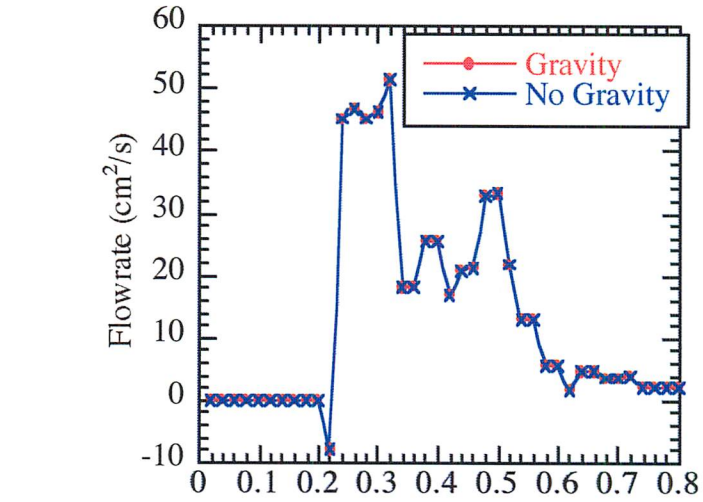

A) Low 10 mL

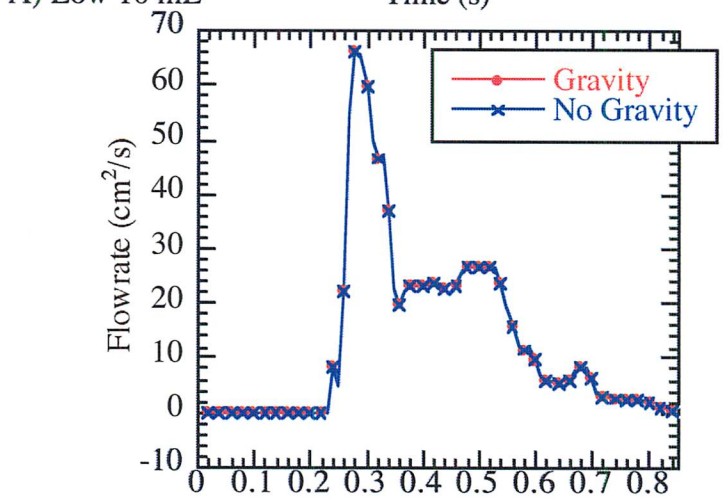

B) Mid 10 mL

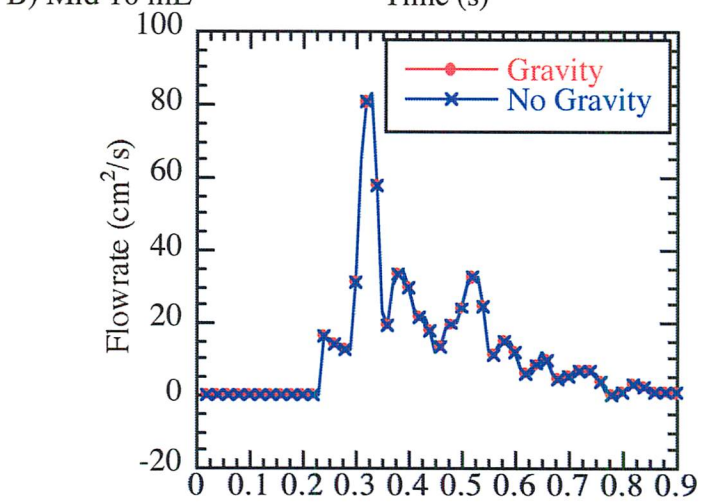

C) High 10 mL

Figure 7.5.2.--Flowrate through the UES for the A) low-, B) mid-, and C) high-viscosity 10 mL boluses demonstrating the effect of gravity.

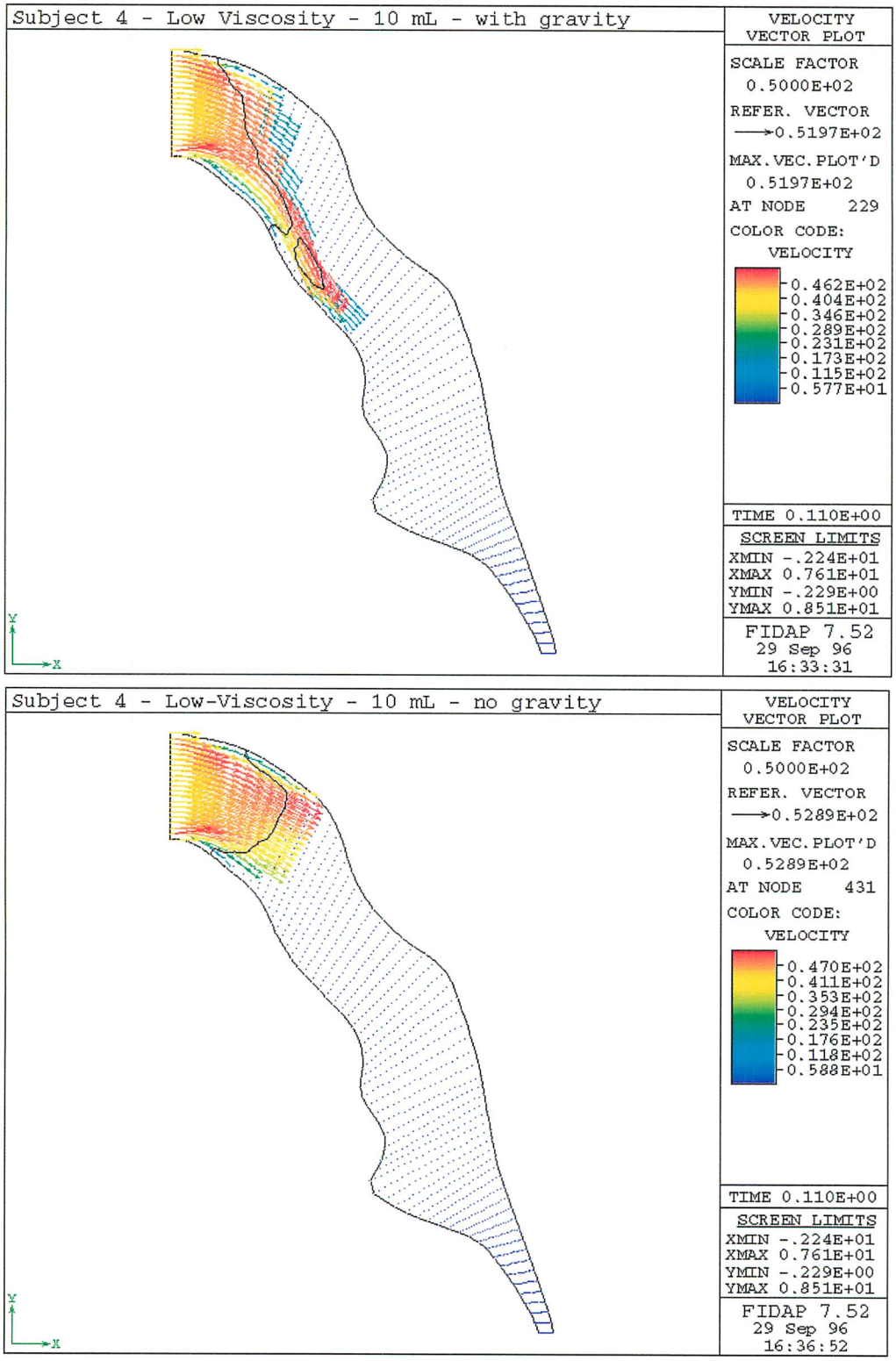

Figure 7.5.3.--Velocity vector plots at t = 0.11 demonstrating the effect of gravity on the low-viscosity, 10 mL swallow.

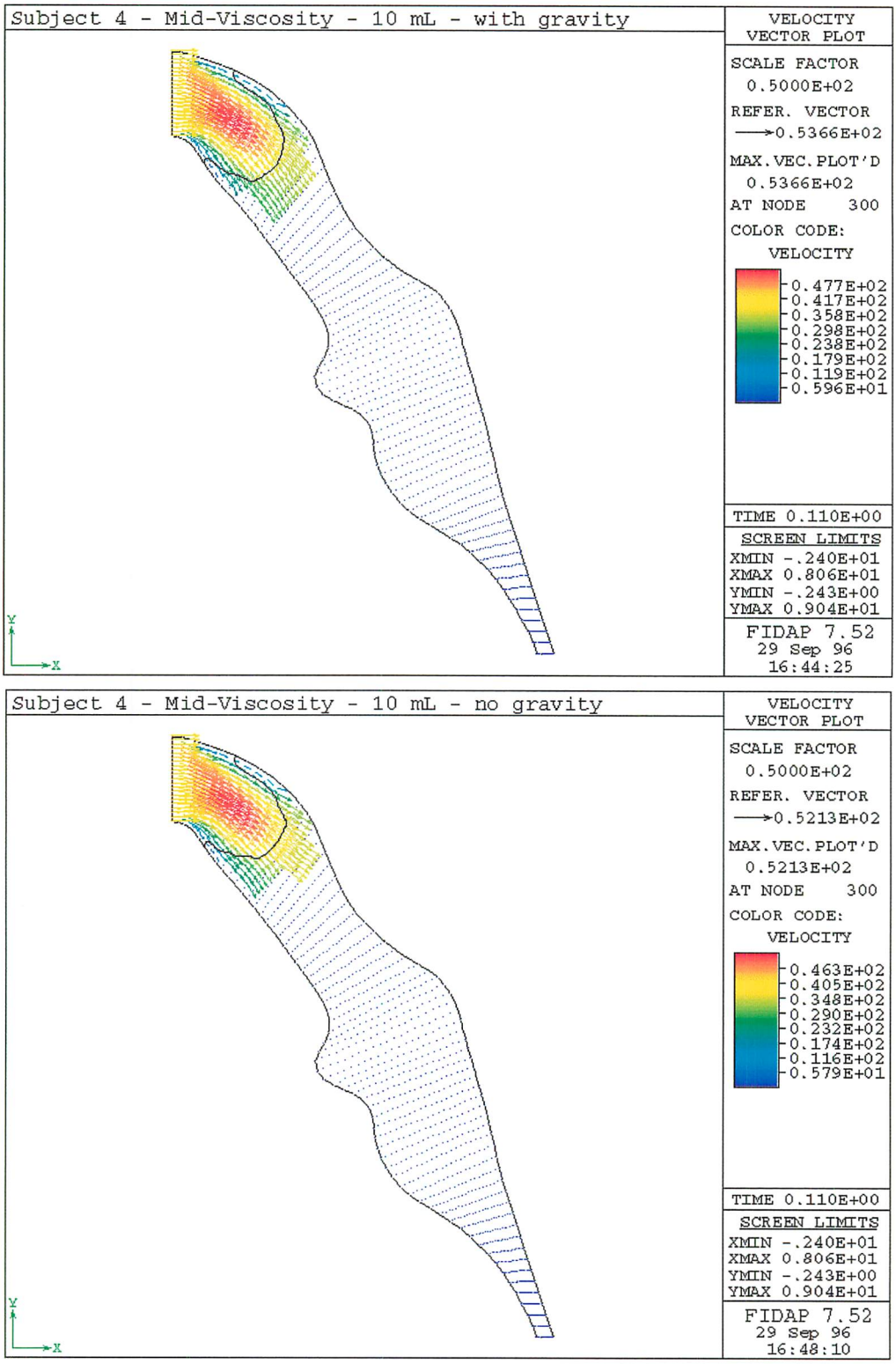

Figure 7.5.4.--Velocity vector plots at t = 0.11 demonstrating the effect of gravity on the mid-viscosity, 10 mL swallow.

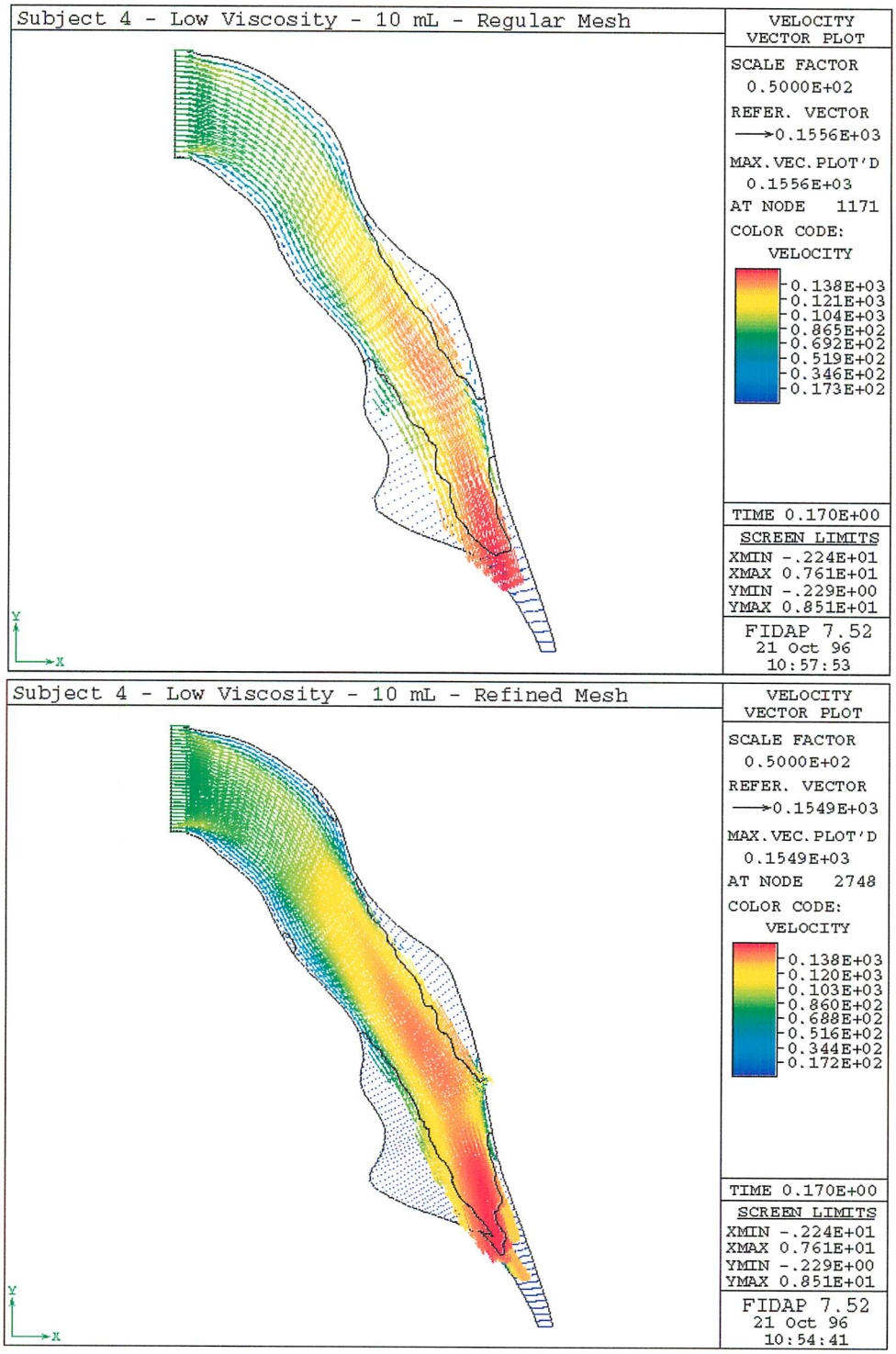

Figure 7.6.1.--Velocity vector plots at t = 0.17 for the regular and refined mesh demonstrating the accuracy of the numerical solution.

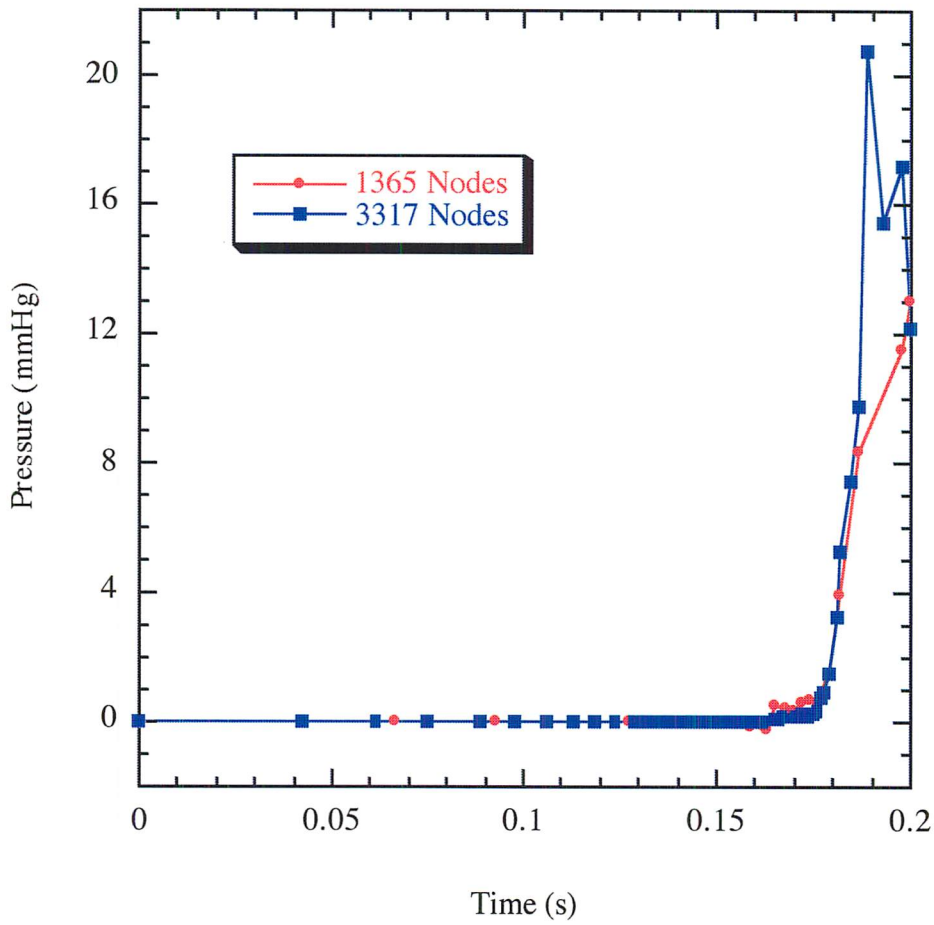

Figure 7.6.2.--Pressure histories near the entrance to the larynx for the regular and refined mesh demonstrating the accuracy of the numerical solution.

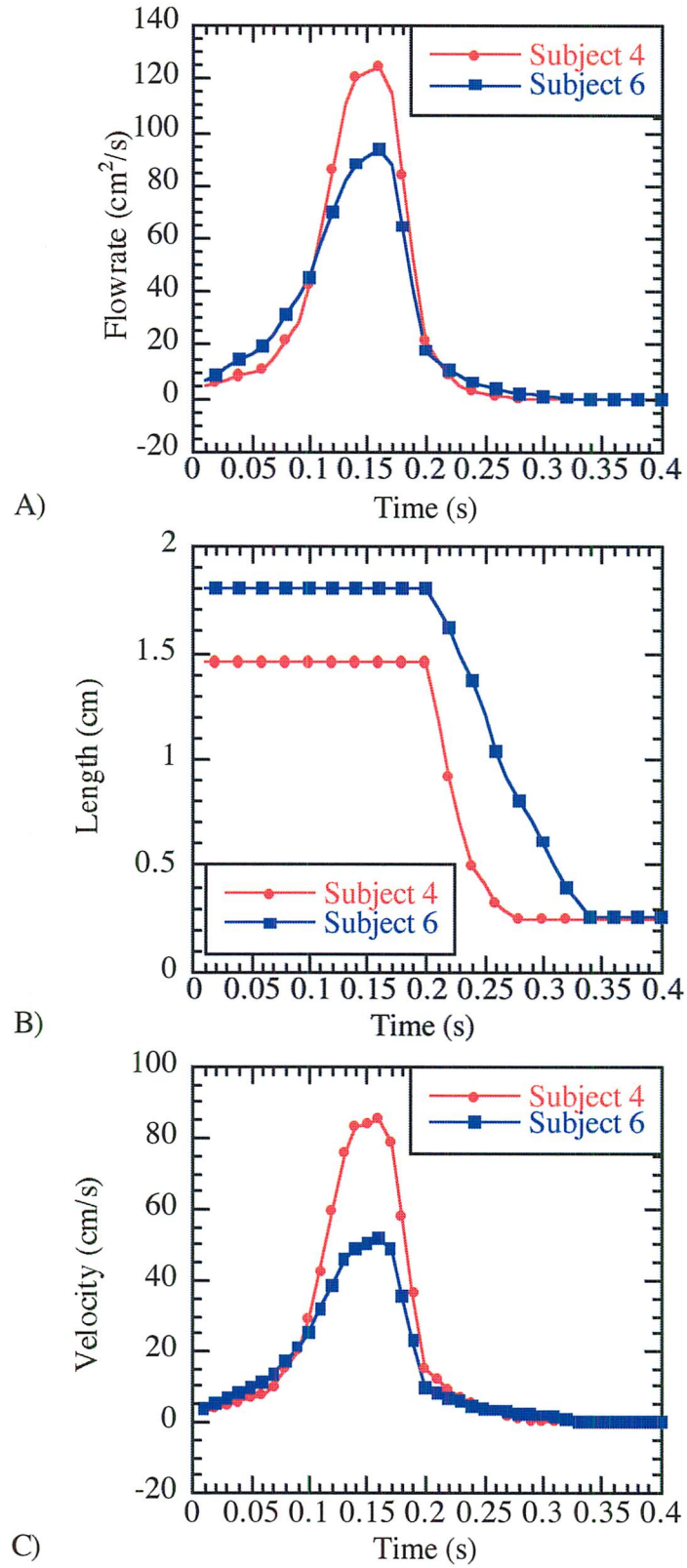

Figure 7.7.1.--Volumetric flowrate (A), width (B), and velocity (C) at the GPJ demonstrating the variability between subjects.

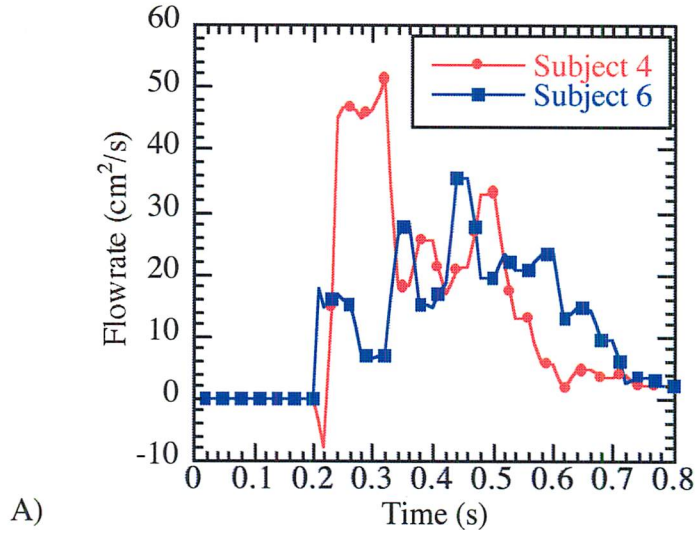

A)

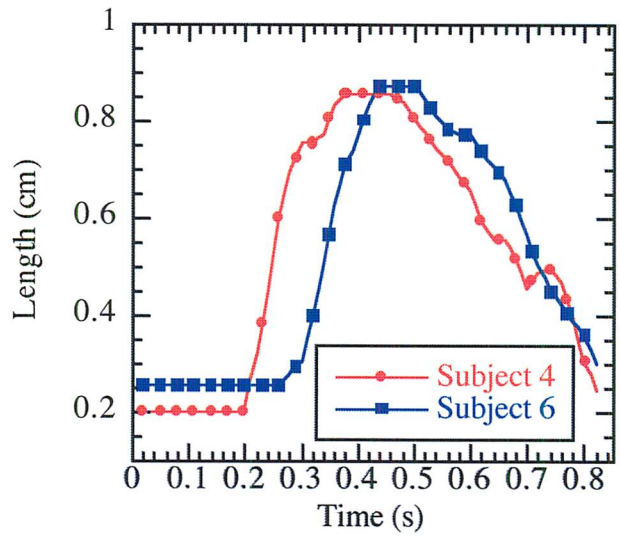

B)

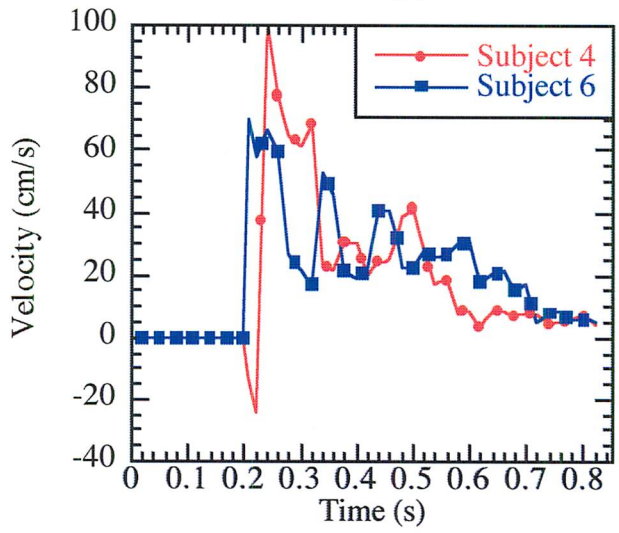

C)

Figure 7.7.2.--Volumetric flowrate (A), width (B), and velocity (C) at the UES demonstrating the variability between subjects.

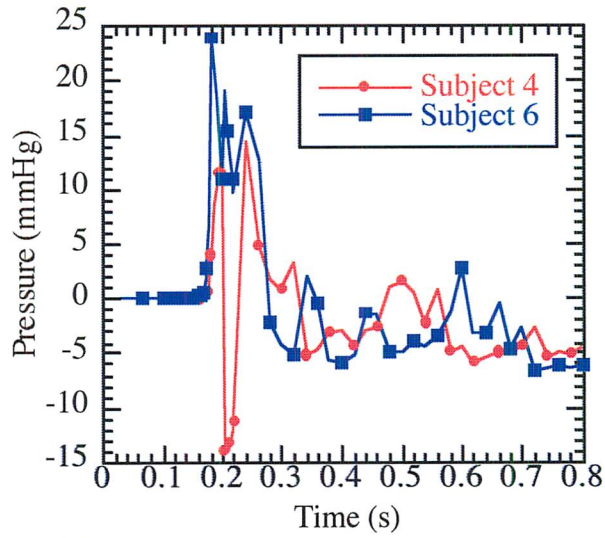

A)

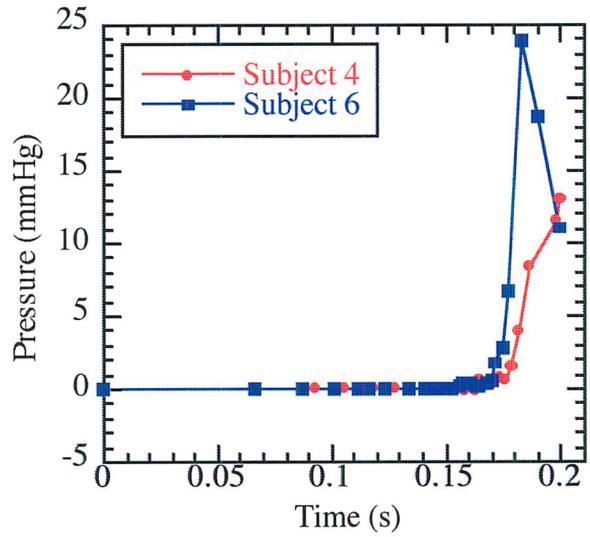

B)

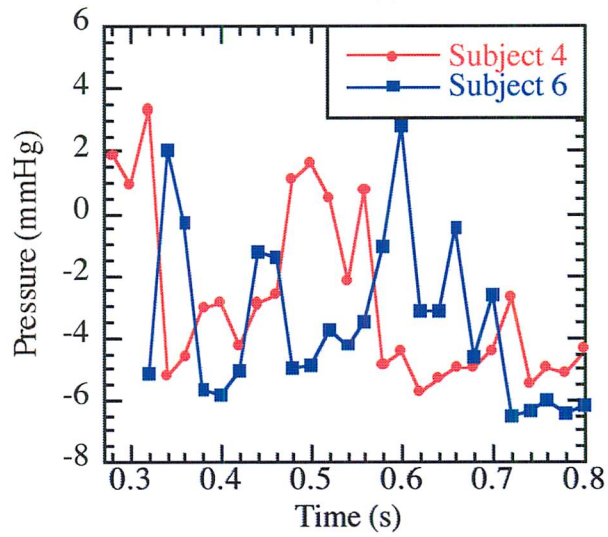

C)

Figure 7.7.3.--Pressure histories at the level of the larynx demonstrating the variability between subjects. (A) Total time, (B) Filling, (C) UES open.

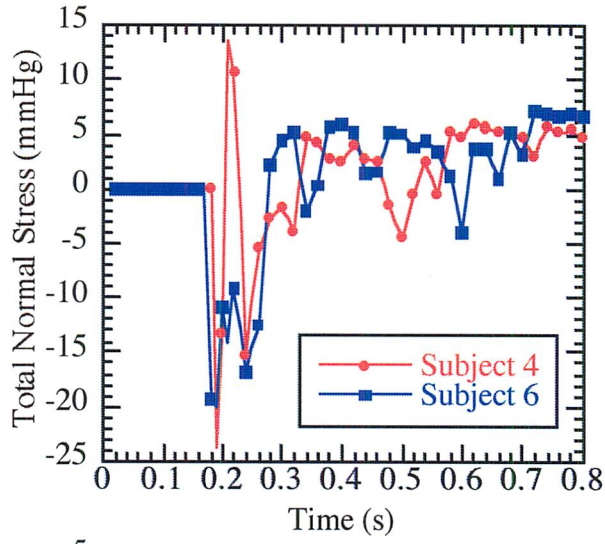

A)

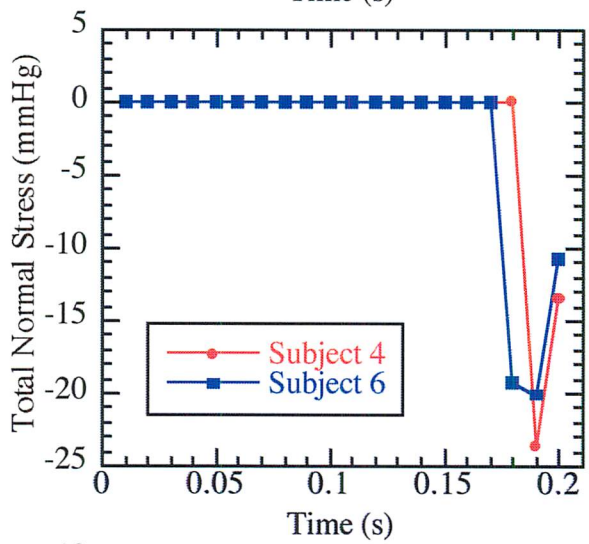

B)

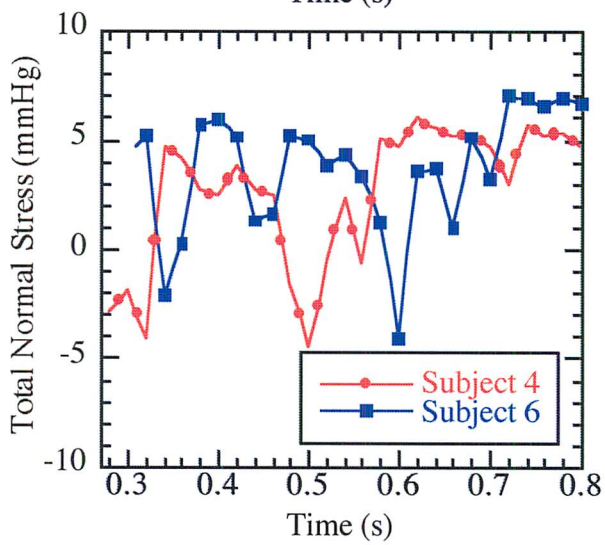

C)

Figure 7.7.4.--Total normal stresses at the entrance of the larynx demonstrating the variability between subjects. (A) Total time, (B) Filling, (C) UES open.

CHAPTER 8.--DISORDERED SWALLOWING

8.1.--Introduction

The analysis presented in the previous chapter demonstrated how the mathematical model can be used to gain insight on the normal swallow. In this chapter, how the model can be used to learn more about the parameters affecting swallowing disorders is discussed. As discussed in chapter 1, there are many causes of dysphagia. The main symptom of dysphagia that we are most interesting in modeling is laryngeal penetration. Laryngeal penetration is when the bolus enters the laryngeal vestibule. Laryngeal penetration can lead to aspiration. Aspiration occurs during normal breathing when liquid that has entered the larynx is inhaled, soiling the bronchial tree. Chronic aspiration can lead to asthma and/or lung infections, such as pneumonia.

The most common cause of laryngeal penetration is poor timing between the oral and pharyngeal phases of swallowing (Rubesin 1995). In this situation, the elevation of the larynx does not complete before the initiation of the oral phase. This premature leakage of bolus from the oral cavity into the pharynx enters the laryngeal vestibule.

Retention of the bolus in the pharynx can also lead to laryngeal penetration. Stasis of bolus material in the pharynx is generally due to neuromuscular diseases, tumors, or structural disorders such as diverticula. Esophageal disorders, such at gastroesophageal reflux disease or obstructions can also lead to laryngeal penetration.

In this chapter, the mathematical model is used to study two common occurrences that can result in laryngeal penetration. The filling simulation is applied to study the premature leakage of the bolus into the pharynx due to poor coordination between the oral and pharyngeal phases. Specifically, the effect of bolus volume, bolus viscosity, and gravity on laryngeal penetration is investigated. These effects will be discussed in section 8.2. The moving boundary simulation is applied to a fluoroscopy study of a patient who

had suffered a recent cerebrovascular accident. This patient displayed bolus retention in the pharynx due to weakened pharyngeal musculature. How the model can be used to estimate possible methods for improving swallowing function is investigated. The results of the model applied to the dysphagic patient is discussed in section 8.3. Section 8.4 summarizes the chapter.

8.2.--Simulating Laryngeal Penetration

The model applied to subject 4 is used to simulate laryngeal penetration. This section presents a model of the most common occurrence of penetration; the discoordination of the oral and pharyngeal phases. As discussed above, this occurs due to incomplete elevation of the larynx before arrival of the bolus at this location. In many situations, the larynx completes the elevation, protecting the airway throughout the remainder of the swallow after penetration of a small portion of the bolus. This is well demonstrated by the MPEG movie, larpen.mpg, on the CD included with this dissertation showing a fluoroscopy study of a normal subject where laryngeal penetration occurs. Frames 19 and 20 show the bolus penetrating the laryngeal vestibule. Elevation completes in frame 21 and the remainder of the bolus is transported to the esophagus following pharyngeal peristalsis.

Since this type of penetration occurs early in the swallow, we can model it with just the filling simulation. The amount of bolus penetrating the larynx can be quantified by allowing flow in the region of the entrance to the larynx. This location is determined by analysis of the fluoroscopic images just prior to the completion of elevation. A stress-free boundary condition is specified in this location. The boundary conditions at the GPJ, UES, and posterior and remaining anterior walls are the same as for the normal swallow. Figure 8.2.1 details the boundary conditions for this model.

8.2.1.--Bolus Viscosity

The purpose of simulating laryngeal penetration is to determine what combination

of bolus variables cause the greatest amount of penetration. The 5, 10, and 20 mL, low-viscosity swallows from subject 4 were used for this purpose. Since it was found in chapter 7 that geometrical differences were only great between different volumes and not viscosities, the properties of the mid- and high-viscosity boluses were used in the 5, 10, and 20 mL, low-viscosity geometries to study the effect of viscosity on different volumes.

Figure 8.2.2 shows the flowrate through the larynx for the low-viscosity, 5, 10, and 20 mL geometries. These simulations were re-run using the properties for the mid- and high-viscosity boluses to demonstrate the effect of viscosity on the amount of penetration. The numbers in parentheses in the legend indicate the total amount penetrating during the entire simulation. For all volumes, the low-viscosity fluid shows the greatest amount of penetration. This should be expected based on the discussion in chapter 7. The low-viscosity fluid fills the pharyngeal chamber faster reaching the opening to the larynx sooner due to the increased significance of inertial forces. More of the bolus is transported early in the swallow due to the increased velocity of the bolus head. Notice that the high-viscosity bolus shows a greater amount of penetration than the mid-viscosity fluid. MPEG movies of these simulations (larlow.mpg, larmid.mpg, and larhigh.mpg), included on the CD included with this dissertation, demonstrate why. The higher viscosity bolus spreads out less than the lower viscosity boluses due to increased viscous forces. This bolus clings to the walls of the pharynx more resulting in longer contact time with the opening to the larynx.

In chapter 7, it was found that the higher viscosity fluids take longer to fill the pharyngeal chamber. These simulations stop at the point of fill for the low-viscosity fluid. The simulations are not continued to the point of fill for the mid- and high-viscosity fluids because we want to compare penetration amounts over the same duration of laryngeal exposure for all fluids in order to compare differences between the same swallow. Continuing the simulations to the point of fill for the mid- and high-viscosity

fluids effectively leaves the entrance to the larynx open longer. We need to compare over the same duration of laryngeal opening, not the filling duration.

8.2.2.--Bolus Volume

Figure 8.2.3 shows the effect of bolus volume for the three fluids. Above, we discussed the need to do the simulations over the same time period in order to compare viscosity effects. Recall from chapter 7 that the difference in the time to fill between volumes was entirely due to the time to open the GPJ. We want the time for comparison to be constant over the time the larynx is exposed to the bolus. This duration begins after the GPJ has fully open. The time from the GPJ fully open to fill is constant among volumes and therefore, the time that is used to compare for constant laryngeal exposure.

To compare between bolus volumes, the data are normalized over the length of the opening to the larynx. The opening to the larynx was chosen arbitrarily over the length of two elements for each mesh. The lengths of these opening vary slightly between volumes. The length in the 5 mL, 10 mL, and 20 mL meshes is 0.9 cm, 0.64 cm, and 0.60 cm, respectively. The total flowrate integrated over time normalized by length is shown in parentheses in the legends of these plots. These data show no correlation with bolus volume. The volume demonstrating the largest amount of penetration changes between viscosities. Also, for each viscosity, there is only a small variation in the magnitude of penetration between volumes.

8.2.3.--Gravity

The effect of gravity on laryngeal penetration was also studied using the low-viscosity, 20 mL geometry from subject 4. Figure 8.2.4 shows the results for the low-, mid-, and high-viscosity bolus samples. As discussed in section 7.5, the gravitational forces play a significant role in the transport of the low-viscosity fluid. Without including gravitational forces in this simulation, none of the low-viscosity bolus penetrates the entrance to the larynx. The reason for this effect is demonstrated in figure

8.2.5. The effect of the force of gravity is to pull the bolus closer to the entrance of the larynx as seen in this figure. Without gravity, the bolus is positioned more toward the back of the pharynx effectively eliminating exposure to the entrance of the larynx. Obviously, eliminating the force of gravity is not an option for treatment in dysphagic subjects, but this result does suggest the importance of body positioning. Further studies, including varying the body position, should be done to fully investigate the significance of gravity on laryngeal penetration.

Similar amounts of penetration are seen for the mid- and high-viscosity fluids. The amount of penetration actually increases for the high-viscosity fluid without gravity. Whether or not this small difference is significant requires investigation of more swallows and more subjects.

From this limited study, we can see how the model can be used to learn more about parameters affecting laryngeal penetration. It has been demonstrated that the viscosity of the bolus has a large effect on the amount of penetration. Low-viscosity fluids fill the pharynx faster resulting in a greater risk of penetration before laryngeal elevation can complete. In fact, it is common clinical practice to restrict dysphagic patients diets to thick liquids (Ganger and Craig 1990). The model helps us to understand why this practice is needed.

8.3.--Simulating Ineffective Peristalsis

The same modeling techniques used on the normal subject were applied to a patient with weakened pharyngeal musculature. This person had suffered a recent cerebrovascular accident. This patient demonstrated poor control in both the oral and pharyngeal phases of the swallow. Each bolus required multiple attempts to be transported from the oral cavity to the pharyngeal chamber. We chose to model the portion of the swallowing sequence where pharyngeal peristalsis was first initiated. At this time, most of the bolus had been transported to the pharyngeal cavity, but peristalsis,

laryngeal elevation, or opening of the UES hadn't occurred. The next attempt to swallow resulted in elevation, initiation of peristalsis, and transport of some of the contents of the pharyngeal chamber through the UES. The time from initiation of peristalsis to UES closure is the duration modeled.

An MPEG movie, dysfluor.mpg, of the portion of the fluoroscopy study modeled is included on the CD with this dissertation. For this first swallow in the fluoroscopy study, 5 mL of the high-viscosity sample was placed in the patients mouth. Notice that the dysphagic patient never achieves complete closure of the pharyngeal lumen behind the bolus. Since complete closure of the pharyngeal lumen was never observed, later swallows could not be modeled since the residual bolus from the previous swallow was not cleared during the duration of the study. Even though 5 mL of the sample was placed in the patient's mouth, the amount of this bolus transported to the pharynx and UES is unknown due to the residual remaining in the mouth and pharynx. Multiple swallows were required to transport the bolus from the mouth to the pharynx, and into the esophagus. Also notice that the patient displays reverse peristalsis resulting in penetration into the nasopharynx. Because the movement of each node is prescribed, these events can be accounted for with the moving boundary simulation.

Since the bolus was already filling the pharyngeal chamber, only a moving boundary simulation was run. The velocity of the boundary of the bolus was prescribed in the same manner as discussed in section 6.5.5. The boundary condition at the GPJ was left free (no-stress) since there seem to be little oral control and closure of the GPJ was never observed. The boundary condition at the UES was also free, the same as in the normal model.

An MPEG movie, dys5h.mpg, of the moving boundary simulation can also be found on the CD included with this dissertation. Notice that reverse flow is seen during much of the simulation. Figure 8.3.1 shows the flowrate through the GPJ, UES, and

width of the UES for this simulation compared to the results from the moving boundary simulation of the 5 mL, high-viscosity swallow from a normal subject (subject 4). This figure further demonstrates the ineffective transport of the bolus for the dysphagic patient. The total flow through the UES is only 0.97 cm^2 compared to 7.89 cm^2 for the normal subject. There is continuous flow through the GPJ for the dysphagic subject, but the net flow is nearly zero (0.0008 cm^2). Also notice that the UES opens much wider for the normal subject.

Figure 8.3.2 compares the stresses near the entrance to the larynx for the normal and dysphagic subjects. The stresses are negative because they are acting in the negative x-direction. Note that the magnitude of the stress is decreased in the dysphagic subject. From the analysis of squeezing flow presented in section 3.6, this can be attributed to the reduced velocity of wall movement and increased separation between the anterior and posterior walls of the pharynx. Since the forces at the boundary of the fluid must equal the forces at the walls of the pharynx, it can be concluded that the muscles are not generating as much force in the dysphagic patient as in the normal subject.

To determine if different fluids would increase the effectiveness of bolus transport, the simulation was re-run using the properties of the low- and mid-viscosity samples. MPEG movies of these simulations, dys5l.mpg, dys5m.mpg, are also included on the CD with this dissertation. Notice that the amount of reverse flow is dramatically decreased for the low-viscosity fluid. Figure 8.3.3 shows the flowrate through the GPJ and the UES for these three fluids. Note the significant increase in the transport of the bolus for the low-viscosity fluid. As discussed in chapter 7, less viscous fluids require less force to transport; thus, the weakened muscles are able to transport the lower viscosity fluid much more effectively.

This analysis suggests that a dysphagic patient with weakened pharyngeal musculature may be able to transport fluids with lower viscosities more effectively than

fluids where viscous forces dominate. The amount of residual bolus remaining in the pharyngeal chamber will be reduced with increased efficiency of fluid transport. This will also decrease the number of swallows required to clear any residual bolus. If the amount of residual bolus is reduced, the risk of aspiration after the swallow is lessened.

8.4.--Summary

In this chapter, the model was used to investigate the parameters affecting swallowing disorders. The filling simulation was applied to study the most common cause of laryngeal penetration; premature leakage of the bolus into the pharynx. This investigation of the parameters influence laryngeal penetration suggest fluids with higher viscosities, where viscous forces dominate, result in slower filling of the pharynx allowing more time for the entrance to the larynx to close. It was also found that bolus volume has no significant effect on the amount of laryngeal penetration. As in chapter 7, it was found that gravitational forces only play a significant role in the transport of the low-viscosity fluid. The amount of penetration without gravitational forces was significantly greater with the force of gravity included in the model for the low-viscosity fluid. Gravitational forces had no effect for the mid- or high-viscosity fluids. The effect of gravitational forces and body positioning requires further study for lower viscosity fluids to make significant conclusions about clinical applications.

The same modeling techniques were also applied to fluoroscopy data from a dysphagic patient exhibiting weakened pharyngeal musculature. The model demonstrated the ineffective bolus transport by showing that reverse flow occurs during the moving boundary simulation. The results of the model confirmed that the flowrate through the UES is dramatically reduced compared to a normal subject. The forces at the walls of the pharynx were also shown to be reduced for the dysphagic patient. Re-running the simulation using the properties of the low-viscosity fluid showed a dramatic increase in the amount of bolus transported to the esophagus.

The results of these two investigations of possible causes of laryngeal penetration give conflicting results. In the case of laryngeal penetration due to premature leakage of the bolus, it was found that higher viscosity fluids results in a reduced risk of penetration. For the situation where penetration occurs due to insufficient clearing of the bolus from the pharyngeal cavity, we find that the low-viscosity fluids reduce the risk of bolus retention. The difference in the conclusion is due to the difference in the problem. The application of the model provides insight into the effects of different parameters on the pharyngeal phase of swallowing, but the results should be interpreted carefully. It cannot be concluded which answer is best for any given situation. The model is intended to be used as a tool to aid in the understanding of dysphagia. It cannot be used without standard evaluation techniques and good clinical judgment.

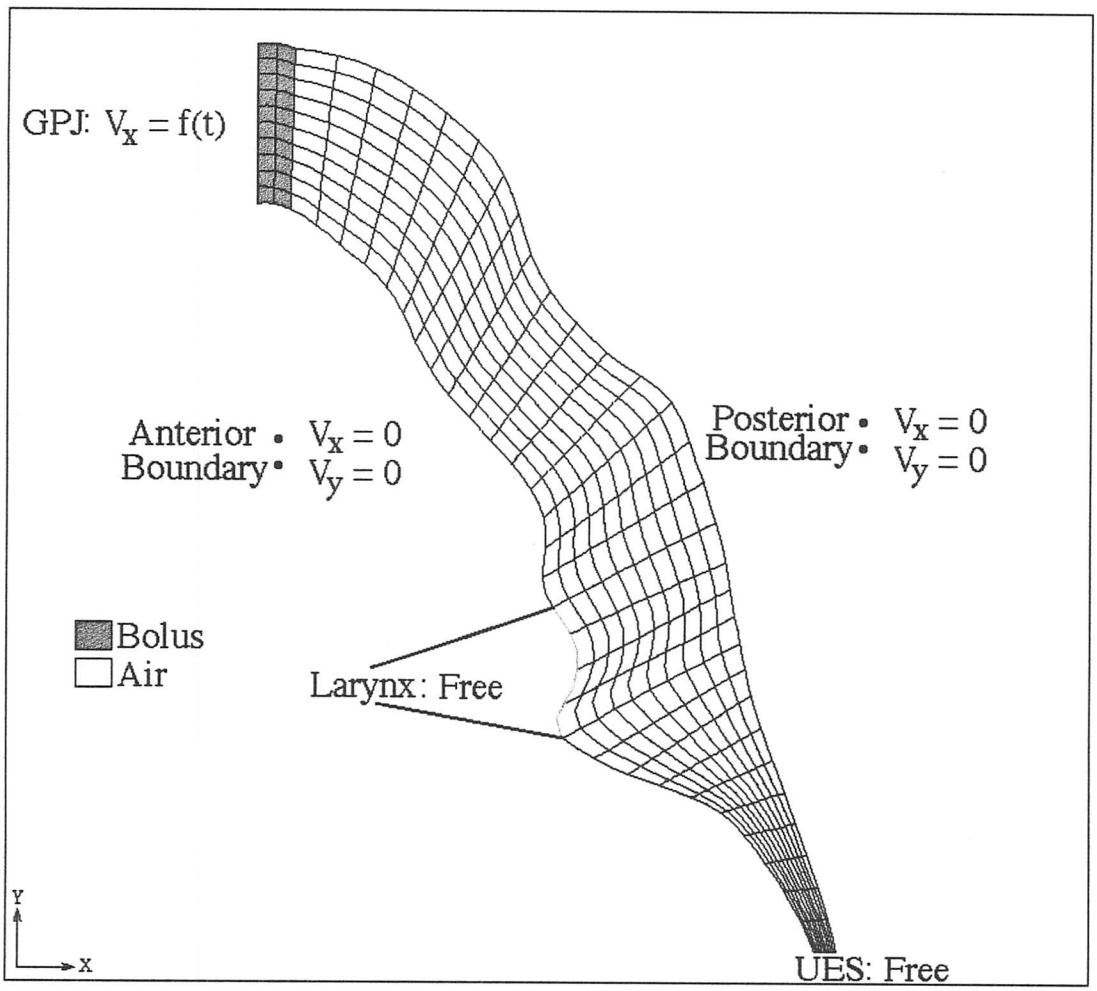

Figure 8.2.1.--Representative finite element mesh demonstrating the boundary conditions for the laryngeal penetration simulations.

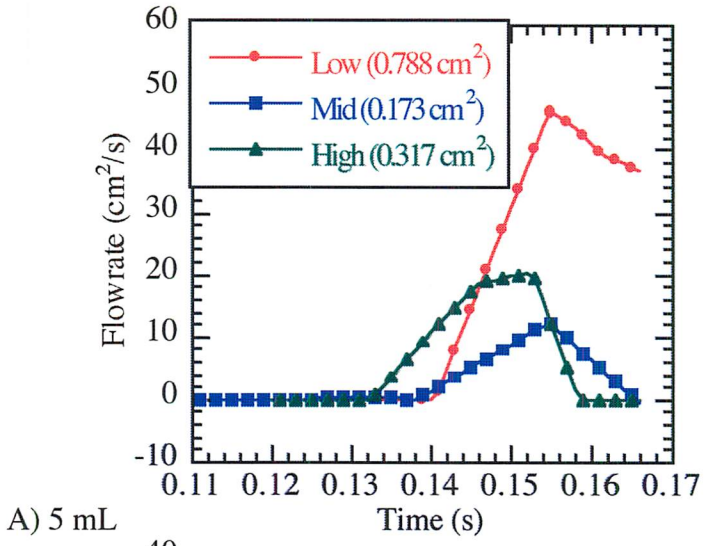

A) 5 mL

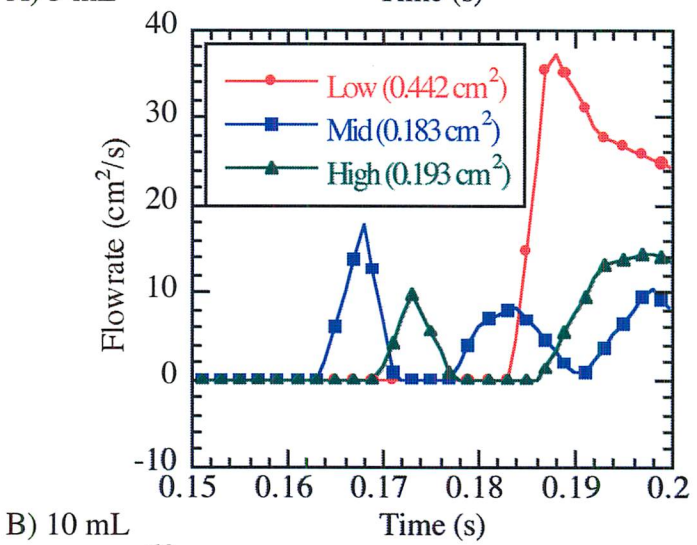

B) 10 mL

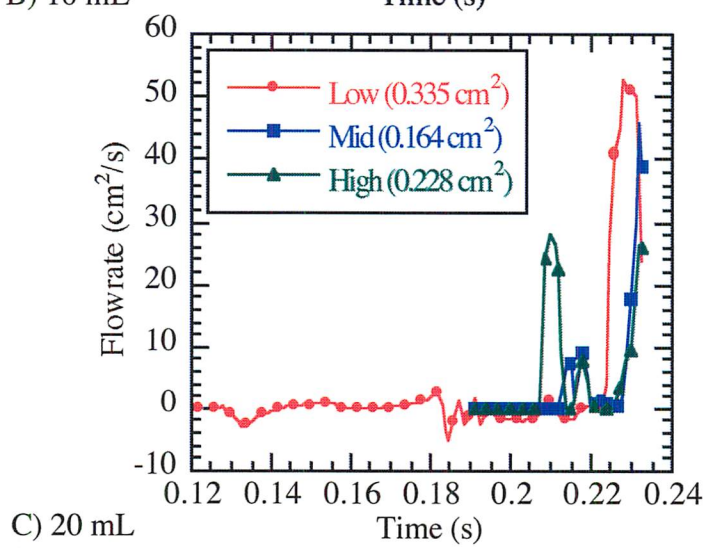

C) 20 mL

Figure 8.2.2.--Flowrate through the larynx demonstrating the effect of viscosity on laryngeal penetration. A) 5 mL B) 10 mL, C) 20 mL.

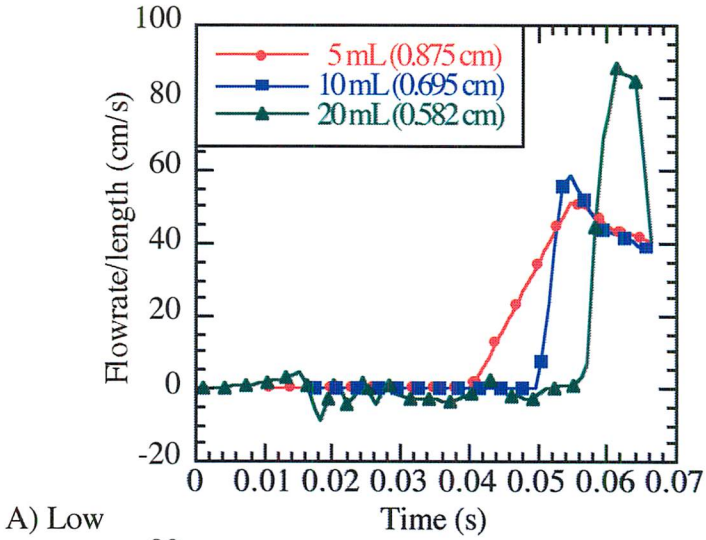

A) Low

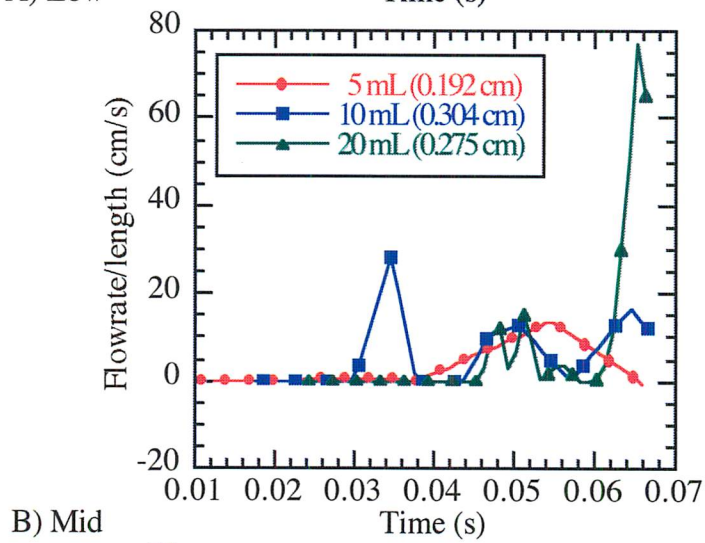

B) Mid

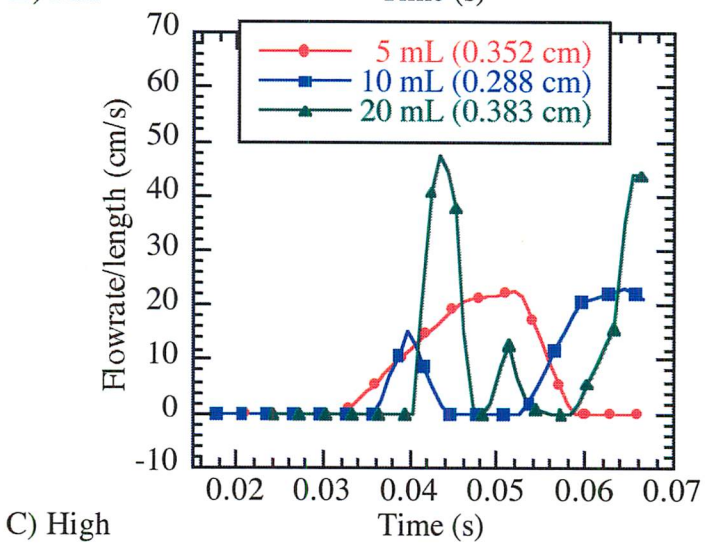

C) High

Figure 8.2.3.--Flowrate through the larynx demonstrating the effect of volume on laryngeal penetration. A) low-viscosity, B) mid-viscosity, C) high-viscosity.

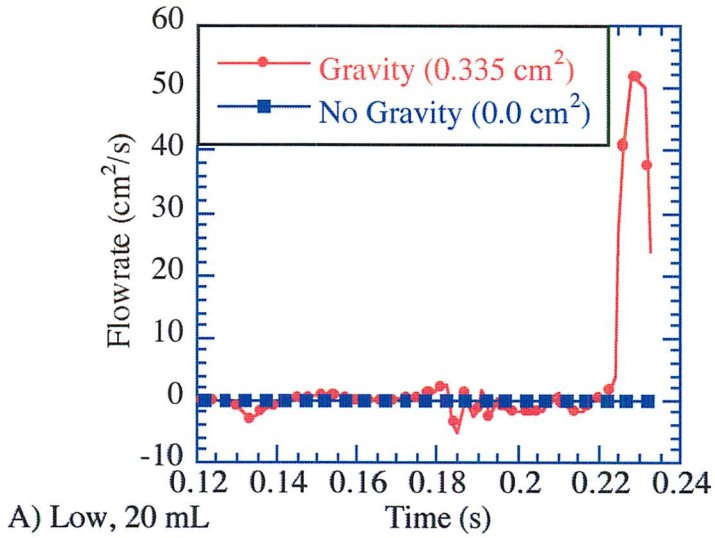

A) Low, 20 mL

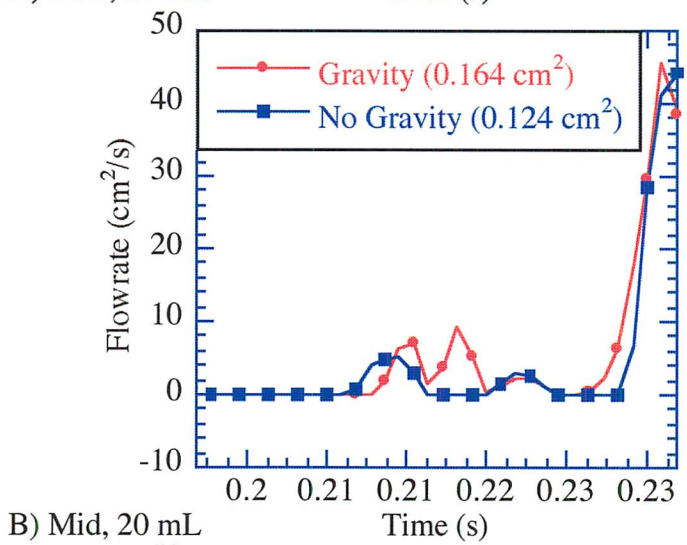

B) Mid, 20 mL

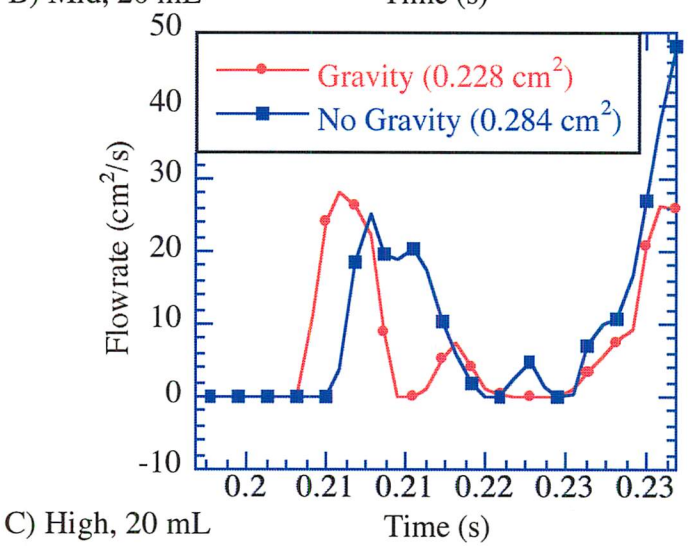

C) High, 20 mL

Figure 8.2.4.--Flowrate through the larynx demonstrating the effect of gravity on laryngeal penetration in the 20 mL geometry. A) low-, B) mid-, and C) high-viscosity.

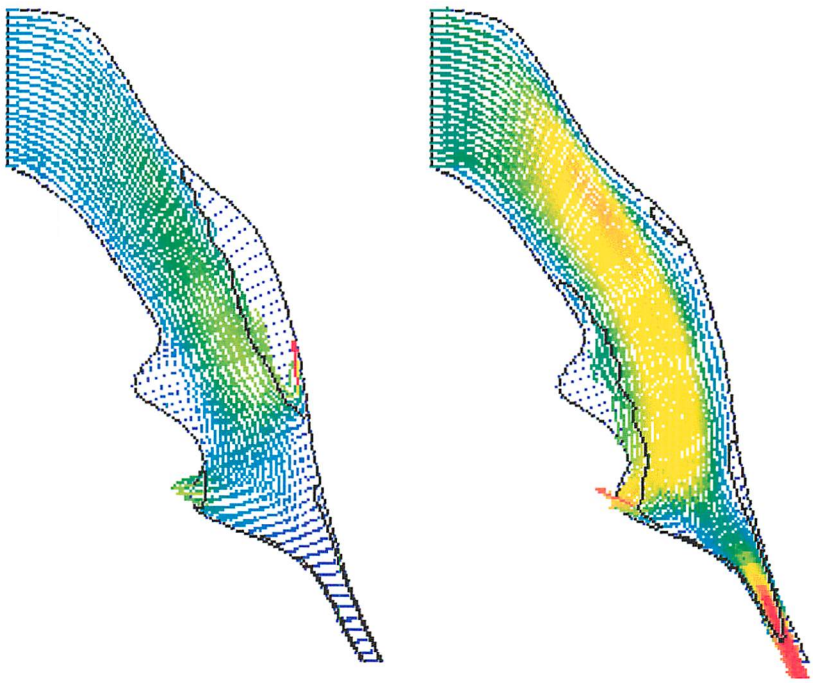

A) Gravity B) no Gravity

Figure 8.2.5.--Velocity vector plots demonstrating the effect of gravity on laryngeal penetration in the low-viscosity, 20 mL simulation.

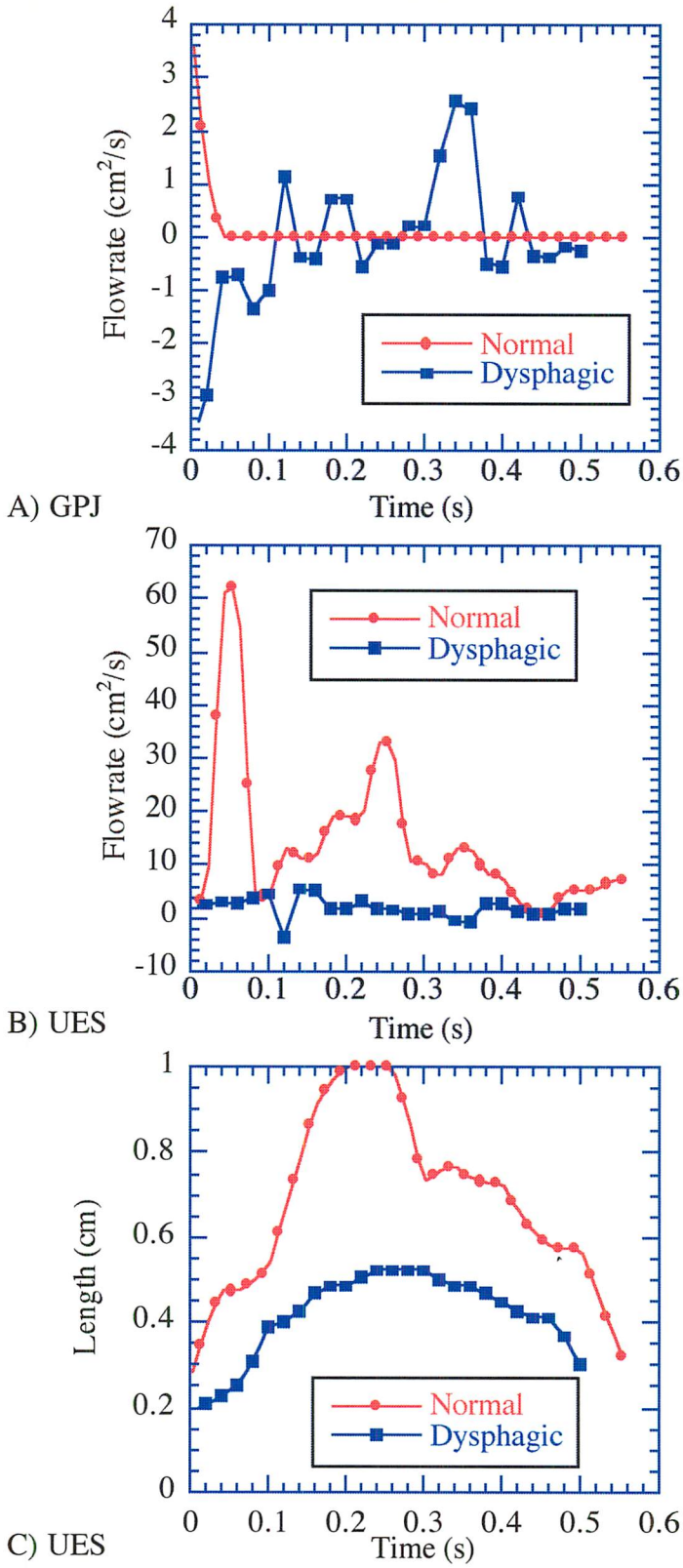

Figure 8.3.1.--Comparison of a normal subject with a patient exhibiting weakened peristalsis. A) flow through the GPJ, B) flow through the UES, C) Width of the UES.

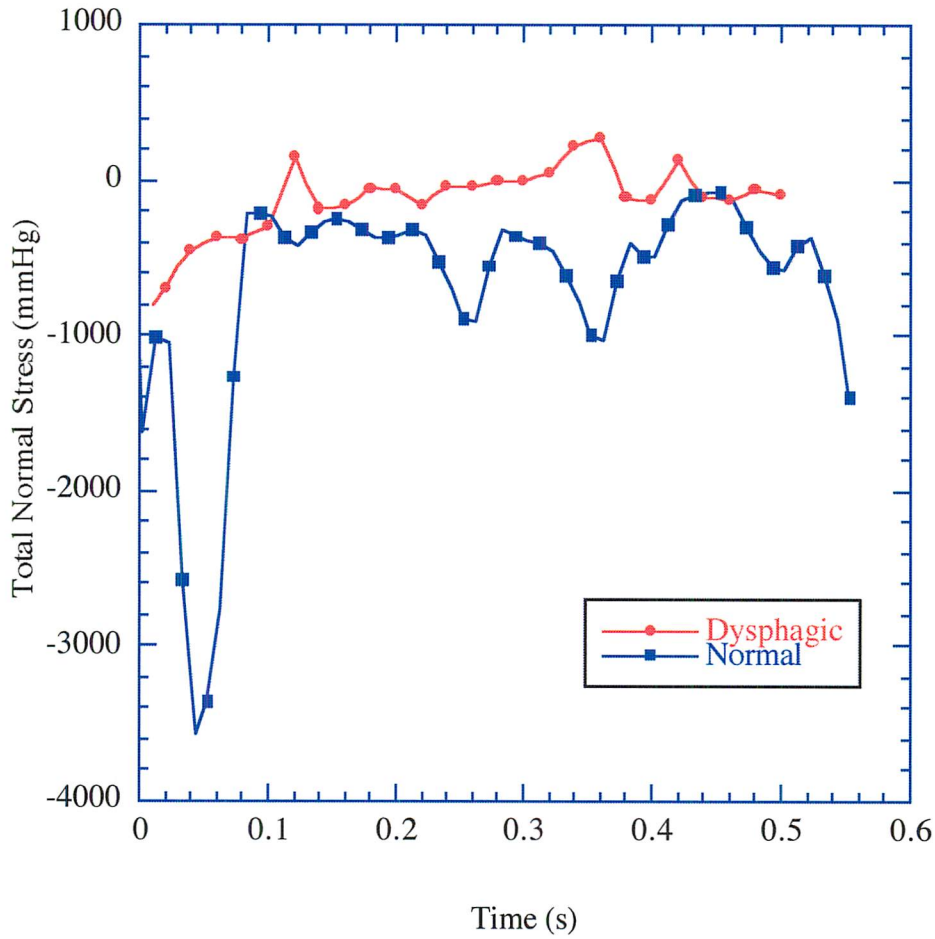

Figure 8.3.2.--Total normal stresses near the entrance to the larynx for the high-viscosity, 5 mL swallows demonstrating the difference between the normal and dysphagic subjects.

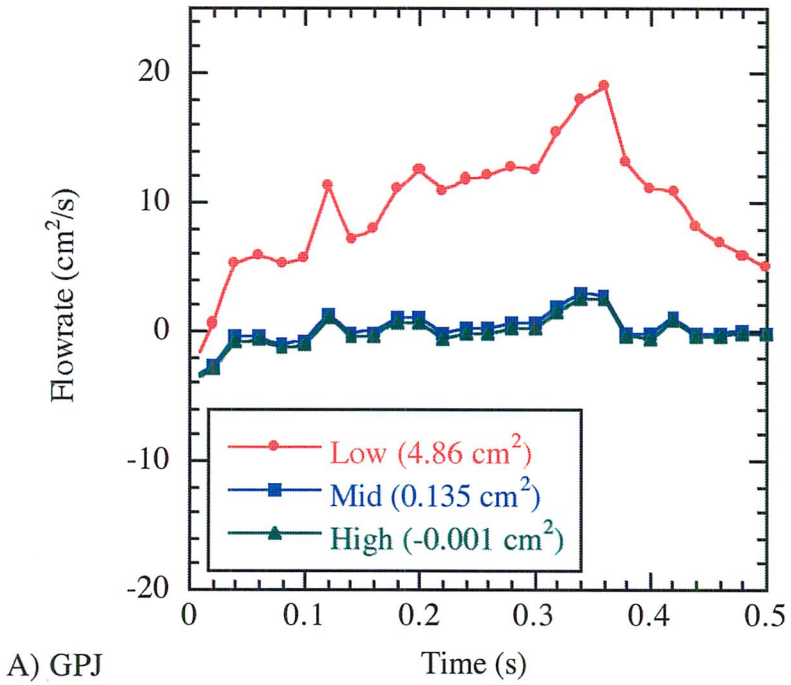

A) GPJ

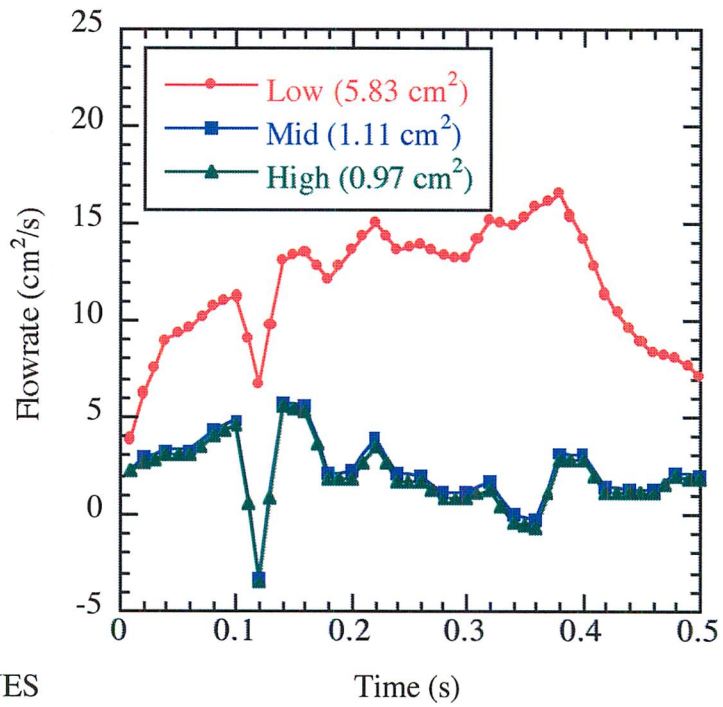

B) UES

Figure 8.3.3.--Flowrate through A) the GPJ and B) the UES for the dysphagic patient demonstrating the effect of viscosity.

CHAPTER 9.--CONCLUSIONS AND RECOMMENDATIONS

9.1.--Introduction

This final chapter summarizes this dissertation by highlighting the major conclusions of this work. This chapter also provides suggestions for the many directions in which this research can continue. Suggestions for improvements on the current model along with ideas for future models are also presented.

9.2.--Conclusions

Dysphagia is a significant medical problem most commonly affecting the elderly population. Twelve to thirteen percent of hospitalized patients and 40% of nursing home patients suffer from dysphagia (Groher and Bukatman 1986 and Donner 1986). Thirty to forty percent of the patients who have suffered from cerebrovascular accidents experience complete or partial loss of the swallowing function (Reddy, *et al.* 1990). With the increasing numbers of the elderly population, improvement in the understanding of such disorders is needed. A mathematical model can aid in the understanding of dysphagia by allowing the clinician to learn more about how different parameters affect the swallowing function.

Many studies in the literature have shown the current analysis techniques, such as manometry and fluoroscopy, provide detailed information about the swallowing function. These methods are also useful in the development of the mathematical model. The mathematical model can provide flow information these methods cannot. The advantage of the mathematical model is the ability to study the effect of changing parameters without exposing the patient to the invasiveness of manometry or excessive radiation exposure from fluoroscopy.

There are many models in the literature for flow situations similar to flow in the pharynx, but these models cannot adequately predict the fluid mechanics in the pharynx.

They cannot account for the complex movements of the pharyngeal wall. The model developed in this dissertation can. Its major advantage is the ability to specify these movements on an individual patient basis since the movement data are provided from a fluoroscopy study of each subject.

This dissertation has demonstrated the ability to use the model to investigate parameters affecting the normal swallow: volume, viscosity, head position, and gravitational forces. The effect of these parameters on swallowing has been studied extensively in the literature. The mathematical model confirms much of these findings and had provided additional information about the pharyngeal phase of swallowing. It has been found that the volume effect on the timing of the swallow and bolus geometry varies between subjects. Through application of the model, this effect has been attributed to the geometrical differences of the pharynx between subjects. The effect of viscosity has been ascribed to the relative significance of viscous forces to inertial forces in the equations of motion. When inertial forces dominate ($Re > 1$), recirculation patters can be seen in the flow simulations. When viscous forces dominate ($Re < 1$), no recirculations are seen in the flow field. The pressures predicted with the model show a direct correlation with bolus viscosity. This prediction agrees with other mathematical models of similar flow situations, but disagrees with manometry data. This is due to the presence of air during the pharyngeal phase of the swallow not accounted for in the moving boundary simulations. The application of the model to the study of head positioning was inconclusive, but could show an effect for flow situations where inertial forces become more important than viscous forces. It has been shown that gravitational forces are negligible in the transport of the bolus through the pharynx except when inertial forces dominate.

The numerical accuracy of the model was verified through mesh refinement. Application of the model to a second normal subject demonstrated the flexibility of the

model in accounting for geometrical differences while still predicting similar flow characteristics.

Application of the model to the study of the swallowing disorders provided insight into how laryngeal penetration can be reduced. It has been shown that the pharynx fills faster for the low-viscosity fluid. This effect increases the risk of pharyngeal penetration before the swallow due to discoordination of the oral and pharyngeal phases of swallowing. The higher-viscosity boluses hold together more reducing the risk of aspiration before the swallow.

The model was applied to a dysphagic patient with weakened pharyngeal musculature. The model demonstrated the ineffective bolus transport. It has been demonstrated that because viscous boluses require a greater force to propel through the pharynx, the risk of bolus retention after the swallow increases. The effectiveness of bolus transport was increased for fluids where inertial effects dominate.

The application of the mathematical model to normal and disordered swallowing has provided additional insight on the effects of bolus volume and viscosity, head positioning, and gravity on the pharyngeal phase of swallowing. The mathematical model helps to explain the effects of different parameters, but cannot tell *a priori* which solution is best for any given swallowing disorder. The model can be used to aid in the treatment of dysphagia, but is only useful when combined with standard evaluation techniques and good clinical judgment.

9.3.--Recommendations

Many ideas have been generated in the process of developing, applying, and presenting this model. This section will discuss the many directions this research can continue, including additional simulations with the current model, improving the current model, additional human subject studies, and ideas for new models.

9.3.1.--Applying the current model

Currently, there are data from 6 fluoroscopy studies. With these data, the differences between subjects could be studied more thoroughly. The sixth study used a modified protocol using the low-viscosity fluid for the head-tilt forward and back swallows. The model could be applied to this study to see if head position has any effect when inertial forces dominate. The effect of viscosity could be estimated with the current model for subject 4 just by using the properties of the low-viscosity fluid in the geometry from the mid-viscosity swallow. It would also be interesting to study the effect of head position on laryngeal penetration. Analysis of the images from subject 4 could show where to locate the entrance to the larynx. The same procedure as described in section 8.2 could be applied to these data to learn the effect of head position on laryngeal penetration. The effect of gravity could also be further investigated with the current data. The model could be easily modified to have gravity acting in any direction.

9.3.2.--Improving the current model

A major disadvantage of applying the current model is the time investment required to analyze the images. Currently, the image analysis is done by hand. Automation of this procedure could greatly reduce the time to generate the model. Automation is difficult due to the poor resolution of the bolus. Each pixel has a value between 0 and 256 assigned to it. The difference between the value of the pixels in the bolus with the pharyngeal musculature is only on the order of 10 to 20. Increasing the contrast of the fluoroscopic image would make automation of the image analysis much easier, especially in the region of the GPJ. Increasing the intensity of the X-rays would increase the contrast, but is not an option due to the increased risk to the patient and examiner. Another possible way to increase the contrast is to reduce the fluoroscopic flaring. Flaring is seen at the boundary of the body where nothing is being imaged. This is the brightest area on the images with the smallest pixel values. Johnsson, *et al.* (1995) use a protocol where a water filled latex glove is held under the chin to reduce the amount

of dead space on the fluoroscopic images reducing flaring. Future studies should incorporate this addition to the protocol to see if the contrast of the images is enhanced.

The model as it exists has been shown to be useful in understanding gross effects of various parameters, but needs improvement to provide further understanding of the causes of these effects. It has been found that the largest flaw of the model to be ignoring the air phase during the moving boundary simulation. The key to improving the model is to include the air phase by allowing for a moving boundary during a filling simulation. This currently is a limitation of the software used to solve the mathematical model. Two solutions exists; development of new software for this purpose, or waiting for Fluid Dynamics International, Inc. to include this capability in their product. The best option is the one requiring less time. FDI plans to incorporate this capability in the version 8.0.

Another improvement of the current model would be to account for the non-Newtonian behavior of the bolus. As discussed in section 3.7 many foods exhibit non-Newtonian behavior. It may be worthwhile to investigate the how a non-Newtonian fluid model affects the results of the simulations. Non-Newtonian models supported by FIDAP were discussed in section 3.3. If new software is developed, it can be developed to include any non-Newtonian model desired.

9.3.3.--Additional studies

The same modeling techniques can be applied to additional human subject studies. A study including larger volumes could indicate if there is a maximum flowrate through the pharynx. Also of interest is the effect of volume on different viscosity swallows. The effect of viscosity has been reported to be more profound for higher volumes (Dantas, *et al.* 1993). Confirmation of the scant data in the literature is needed. Combined fluoroscopy and manometry studies could be done to see if the catheter affects the bolus flow. The effect with viscosity would be the most interesting. This could shed light on the discrepancy between the data from Dantas, *et al.* (1993) and Hamlet, *et al.*

(1996) discussed in section 7.3.1. Also, manometric studies could provide further insight on the discrepancy between manometric data and the results from the model. Fluoroscopic images of swallows in the supine position could give additional information about the role of gravity in the swallow. It would also be worthwhile to study the reproducibility of the model by having the same subject swallowing the same bolus multiple times and modeling each swallow. From these data, the variation of the boundary condition at the GPJ, flowrates and pressures can be statistically analyzed.

Further human subject studies using ultra-fast computerized tomography should be done to study the role of air in the pharyngeal swallow. Ultra-fast CT scans show the cross-section of the pharyngeal chamber. Temporal and spatial resolution is limited, but these data could provide valuable information that could be used in the development of future models. It would also be interesting to combine these studies with manometry to further elucidate whether the sensor is in contact with bolus or air. The effect of bolus volume and viscosity on the amount of air contacting the pressure sensor would also be interesting data to analyze. It would also be informative to use this procedure, if possible, to study the variation due to head and body position.

The validity of using the different parameters in the simulations should be investigated. A fluoroscopy study of a subject in the supine position could be modeled. These results can be compared to a similar study in the upright position but with gravity acting in the direction of gravity in the supine swallow. This could indicate if gravity has any significance on the geometry of the bolus. It also will lend validity to models where the direction of gravity is arbitrarily assigned. Models where the viscosity is arbitrarily assigned could be verified by comparing the results of a simulation based on the actual bolus properties to the simulation that has a similar volume with arbitrary viscosity.

9.3.4.--Additional models

The model presented in this dissertation only accounted for the fluid mechanics of

the bolus in a two-dimensional geometry. To further understand the mechanism of swallowing, the role of the fluid-solid interaction should be investigated. This requires a different constitutive relationship for each muscle type involved in the pharyngeal swallow. There is currently no data in the literature describing the behavior of any of the muscles involved in the pharyngeal phase of swallowing. Constitutive relations would need to be developed or borrowed from similar muscle types within the human body. Software that can solve the combined fluid-solid model would have to be developed or purchased for this purpose.

Expanding the current model to a three-dimensional geometry would result in greater accuracy. As discussed in section 2.4.2, the best description of the cross-section of the pharynx is elliptical. To generate a three-dimensional model, the cross-section of the pharyngeal chamber would need to imaged. As mentioned above, ultrafast CT scans can be used for this purpose. These data, combined with bi-planar fluoroscopic data, can be used to generate three-dimensional geometry data as a function of time as demonstrated by Kahrilas, *et al.* (1993). An alternate method would be to use data from bi-planar fluoroscopy and assume elliptical geometry. The current version of FIDAP can handle a three-dimensional model, but limits the number of nodes with prescribed velocities via the time function command. This limitation may be eliminated in future versions of the software and can be circumvented by prescribing the movements through the use of a FORTRAN subroutine. The amount of data involved in prescribing individual movements of every node on a three-dimensional finite element mesh may be too large for many computer platforms to handle. As always, certain assumptions can be made to simplify the model.

This is just a brief summary of the many directions this research could continue. The amount of literature data on the subject of the pharyngeal swallow is proof that there is considerable interest in investigating this topic. This mathematical model is simply

another tool that can be used in the study of swallowing. This dissertation has demonstrated that a mathematical model can be used to provide additional insight into both normal and disordered pharyngeal swallowing.

LIST OF REFERENCES

Adnerhill, I., O. Ekberg, and M. E. Groher. "Determining normal bolus size for thin liquids." *Dysphagia* **4**(1): 1-3, 1989.

Ali, G. N., T. M. Laundl, K. L. Wallace, D. J. deCarle, and I. J. Cook. "Influence of cold stimulation on the normal pharyngeal swallow response [see comments]." *Dysphagia* **11**(1): 2-8, 1996.

Bastian, R. W. "The videoendoscopic swallowing study: an alternative and partner to the videofluoroscopic swallowing study." *Dysphagia* **8**(4): 359-67, 1993.

Beck, T. J., and B. W. Gayler. "Image quality and radiation levels in videofluoroscopy for swallowing studies: a review [see comments]." *Dysphagia* **5**(3): 118-28, 1990.

Bilder, C. R., C. P. Dooley, and J. E. Valenzuela. "Effect of bolus volume on the response of the human esophagus to a viscous bolus." *Scand J Gastroenterol* **25**(5): 467-70, 1990.

Birch-Iensen, M., P. S. Borgstrom, and O. Ekberg. "Cineradiography in closed and open pharyngeal swallow." *Acta Radiol* **29**(4): 407-10, 1988.

Bird, R. B., R. C. Armstrong, and O Hassager. Dynamics of Polymeric Liquids. 2nd ed. New York: John Wiley & Sons, 1987.

Bird, R. B., W. E. Stewart, and E. N. Lightfoot. Transport Phenomena. New York: John Wiley & Sons, 1960.

Bisch, E. M., J. A. Logemann, A. W. Rademaker, P. J. Kahrilas, and C. L. Lazarus. "Pharyngeal effects of bolus volume, viscosity, and temperature in patients with dysphagia resulting from neurologic impairment and in normal subjects." *J Speech Hear Res* **37**(5): 1041-59, 1994.

Bohme, G., and R. Friedrich. "Peristaltic flow of viscoelastic liquids." *J. Fluid Mech.* **128**: 109-122, 1983.

Borgstrom, P. S., and O. Ekberg. "Peristalsis in pharyngeal constrictor musculature in relation to positioning and gravity." *Acta Radiol* **30**(2): 183-5, 1989.

Borgstrom, P. S., and O. Ekberg. "Speed of peristalsis in pharyngeal constrictor musculature: correlation to age." *Dysphagia* **2**(3): 140-4, 1988.

Bosma, J. F., M. W. Donner, E. Tanaka, and D. Robertson. "Anatomy of the pharynx, pertinent to swallowing." *Dysphagia* **1**(1): 23-33, 1986.

Brasseur, J. G. "A fluid mechanical perspective on esophageal bolus transport." *Dysphagia* **2**(1): 32-9, 1987.

Brasseur, J. G. "Mechanical studies of the esophageal function." *Dysphagia* **8**(4): 384-6, 1993.

Brasseur, J. G., S. Corrsin, and N. Q. Lu. "The influence of a peripheral layer of different viscosity on peristaltic pumping with newtonian fluids." *J. Fluid Mech.* **174**: 495-519, 1987.

Brasseur, J. G., and W. J. Dodds. "Interpretation of intraluminal manometric measurements in terms of swallowing mechanics." *Dysphagia* **6**(2): 100-19, 1991.

Brown, T. D., and T. Hung. "Computational and experimental investigations of two-dimensional nonlinear peristaltic flows." *J. Fluid Mech.* **83**: 249-272, 1977.

Burden, R. L., and J. D. Faires. Numerical Analysis. Boston: PWS-KENT Publishing Company, 1989.

Burnett, D. S. Finite Element Analysis. Reading, MA: Addison-Wesley Publishing Company, 1987.

Caruso, A. J., S. J. Stanhope, and D. A. McGuire. "New technique for acquiring three-dimensional orofacial nonspeech movements." *Dysphagia* **4**(2): 127-32, 1989.

Castell, D. O. "Manometric evaluation of the pharynx." *Dysphagia* **8**(4): 337-8, 1993.

Castell, J. A., and D. O. Castell. "Manometric analysis of the pharyngo-esophageal segment." *Indian J Gastroenterol* **13**(2): 58-63, 1994.

Castell, J. A., and D. O. Castell. "Modern solid state computerized manometry of the pharyngoesophageal segment." *Dysphagia* **8**(3): 270-5, 1993.

Castell, J. A., D. O. Castell, A. R. Schultz, and S. Georgeson. "Effect of head position on the dynamics of the upper esophageal sphincter and pharynx." *Dysphagia* **8**(1): 1-6, 1993.

Castell, J. A., and C. B. Dalton. "Esophageal Manometry." In *The Esophagus*, edited by D. O. Castell, 143-159. Boston: Little Brown, 1992.

Castell, J. A., C. B. Dalton, and D. O. Castell. "Effects of body position and bolus consistency on the manometric parameters and coordination of the upper esophageal sphincter and pharynx." *Dysphagia* **5**(4): 179-86, 1990.

Castell, J. A., C. B. Dalton, and D. O. Castell. "Pharyngeal and upper esophageal sphincter manometry in humans." *Am J Physiol* **258**(2 Pt 1): G173-8, 1990.

Cerenko, D., F. M. McConnel, and R. T. Jackson. "Quantitative assessment of pharyngeal bolus driving forces." *Otolaryngol Head Neck Surg* **100**(1): 57-63, 1989.

Cherney, L. R., C. A. Cantieri, and J. J. Pannell. Clinical evaluation of dysphagia. Rockvill, MD: Aspen Systems Corp, 1986.

Cook, I. J. "Cricopharyngeal function and dysfunction [see comments]." *Dysphagia* **8**(3): 244-51, 1993.

Cook, I. J. "Normal and disordered swallowing: new insights." *Baillieres Clin Gastroenterol* **5**(2): 245-67, 1991.

Cook, I. J., J. Dent, and S. M. Collins. "Upper esophageal sphincter tone and reactivity to stress in patients with a history of globus sensation." *Dig Dis Sci* **34**(5): 672-6, 1989.

Cook, I. J., J. Dent, S. Shannon, and S. M. Collins. "Measurement of upper esophageal sphincter pressure. Effect of acute emotional stress." *Gastroenterology* **93**(3): 526-32, 1987.

Cook, I. J., W. J. Dodds, R. O. Dantas, M. K. Kern, B. T. Massey, R. Shaker, and W. J. Hogan. "Timing of videofluoroscopic, manometric events, and bolus transit during the oral and pharyngeal phases of swallowing." *Dysphagia* **4**(1): 8-15, 1989.

Cook, I. J., W. J. Dodds, R. O. Dantas, B. Massey, M. K. Kern, I. M. Lang, J. G. Brasseur, and W. J. Hogan. "Opening mechanisms of the human upper esophageal sphincter." *Am J Physiol* **257**(5 Pt 1): G748-59, 1989.

Cook, I. J., M. Gabb, V. Panagopoulos, G. G. Jamieson, W. J. Dodds, J. Dent, and D. J. Shearman. "Pharyngeal (Zenker's) diverticulum is a disorder of upper esophageal sphincter opening." *Gastroenterology* **103**(4): 1229-35, 1992.

Cook, I. J., M. D. Weltman, K. Wallace, D. W. Shaw, E. McKay, R. C. Smart, and S. P. Butler. "Influence of aging on oral-pharyngeal bolus transit and clearance during swallowing: scintigraphic study." *Am J Physiol* **266**(6 Pt 1): G972-7, 1994.

Dantas, R. O., I. J. Cook, W. J. Dodds, M. K. Kern, I. M. Lang, and J. G. Brasseur. "Biomechanics of cricopharyngeal bars." *Gastroenterology* **99**(5): 1269-74, 1990.

Dantas, R. O., and W. J. Dodds. "[Influence of the viscosity of the swallowed food bolus on the motility of the pharynx]." *Arq Gastroenterol* **27**(4): 164-8, 1990.

Dantas, R. O., W. J. Dodds, B. T. Massey, and M. K. Kern. "The effect of high- vs low-density barium preparations on the quantitative features of swallowing." *Ajr Am J Roentgenol* **153**(6): 1191-5, 1989.

Dantas, R. O., W. J. Dodds, B. T. Massey, R. Shaker, and I. J. Cook. "Manometric characteristics of glossopalatal sphincter." *Dig Dis Sci* **35**(2): 161-6, 1990.

Dantas, R. O., M. K. Kern, B. T. Massey, W. J. Dodds, P. J. Kahrilas, J. G. Brasseur, I. J. Cook, and I. M. Lang. "Effect of swallowed bolus variables on oral and pharyngeal phases of swallowing." *Am J Physiol* **258**(5 Pt 1): G675-81, 1990.

de Bruijne, D. W., H. A. C. M. Hendrickx, L. Alderliested, and J. de Looff. "Mouthfeel of foods." In *Food Colloids and Polymers: Stability and Mechanical Properties*, edited by E. Dickinson and P. Walstra. Cambridge: Royal Society of Chemistry, 1993.

Dejaeger, E., W. Pelemans, E. Ponette, and G. Vantrappen. "Effect of body position on deglutition." *Dig Dis Sci* **39**(4): 762-5, 1994.

Dengel, G., J. Robbins, and J. C. Rosenbek. "Image processing in swallowing and speech research." *Dysphagia* **6**(1): 30-9, 1991.

Dodds, W. J., J. A. Logemann, and E. T. Stewart. "Radiologic assessment of abnormal oral and pharyngeal phases of swallowing." *Ajr Am J Roentgenol* **154**(5): 965-74, 1990.

Dodds, W. J., K. M. Man, I. J. Cook, P. J. Kahrilas, E. T. Stewart, and M. K. Kern. "Influence of bolus volume on swallow-induced hyoid movement in normal subjects." *Ajr Am J Roentgenol* **150**(6): 1307-9, 1988.

Dodds, W. J., E. T. Stewart, and J. A. Logemann. "Physiology and radiology of the normal oral and pharyngeal phases of swallowing [see comments]." *Ajr Am J Roentgenol* **154**(5): 953-63, 1990.

Dodds, W. J., A. J. Taylor, E. T. Stewart, M. K. Kern, J. A. Logemann, and I. J. Cook. "Tipper and dipper types of oral swallows." *Ajr Am J Roentgenol* **153**(6): 1197-9, 1989.

Donner, M. W. "Editorial." *Dysphagia* **1**(1): 1-2, 1986.

Donner, M. W., and B. Jones. "Editorial." *Gastrointest Radiol* **10**(3): 194-95, 1985.

Donner, M. W., J. F. Bosma, and D. L. Robertson. "Anatomy and physiology of the pharynx." *Gastrointest Radiol* **10**(3): 196-212, 1985.

Dudnick, R. S., J. A. Castell, and D. O. Castell. "Abnormal upper esophageal sphincter function in achalasia." *Am J Gastroenterol* **87**(12): 1712-5, 1992.

Dusey, M. P. "Numerical analysis of lubrication theory and peristaltic transport in the esophagus." Ph.D. Thesis, Pennsylvania State University, 1993.

Ekberg, O. "Dimension of the pharyngo-esophageal segment in dysfunction of the cricopharyngeal muscle." *Acta Radiol Diagn Stockh* **27**(5): 539-41, 1986.

Ekberg, O. "Dysfunction of the pharyngo-oesophageal segment in patients with normal opening of the upper oesophageal sphincter: a cineradiographic study." *Br J Radiol* **60**(715): 637-44, 1987.

Ekberg, O. "Elevation of the pharynx and the width of the pharyngo-esophageal segment during swallow." *Acta Radiol Diagn Stockh* **27**(3): 293-5, 1986.

Ekberg, O. "Posture of the head and pharyngeal swallowing." *Acta Radiol Diagn Stockh* **27**(6): 691-6, 1986.

Ekberg, O. "The width of the pharyngo-esophageal junction area." *Acta Radiol Diagn Stockh* **27**(2): 205-8, 1986.

Ekberg, O., and P. S. Borgstrom. "Graphic representation of pharyngeal wall motion during swallow: technical note." *Dysphagia* **4**(1): 43-7, 1989.

Ekberg, O., and M. Feinberg. "Clinical and demographic data in 75 patients with near-fatal choking episodes." *Dysphagia* **7**(4): 205-8, 1992.

Ekberg, O., and M. J. Feinberg. "Altered swallowing function in elderly patients without dysphagia: radiologic findings in 56 cases [see comments]." *Ajr Am J Roentgenol* **156**(6): 1181-4, 1991.

Ekberg, O., and H. Hilderfors. "Defective closure of the laryngeal vestibule: frequency of pulmonary complications." *Ajr Am J Roentgenol* **145**(6): 1159-64, 1985.

Ekberg, O., B. Liedberg, and B. Owall. "Barium and meat. A comparison between pharyngeal swallow of fluid and solid boluses." *Acta Radiol Diagn Stockh* **27**(6): 701-4, 1986.

Ekberg, O., and C. Lindstrom. "The upper esophageal sphincter area." *Acta Radiol* **28**(2): 173-6, 1987.

Ekberg, O., and G. Nylander. "Double-contrast examination of the pharynx." *Gastrointest Radiol* **10**(3): 263-71, 1985.

Ekberg, O., G. Nylander, F. T. Fork, S. Sjoberg, M. Birch-Iensen, and B. Hillarp. "Interobserver variability in cineradiographic assessment of pharyngeal function during swallow." *Dysphagia* **3**(1): 46-8, 1988.

Ekberg, O., R. Olsson, and P. Sundgren-Borgstrom. "Relation of bolus size and pharyngeal swallow." *Dysphagia* **3**(2): 69-72, 1988.

Ekberg, O., and L. Wahlgren. "Dysfunction of pharyngeal swallowing. A cineradiographic investigation in 854 dysphagia patients." *Acta Radiol Diagn Stockh* **26**(4): 389-95, 1985.

Ekberg, O., and L. Wahlgren. "Pharyngeal dysfunctions and their interrelationship in patients with dysphagia." *Acta Radiol Diagn Stockh* **26**(6): 659-64, 1985.

Ergun, G. A., P. J. Kahrilas, S. Lin, J. A. Logemann, and J. M. Harig. "Shape, volume, and content of the deglutitive pharyngeal chamber imaged by ultrafast computerized tomography." *Gastroenterology* **105**(5): 1396-403, 1993.

Fass, J., J. Silny, J. Braun, U. Heindrichs, B. Dreuw, V. Schumpelick, and G. Rau. "Measuring esophageal motility with a new intraluminal impedance device. First clinical results in reflux patients." *Scand J Gastroenterol* **29**(8): 693-702, 1994.

Finlayson, B. A. The Method of Weighted Residuals and Variational Principles. New York: Academic Press, 1972.

Finlayson, B. A. Nonlinear Analysis in Chemical Engineering. New York: McGraw-Hill, 1980.

Finlayson, B. A. Numerical Methods for Problems with Moving Fronts. Seattle: Ravenna Park Publishing, 1992.

Fisher, M. A., T. R. Hendrix, J. N. Hunt, and A. J. Murrills. "Relation between volume swallowed and velocity of the bolus ejected from the pharynx into the esophagus." *Gastroenterology* **74**(6): 1238-40, 1978.

Fluid Dynamics International, Inc. FIDAP 7.5 Update Manual. Evanston, IL, 1995.

Fluid Dynamics International, Inc. FIDAP 7.0 Theory Manual. Evanston, IL, 1993.

Fulp, S. R., C. B. Dalton, J. A. Castell, and D. O. Castell. "Aging-related alterations in human upper esophageal sphincter function." *Am J Gastroenterol* **85**(12): 1569-72, 1990.

Fung, Y. C. "Peristaltic pumping: a bioengineering model." In *Urodynamics: Hydrodynamics of the Ureter and Renal Pelvis*, edited by S. Boyarsky, 177-199. New York: Academic Press, 1971.

Fung, Y. C., and C. S. Yih. "Peristaltic transport." *Trans. ASME, J. Appl. Mech.* **35**: 669-675, 1968.

Ganger, D., and R. M. Craig. "Swallowing disorders and nutritional support." *Dysphagia* **4**(4): 213-9, 1990.

Gerhardt, D. C., T. J. Shuck, R. A. Bordeaux, and D. H. Winship. "Human upper esophageal sphincter. Response to volume, osmotic, and acid stimuli." *Gastroenterology* **75**(2): 268-74, 1978.

Gramiak, R., M. L. Kelley, Jr., and R. F. Gravina. "Nasal pressure changes during swallowing; an analysis of 1,219 swallows in 88 healthy subjects." *Am J Roentgenol Radium Ther Nucl Med* **99**(3): 562-76, 1967.

Gresho, P. M., S. T. Chan, R. L. Lee, and C. D. Upson. "A modified Finite Element Method for solving the time-dependent incompressible Navier-Stokes equations." *Int. J. Num. Meth. Fluid.* **4**: 557, 1984.

Groher, M. E., and R. Bukatman. "The prevalence of swallowing disorders in two teaching hospitals." *Dysphagia* **4**(1): 1-3, 1989.

Groher, Michael E, ed. Dysphagia : diagnosis and management. Boston: Butterworth-Heinemann, 1992.

Gupta, B. B., and V. Seshadri. "Peristaltic pumping in non-uniform tubes." *J. Biomechanics* **9**: 105-109, 1976.

Hamlet, S., J. Choi, M. Zormeier, F. Shamsa, R. Stachler, J. Muz, and L. Jones. "Normal adult swallowing of liquid and viscous material: scintigraphic data on bolus transit and oropharyngeal residues." *Dysphagia* **11**(1): 41-7, 1996.

Hamlet, S. L. "Dynamic aspects of lingual propulsive activity in swallowing." *Dysphagia* **4**(3): 136-45, 1989.

Hamlet, S. L., J. Muz, R. Patterson, and L. Jones. "Pharyngeal transit time: assessment with videofluoroscopic and scintigraphic techniques." *Dysphagia* **4**(1): 4-7, 1989.

Hendrix, T. R. "Coordination of peristalsis in pharynx and esophagus." *Dysphagia* **8**(2): 74-8, 1993.

Holt, S., S. D. Miron, M. C. Diaz, R. Shields, D. Ingraham, and E. M. Bellon. "Scintigraphic measurement of oropharyngeal transit in man." *Dig Dis Sci* **35**(10): 1198-204, 1990.

Howard, P. J., A. Pryde, and R. C. Heading. "Oesophageal manometry during eating in the investigation of patients with chest pain or dysphagia." *Gut* **30**(9): 1179-86, 1989.

Hughes, T. A., P. Liu, H. Griffiths, B. W. Lawrie, and C. M. Wiles. "An analysis of studies comparing electrical impedance tomography with x-ray videofluoroscopy in the assessment of swallowing." *Physiol Meas* **15**(209): A199-209, 1994.

Ingervall, B., and B. Lantz. "Significance of gravity on the passage of bolus through the human pharynx." *Arch Oral Biol* **18**(3): 351-6, 1973.

Isberg, A., M. E. Nilsson, and H. Schiratzki. "Movement of the upper esophageal sphincter and a manometric device during deglutition. A cineradiographic investigation." *Acta Radiol Diagn Stockh* **26**(4): 381-8, 1985.

Isberg, A., M. E. Nilsson, and H. Schiratzki. "The upper esophageal sphincter during normal deglutition. A simultaneous cineradiographic and manometric investigation." *Acta Radiol Diagn Stockh* **26**(5): 563-8, 1985.

Jacob, P., P. J. Kahrilas, J. A. Logemann, V. Shah, and T. Ha. "Upper esophageal sphincter opening and modulation during swallowing." *Gastroenterology* **97**(6): 1469-78, 1989.

Jaffrin, M. Y. "Inertia and streamline curvature: effects on peristaltic pumping." *Int. J. Engng. Sci.* **11**: 681-699, 1973.

Johnsson, F., D. Shaw, M. Gabb, J. Dent, and I. Cook. "Influence of gravity and body position on normal oropharyngeal swallowing." *Am J Physiol* **269**(5 Pt 1): G653-8, 1995.

Jones, B., and M. W. Donner. "How I do it: examination of the patient with dysphagia [published erratum appears in Dysphagia 1991;6(1):65]." *Dysphagia* **4**(3): 162-72, 1989.

Jones, B., S. S. Kramer, and M. W. Donner. "Dynamic imaging of the pharynx." *Gastrointest Radiol* **10**(3): 213-24, 1985.

Jowitt, R., F. Escher, M. Kent, B. McKenna, and M. Roques, eds. *Physical Properties of Foods-2*. New York: Elsevier Applied Science, 1987.

Kahrilas, P. J. "Anatomy, physiology and pathophysiology of dysphagia." *Acta Otorhinolaryngol Belg* **48**(2): 97-117, 1994.

Kahrilas, P. J. "Pharyngeal structure and function." *Dysphagia* **8**(4): 303-7, 1993.

Kahrilas, P. J., R. E. Clouse, and W. J. Hogan. "American Gastroenterological Association technical review on the clinical use of esophageal manometry [see comments]." *Gastroenterology* **107**(6): 1865-84, 1994.

Kahrilas, P. J., J. Dent, W. J. Dodds, W. J. Hogan, and R. C. Arndorfer. "A method for continuous monitoring of upper esophageal sphincter pressure." *Dig Dis Sci* **32**(2): 121-8, 1987.

Kahrilas, P. J., W. J. Dodds, J. Dent, J. A. Logemann, and R. Shaker. "Upper esophageal sphincter function during deglutition." *Gastroenterology* **95**(1): 52-62, 1988.

Kahrilas, P. J., W. J. Dodds, and W. J. Hogan. "Effect of peristaltic dysfunction on esophageal volume clearance." *Gastroenterology* **94**(1): 73-80, 1988.

Kahrilas, P. J., and G. A. Ergun. "Esophageal dysphagia." *Acta Otorhinolaryngol Belg* **48**(2): 171-90, 1994.

Kahrilas, P. J., S. Lin, J. Chen, and J. A. Logemann. "Three-dimensional modeling of the oropharynx during swallowing." *Radiology* **194**(2): 575-9, 1995.

Kahrilas, P. J., S. Lin, J. A. Logemann, G. A. Ergun, and F. Facchini. "Deglutitive tongue action: volume accommodation and bolus propulsion." *Gastroenterology* **104**(1): 152-62, 1993.

Kahrilas, P. J., and J. A. Logemann. "Volume accommodation during swallowing." *Dysphagia* **8**(3): 259-65, 1993.

Kahrilas, P. J., J. A. Logemann, and P. Gibbons. "Food intake by maneuver; an extreme compensation for impaired swallowing." *Dysphagia* **7**(3): 155-9, 1992.

Kahrilas, P. J., J. A. Logemann, C. Krugler, and E. Flanagan. "Volitional augmentation of upper esophageal sphincter opening during swallowing." *Am J Physiol* **260**(3 Pt 1): G450-6, 1991.

Kahrilas, P. J., J. A. Logemann, S. Lin, and G. A. Ergun. "Pharyngeal clearance during swallowing: a combined manometric and videofluoroscopic study." *Gastroenterology* **103**(1): 128-36, 1992.

Karstoft, J., O. Ekberg, and S. E. Rubesin. "Topographic representation of the pharyngoesophageal segment during swallowing." *Invest Radiol* **25**(2): 184-8, 1990.

Kim, C. H., J. J. Hsu, M. K. O'Connor, A. L. Weaver, M. L. Brown, and A. R. Zinsmeister. "Effect of viscosity on oropharyngeal and esophageal emptying in man." *Dig Dis Sci* **39**(1): 189-92, 1994.

Knauer, C. M., J. A. Castell, C. B. Dalton, L. Nowak, and D. O. Castell. "Pharyngeal/upper esophageal sphincter pressure dynamics in humans. Effects of pharmacologic agents and thermal stimulation." *Dig Dis Sci* **35**(6): 774-80, 1990.

Kokini, J. L., and A. M. Dickie. "An attempt to identify and model transient viscoelastic flow in foods." *J. Texture Studies* **121**: 539-557, 1981.

Ku, D. N., P. P. Ma, F. M. McConnel, and D. Cerenko. "A kinematic study of the oropharyngeal swallowing of a liquid." *Ann Biomed Eng* **18**(6): 655-69, 1990.

Lazarus, C., J. A. Logemann, and P. Gibbons. "Effects of maneuvers on swallowing function in a dysphagic oral cancer patient." *Head Neck* **15**(5): 419-24, 1993.

Lazarus, C. L., J. A. Logemann, A. W. Rademaker, P. J. Kahrilas, T. Pajak, R. Lazar, and A. Halper. "Effects of bolus volume, viscosity, and repeated swallows in nonstroke subjects and stroke patients." *Arch Phys Med Rehabil* **74**(10): 1066-70, 1993.

Li, M., and J. G. Brasseur. "Non-steady peristaltic transport in finite-length tubes." *Journal of Fluid Mechanics* **248**: 129-51, 1993.

Li, M., J. G. Brasseur, and W. J. Dodds. "Analyses of normal and abnormal esophageal transport using computer simulations." *Am J Physiol* **266**(4 Pt 1): G525-43, 1994.

Li, M., J. G. Brasseur, M. K. Kern, and W. J. Dodds. "Viscosity measurements of barium sulfate mixtures for use in motility studies of the pharynx and esophagus." *Dysphagia* **7**(1): 17-30, 1992.

Liedberg, B., O. Ekberg, and B. Owall. "Chewing and the dimension of the pharyngoesophageal segment." *Dysphagia* **6**(4): 214-8, 1991.

Linden, P., D. Tippett, J. Johnston, A. Siebens, and J. French. "Bolus position at swallow onset in normal adults: preliminary observations." *Dysphagia* **4**(3): 146-50, 1989.

Loch, W. E., W. E. Loch, H. M. Reiriz, and M. H. Loch. "Swallow apnea--rhinomanometric manifestation and classification." *Rhinology* **20**(4): 179-91, 1982.

Logeman, J.A. Evaluation and Treatment of Swallowing Disorders. San Diego: College-Hill Press, Inc., 1983.

Logemann, J. A. "Criteria for studies of treatment for oral-pharyngeal dysphagia." *Dysphagia* **1**(2): 193-199, 1987.

Logemann, J. A. "Effects of aging on the swallowing mechanism." *Otolaryngol Clin North Am* **23**(6): 1045-56, 1990.

Logemann, J. A. "Factors affecting ability to resume oral nutrition in the oropharyngeal dysphagic individual." *Dysphagia* **4**(4): 202-8, 1990.

Logemann, J. A. "Non-imaging techniques for the study of swallowing." *Acta Otorhinolaryngol Belg* **48**(2): 139-42, 1994.

Logemann, J. A. "Swallowing physiology and pathophysiology." *Otolaryngol Clin North Am* **21**(4): 613-23, 1988.

Logemann, J. A., P. J. Kahrilas, J. Begelman, W. J. Dodds, and B. R. Pauloski. "Interactive computer program for biomechanical analysis of videoradiographic studies of swallowing." *Ajr Am J Roentgenol* **153**(2): 277-80, 1989.

Logemann, J. A., P. J. Kahrilas, J. Cheng, B. R. Pauloski, P. J. Gibbons, A. W. Rademaker, and S. Lin. "Closure mechanisms of laryngeal vestibule during swallow." *Am J Physiol* **262**(2 Pt 1): G338-44, 1992.

Logemann, J. A., P. J. Kahrilas, M. Kobara, and N. B. Vakil. "The benefit of head rotation on pharyngoesophageal dysphagia." *Arch Phys Med Rehabil* **70**(10): 767-71, 1989.

Logemann, J. A., A. W. Rademaker, B. R. Pauloski, and P. J. Kahrilas. "Effects of postural change on aspiration in head and neck surgical patients." *Otolaryngol Head Neck Surg* **110**(2): 222-7, 1994.

Maddock, D. J., and R. J. Gilbert. "Quantitative relationship between liquid bolus flow and laryngeal closure during deglutition." *Am J Physiol* **265**(4 Pt 1): G704-11, 1993.

Martin, A. W. "Dietary management of swallowing disorders." *Dysphagia* **6**(3): 129-34, 1991.

Martin, B. J., J. A. Logemann, R. Shaker, and W. J. Dodds. "Coordination between respiration and swallowing: respiratory phase relationships and temporal integration." *J Appl Physiol* **76**(2): 714-23, 1994.

Massey, B. T., W. J. Dodds, W. J. Hogan, J. G. Brasseur, and J. F. Helm. "Abnormal esophageal motility. An analysis of concurrent radiographic and manometric findings." *Gastroenterology* **101**(2): 344-54, 1991.

McClelland, M. A., and B. A. Finlayson. "Squeezing flow of highly viscous polymers." *Journal of Rheology* **32**(2): 101-33, 1988.

McConnel, F. M. "Analysis of pressure generation and bolus transit during pharyngeal swallowing." *Laryngoscope* **98**(1): 71-8, 1988.

McConnel, F. M., D. Cerenko, T. Hersh, and L. J. Weil. "Evaluation of pharyngeal dysphagia with manofluorography." *Dysphagia* **2**(4): 187-95, 1988.

McConnel, F. M., D. Cerenko, R. T. Jackson, and T. N. Guffin, Jr. "Timing of major events of pharyngeal swallowing." *Arch Otolaryngol Head Neck Surg* **114**(12): 1413-8, 1988.

McConnel, F. M., D. Cerenko, R. T. Jackson, and T. Hersh. "Clinical application of the manofluorogram." *Laryngoscope* **98**(7): 705-11, 1988.

McConnel, F. M., D. Cerenko, and M. S. Mendelsohn. "Dysphagia after total laryngectomy." *Otolaryngol Clin North Am* **21**(4): 721-6, 1988.

McConnel, F. M., D. Cerenko, and M. S. Mendelsohn. "Manofluorographic analysis of swallowing." *Otolaryngol Clin North Am* **21**(4): 625-35, 1988.

McConnel, F. M., T. N. Guffin, Jr., and D. Cerenko. "The effect of asymmetric pharyngoesophageal pressures on manofluorographic measurements." *Laryngoscope* **101**(5): 510-5, 1991.

McConnel, F. M., T. N. Guffin, Jr., D. Cerenko, and A. S. Ko. "The effects of bolus flow on vertical pharyngeal pressure measurement in the pharyngoesophageal segment: clinical significance." *Otolaryngol Head Neck Surg* **106**(2): 169-74, 1992.

McConnel, F. M., T. R. Hester, M. S. Mendelsohn, and J. A. Logemann. "Manofluorography of deglutition after total laryngopharyngectomy." *Plast Reconstr Surg* **81**(3): 346-51, 1988.

McConnel, F. M., M. S. Mendelsohn, and J. A. Logemann. "Examination of swallowing after total laryngectomy using manofluorography." *Head Neck Surg* **9**(1): 3-12, 1986.

McConnel, F. M., M. S. Mendelsohn, and J. A. Logemann. "Manofluorography of deglutition after supraglottic laryngectomy." *Head Neck Surg* **9**(3): 142-50, 1987.

Mendelsohn, M. S., and F. M. McConnel. "Function in the pharyngoesophageal segment." *Laryngoscope* **97**(4): 483-9, 1987.

Motta, G., U. Cesari, M. Iengo, and G. Motta, Jr. "Clinical application of electroglottography." *Folia Phoniatr Basel* **42**(3): 111-7, 1990.

Neumann, S. "Swallowing therapy with neurologic patients: results of direct and indirect therapy methods in 66 patients suffering from neurological disorders." *Dysphagia* **8**(2): 150-3, 1993.

Olsson, R., H. Nilsson, and O. Ekberg. "An experimental manometric study simulating upper esophageal sphincter narrowing." *Invest Radiol* **29**(6): 630-5, 1994.

Olsson, R., H. Nilsson, and O. Ekberg. "Simultaneous videoradiography and computerized pharyngeal manometry--videomanometry." *Acta Radiol* **35**(1): 30-4, 1994.

Olsson, R., H. Nilsson, and O. Ekberg. "Simultaneous videoradiography and pharyngeal solid state manometry (videomanometry) in 25 nondysphagic volunteers." *Dysphagia* **10**(1): 36-41, 1995.

Orlowski, J., W. J. Dodds, J. H. Linehan, J. Dent, W. J. Hogan, and R. C. Arndorfer. "Requirements for accurate manometric recording of pharyngeal and esophageal peristaltic pressure waves." *Invest Radiol* **17**(6): 567-72, 1982.

Palmer, J. B., K. V. Kuhlemeier, D. C. Tippett, and C. Lynch. "A protocol for the videofluorographic swallowing study." *Dysphagia* **8**(3): 209-14, 1993.

Palmer, J. B., N. J. Rudin, G. Lara, and A. W. Crompton. "Coordination of mastication and swallowing." *Dysphagia* **7**(4): 187-200, 1992.

Palmer, J. B., and K. H. Silver. "Effects of pollution on swallowing: how little we know." *Otolaryngol Head Neck Surg* **106**(6): 706-12, 1992.

Palmer, J. B., E. Tanaka, and A. A. Siebens. "Motions of the posterior pharyngeal wall in swallowing." *Laryngoscope* **98**(4): 414-7, 1988.

Peleg, M., ed. Physical Properties of Foods. Westport, Conn.: AVI Publishing Co., 1983.

Perlman, A. L. "Electromyography and the study of oropharyngeal swallowing." *Dysphagia* **8**(4): 351-5, 1993.

Perlman, A. L., J. G. Schultz, and D. J. VanDaele. "Effects of age, gender, bolus volume, and bolus viscosity on oropharyngeal pressure during swallowing." *J Appl Physiol* **75**(1): 33-7, 1993.

Pouderoux, P., G. A. Ergun, S. Lin, and P. J. Kahrilas. "Esophageal bolus transit imaged by ultrafast computerized tomography." *Gastroenterology* **110**(5): 1422-8, 1996.

Pouderoux, P., and P. J. Kahrilas. "Deglutitive tongue force modulation by volition, volume, and viscosity in humans." *Gastroenterology* **108**(5): 1418-26, 1995.

Rao, M. A., and S. S. H. Rizvi, eds. Engineering Properties of Foods. New York: Dekker, 1986.

Rasley, A., J. A. Logemann, P. J. Kahrilas, A. W. Rademaker, B. R. Pauloski, and W. J. Dodds. "Prevention of barium aspiration during videofluoroscopic swallowing studies: value of change in posture." *Ajr Am J Roentgenol* **160**(5): 1005-9, 1993.

Ravich, W. J. "The unrealized potential of pharyngeal manometry [editorial]." *Dysphagia* **10**(1): 42-3, 1995.

Reddy, N. P., E. P. Canilang, J. Casterline, M. B. Rane, A. M. Joshi, R. Thomas, and R. Candadai. "Noninvasive acceleration measurements to characterize the pharyngeal phase of swallowing." *J Biomed Eng* **13**(5): 379-83, 1991.

Reddy, N. P., B. R. Costarella, R. C. Grotz, and E. P. Canilang. "Biomechanical measurements to characterize the oral phase of dysphagia." *Ieee Trans Biomed Eng* **37**(4): 392-7, 1990.

Ren, J., B. T. Massey, W. J. Dodds, M. K. Kern, J. G. Brasseur, R. Shaker, S. S. Harrington, W. J. Hogan, and R. C. Arndorfer. "Determinants of intrabolus pressure during esophageal peristaltic bolus transport." *Am J Physiol* **264**(3 Pt 1): G407-13, 1993.

Ren, J., R. Shaker, Z. Zamir, W. J. Dodds, W. J. Hogan, and R. G. Hoffmann. "Effect of age and bolus variables on the coordination of the glottis and upper esophageal sphincter during swallowing." *Am J Gastroenterol* **88**(5): 665-9, 1993.

Rohrmann, C. A. "Assessment of Swallowing: Radiologic Why and How." Department of Radiology, University of Washington, 1994.

Rosenbek, J. C., J. Robbins, B. Fishback, and R. L. Levine. "Effects of thermal application on dysphagia after stroke." *J Speech Hear Res* **34**(6): 1257-68, 1991.

Rubesin, S. E. "Oral and pharyngeal dysphagia." *Gastroenterol Clin North Am* **24**(2): 331-52, 1995.

Rubesin, S. E., and I. Laufer. "Pictorial review: principles of double-contrast pharyngography." *Dysphagia* **6**(3): 170-8, 1991.

Sears, V. W., Jr., J. A. Castell, and D. O. Castell. "Comparison of effects of upright versus supine body position and liquid versus solid bolus on esophageal pressures in normal humans." *Dig Dis Sci* **35**(7): 857-64, 1990.

Sears, V. W., Jr., J. A. Castell, and D. O. Castell. "Radial and longitudinal asymmetry of human pharyngeal pressures during swallowing." *Gastroenterology* **101**(6): 1559-63, 1991.

Shaker, R., I. J. Cook, W. J. Dodds, and W. J. Hogan. "Pressure-flow dynamics of the oral phase of swallowing." *Dysphagia* **3**(2): 79-84, 1988.

Shaker, R., W. J. Dodds, R. O. Dantas, W. J. Hogan, and R. C. Arndorfer. "Coordination of deglutitive glottic closure with oropharyngeal swallowing." *Gastroenterology* **98**(6): 1478-84, 1990.

Shaker, R., J. Ren, B. Podvrsan, W. J. Dodds, W. J. Hogan, M. Kern, R. Hoffmann, and J. Hintz. "Effect of aging and bolus variables on pharyngeal and upper esophageal sphincter motor function." *Am J Physiol* **264**(3 Pt 1): G427-32, 1993.

Shaker, R., J. Ren, Z. Zamir, A. Sarna, J. Liu, and Z. Sui. "Effect of aging, position, and temperature on the threshold volume triggering pharyngeal swallows." *Gastroenterology* **107**(2): 396-402, 1994.

Shanahan, T. K., J. A. Logemann, A. W. Rademaker, B. R. Pauloski, and P. J. Kahrilas. "Chin-down posture effect on aspiration in dysphagic patients." *Arch Phys Med Rehabil* **74**(7): 736-9, 1993.

Shapiro, A. H., M. Y. Jaffrin, and S. L. Weinberg. "Peristaltic pumping with long wavelengths at low Reynolds number." *J. Fluid Mech.* **37**(4): 799-825, 1969.

Siddiqui, A. M., A. Provost, and W. H. Schwarz. "Peristaltic pumping of a second-order fluid in a planar channel." *Rheologica Acta* **30**(3): 249-62, 1991.

Siddiqui, A. M., and W. H. Schwarz. "Peristaltic flow of a second-order fluid in tubes." *Journal of Non Newtonian Fluid Mechanics* **53**: 257-84, 1994.

Siddiqui, A. M., and W. H. Schwarz. "Peristaltic motion of a third-order fluid in a planar channel." *Rheologica Acta* **32**(1): 47-56, 1993.

Sokol, E. M., P. Heitmann, B. S. Wolf, and B. R. Cohen. "Simultaneous cineradiographic and manometric study of the pharynx, hypopharynx, and cervical esophagus." *Gastroenterology* **51**(6): 960-74, 1966.

Stavitsky, D., E. O. Macagno, and J. Christensen. "Finite-element analysis of flow induced by contractions like those of the intestine." *J Biomech* **14**(3): 183-93, 1981.

Steffe, J. P. *Personal Communication*, June 1994.

Steffe, J. P., I. O. Mohamed, and E. W. Ford. "Rheological properties of fluid foods." Paper presented at the 1983 Winter Meeting of the American Society of Agricultural Engineers, Chicago, Ill. 1983.

Suto, Y., M. Kamba, and T. Kato. "Technical note: dynamic analysis of the pharynx during swallowing using Turbo-FLASH magnetic resonance imaging combined with an oral positive contrast agent--a preliminary study." *Br J Radiol* **68**(814): 1099-102, 1995.

Takabatake, S., and K. Ayukawa. "Numerical study of two-dimensional peristaltic flows." *J. Fluid Mech.* **122**: 438-465, 1982.

Takabatake, S., K. Ayukawa, and A. Mori. "Peristaltic pumping in circular cylindrical tubes: a numerical study of fluid transport and its efficiency." *J. Fluid Mech.* **193**: 267-283, 1988.

Tatsch, K., W. A. Voderholzer, M. J. Weiss, W. Schroettle, A. G. Klauser, S. A. Mueller-Lissner, and C. M. Kirsch. "Simultaneous assessment of bolus transport and contraction parameters in multiple-swallow investigations [see comments]." *J Nucl Med* **33**(7): 1291-300, 1992.

Tibbling, L., P. Ask, and C. E. 2d Pope. "Electromyography of human oesophageal smooth muscle." *Scand J Gastroenterol* **21**(5): 559-67, 1986.

Tracy, J. F., J. A. Logemann, P. J. Kahrilas, P. Jacob, M. Kobara, and C. Krugler. "Preliminary observations on the effects of age on oropharyngeal deglutition." *Dysphagia* **4**(2): 90-4, 1989.

Van Der Reijden, W. A., E. C. I. Veerman, and A. V. Nieuw-Amerongen. "Shear rate dependent viscoelastic behavior of human glandular salivas." *Biorheology* **30**(2): 141-52, 1993.

van Westen, D., and O. Ekberg. "Solid bolus swallowing in the radiologic evaluation of dysphagia." *Acta Radiol* **34**(4): 372-5, 1993.

Welch, M. V., J. A. Logemann, A. W. Rademaker, and P. J. Kahrilas. "Changes in pharyngeal dimensions effected by chin tuck." *Arch Phys Med Rehabil* **74**(2): 178-81, 1993.

Wilson, J. A., A. Pryde, P. L. Allan, and A. G. Maran. "Cricopharyngeal dysfunction." *Otolaryngol Head Neck Surg* **106**(2): 163-8, 1992.

Wilson, J. A., A. Pryde, A. Cecilia, C. C. Macintyre, and R. C. Heading. "Normal pharyngoesophageal motility. A study of 50 healthy subjects." *Dig Dis Sci* **34**(10): 1590-9, 1989.

Wilson, J. A., A. Pryde, C. C. Macintyre, A. G. Maran, and R. C. Heading. "The effects of age, sex, and smoking on normal pharyngoesophageal motility." *Am J Gastroenterol* **85**(6): 686-91, 1990.

Wintzen, A. R., U. A. Badrising, R. A. Roos, J. Vielvoye, and L. Liauw. "Influence of bolus volume on hyoid movements in normal individuals and patients with Parkinson's disease." *Can J Neurol Sci* **21**(1): 57-9, 1994.